WTW WANDERTHEWEST

SPRING 2016 RALLY

Photo by Maria Papurello

GEOTOUR
OF
THE
CARRIZO PLAIN NATIONAL MONUMENT

APRIL 9 & 10, 2016

EDITED BY TUFF GUY 62

THERE IS SCIENCE, LOGIC,
REASON;

THERE IS THOUGHT
VERIFIED BY EXPERIENCE.

AND THEN THERE IS
CALIFORNIA.

EDWARD ABBEY

WTW WANDERTHEWEST

April 9, 2016

Fellow Wanderers,

We are pleased to welcome you to the Carrizo Plain National Monument for the Wander the West 2016 Spring Rally. Located in southeastern San Luis Obispo County, between the Caliente and Temblor Ranges, Carrizo Plain offers the most spectacular views to observe the San Andreas fault in the State of California. As a result of tectonic forces that continue to shape this landscape, the drainage of the plain was captured near the end on the last ice age by movement along the San Andreas fault, creating Soda Lake, the only closed basin in the Southern Coast Ranges. On opposite sides of the fault, not only are the basement rocks contrasting, but the oldest corresponding sedimentary sequences are dissimilar, and the successively younger sedimentary sequences less different. This condition has occurred as a result of persistent right-lateral movement on the San Andreas fault beginning about 20 million years ago.

Known to the Californianos as "Llano Estero" or salt marsh plain, this arid and treeless valley retains the largest remaining habitats that once spanned the entire San Joaquin Valley. Most of this habitat is protected within the 246,812-acre Carrizo Plain National Monument. The Carrizo Plain is home to the largest concentration of threatened and endangered vertebrates in the state. Some of these species include the San Joaquin kit fox, the San Joaquin antelope squirrel, the blunt-nosed leopard lizard, the giant kangaroo rat, and the California condor. Black-tailed jackrabbit, western coyotes and Le Conte's thrasher also make their homes in the Carrizo Plain. You will see a wide variety of flora ranging from salt marsh environments to juniper and pine communities. Herds of tule elk and pronghorn antelope, eliminated by uncontrolled hunting in the late 19th and early 20th centuries have been reintroduced to their former range. As one of the state's largest protected alkali wetlands, Soda Lake provides refuge and habitat for shorebirds and waterfowl alike.

In addition to the geology and biology of the Carrizo, this rally will also provide an opportunity to observe the impacts of homo sapiens on this usually hot and dry desolate plain. Chumash and Yokut tribes frequented the area in pre-colonial times as seen at Painted Rock. The landscape also underwent dramatic change as herds of livestock from Spanish and later Mexican missions began to graze on the land in the early 1800s, consuming much of the native grasses and introducing non-native plant species. Early Anglo settlers changed the face of agriculture on plain in the early 20th century with the introduction of dryland farming, sowing the land with tens of thousands of acres of wheat & barley.

This field guide is the result of three reconnaissance trips performed in February and March 2016. Collectively, we have 70 plus years combined experience exploring this surprisingly remote area of central California dating back to the early 1970s. The co-leaders of this geo-tour would like to personally thank **Mr. Bill Harr of Stockton California**, who inspired and organized this get together of like-minded folk. *Now let's get out there and get to work on some trip reports!*

Respectfully Submitted,

Brian Papurello
Tuff Guy 62
WTW WANDERTHEWEST
Spring 2016 Geotour Co-leader

Randy Petersen
RandyP
WTW WANDERTHEWEST
Spring 2016 Geotour Co-leader

WTW WANDERTHEWEST

Spring 2016 Rally *April 2016*

Contents

ROAD LOG

WTW WANDERTHEWEST

SPRING 2016 RALLY
GEO-TOUR ROAD LOG

This road log starts ***in the middle of nowhere*** at the intersection of California State Highway 33/166 and Soda Lake Road (Reyes Station). There are no services in this area, make sure to start the tour with a full tank of fuel, plenty of water and some food. Much of this route is on unpaved roads and dirt tracks that can be traversed with a 2WD passenger vehicle. However, road conditions may change suddenly and through the seasons may be impassable after a light to moderate rainfall that infrequently visits the area. Be sure to carry a spare tire in good repair. ***This is rattlesnake country so watch where you step!!*** The geo-tour route is approximately 58-miles in length ending at the Goodwin Education Center near the northerly end of the monument, still ***in the middle of nowhere.*** Enjoy!!

Miles	***(delta)***	
0.0	*(0.0)*	Start at Reyes Station at the junction of CA 33/166 and Soda Lake Road. It is traditional to pop open your favorite cold beverage at this point to honor the memory of Mrs. Alice Reyes, former proprietor of Reyes Station **(34°57.831'/-119°26.822')**
0.2	*(0.2)*	Alkali sag pond, the fault is 150 yards east of the road and approaches obliquely from the right as we drive northwest. The hills to the east are composed of Plio-Pleistocene age Paso Robles Formation, to the south and west the hills consist of upper Miocene Bitterwater Creek Shale. *Please refer to the block diagram for a depiction for active fault landforms on the back cover of this guidebook.* **(34°58.003'/-119°26.983')**
0.7	*(0.5)*	***STOP #1 – Welcome to the San Andreas fault:*** Turn out right. Low scarp trending in the middle of the valley. Take time to observe other fault related features. How many do you see? **(34° 58.286'/-119° 27.343').**
1.0	*(0.3)*	***STOP #2 – Sag Pond:*** Turn out right. Alkali sag pond on the San Andreas fault. Note hypersaline evaporate deposits. **(34° 58.459'/-119° 27.603')**
1.6	*(0.6)*	***STOP #3 – Earthquake!!:*** Turn out right. View three erosional gullies offset right-laterally from their corresponding alluvial fans. These small fan deposits are offset up to 8 meters most likely from the (~M8.0 1857 Fort Tejon Earthquake. Hills are composed of folded Paso Robles Fm. At this point the fault joins the road for about the next half a mile **(34° 58.851'/-119° 28.063')**
1.9	*(0.3)*	Enter the Carrizo Plain drainage basin. To the south, drainage flows to the Pacific Ocean via the Cuyama River. Northward, it flows into the Carrizo Plain which is a closed basin **(34° 58.994'/-119° 28.272')**

GEO-TOUR ROAD LOG (CONTINUED)

Miles	*(delta)*	
2.4	*(0.5)*	Numerous fault features on the left to include linear ridges, sags, etc. **(34° 59.231'/-119° 28.664')**
2.6	(0.2)	***STOP #4 -Group Photo:*** **(34° 59.353'/-119° 28.834')** Turn out right. Enter Carrizo Plain National Monument. Carrizo Plain National Monument was created by proclamation on January 17, 2001 by President William J. Clinton just prior to leaving office. Encompassing an area of over 204,000-acres, Carrizo Plain is home to many animals with sensitive status. Tule elk and pronghorn antelope have been reintroduced and can be seen at various locations on the plain. Many raptors, including red-tailed hawks, golden eagles, northern harriers, owls, and others can be found at different times throughout the year. The California Condor has been reintroduced nearby and is occasionally detected within the monument. Some of the nocturnal animals found within the monument are federally or state protected species. These include the San Joaquin kit fox and the giant kangaroo rat. The Carrizo is also home to other kangaroo rat species and numerous other rodents. Badgers and bobcats are both quite secretive and are more nocturnal than diurnal but may be seen during the day or night, especially during the spring months. Jackrabbits normally come out at night but can be seen during the day if flushed from their resting spots. There are several owl species that hunt for rodents at night. Great-horned and barn owls are the most common. Burrowing owls can quite often be seen in spring both day and night. Short-eared owls are also found on the Carrizo but are less likely to be seen than the others. Bats too become active as the temperatures warm, some coming out at dusk, clearly visible as they comb the skies for insects. The monument contains hundreds of significant cultural sites. These include everything from prehistoric Native American campsites that are as much as 10,000 years old to 19th century homesteads, some which were farmed and ranched into recent times. Many of the Carrizo sites have been listed on the National Register of Historic Places. The values of the spectacular Painted Rock site are obvious, but other important cultural sites also add to our understanding of life on the Carrizo, even if they may not immediately appear significant at first glance. Old farm buildings, machinery and implements, fence posts, water troughs and even historical period dump sites represent aspects of a way of life to preserve. Look to the north down upon a sag pond. To the northwest you can follow the trace of the fault and see a notch and deformation where the foothills join the plain. Note chemically altered and sheared Paso Robles Formation. The greenish and purple colors are from ground water alteration characteristic of fault gouge. Take a short walk to the south to examine recent fault and earthquake features.
5.2	*(2.6)*	Pavement ends **(35° 0.644'/-119° 31.005')**
10.8	*(5.6)*	Concrete filled gully. This gully was once Soda Lake Road! Realignment of the road to its present route in the 1960s changed the flow dynamics by concentrating runoff and speeding up erosion. The concrete barrier was emplaced in 1992 to protect a buried telecommunication cable where it crosses the gully **(35° 3.345'/-119° 35.582')**
11.3	(0.5)	Pavement begins **(35° 3.349/-119° 36.136)**

GEO-TOUR ROAD LOG (CONTINUED)

Miles	*(delta)*	
11.7	*(0.4)*	***STOP #5 - Sanitary Halt, Traver Ranch:*** **(35° 3.486'/-119° 36.473')** The L.E. Traver Ranch was established in the 1940s when the family purchased approximately 800 acres and began building the large block house that still stands along the edge of Soda Lake Road (see tri-fold handout in map pocket). The family was primarily involved in dryland farming of wheat and occasionally barley. Examples of farming implements that were used are on display in the field east of the block house. The house can be viewed from the small parking lot and information kiosk. The house provides important habitat for the pallid bat and western small-footed bat, as well as other wildlife species. Because of this, the house has been secured with plywood and metal grates to allow wildlife access but prevent human entrance into the structure.
12.7	*(1.0)*	Pavement ends **(35° 3.863'/-119° 37.393')**
14.0	*(1.3)*	Enter a region of low hills (10 million year old Caliente Fm.), turn right on dirt road **(35° 4.121'/-119° 38.772')**
14.4	*(0.4)*	***STOP #6 – Dragon's Back Pressure Ridge Overlook:*** **(35° 4.443'/-119° 38.692')** Examine one of the iconic features of the San Andreas fault. Current theory postulates that the Dragon's Back is a result of a knuckle or bend of the fault plane on the North American plate that results in rapid uplift (~1.7mm/yr) of the overriding Pacific Plate.
15.0	*(0.6)*	Bear right at tank **(35° 5.674'/-119° 38.399')**
16.6	(1.6)	***STOP #7 – Agriculture in the Shadow of the San Andreas:*** **(35° 5.471'/-119° 37.833)** How did the Carrizo get its name? One speculative story is that when the early settlers came to the plain they called it, "llano estero" referring to a salt marsh plain. Then later, as others came to the plain, the name changed to "Carrizo Plain." The word "Carrizo" referred to a grass that grew very tall. It was said that the grass touched the bellies of the vaquero's horses as they rode across that plains. Then, as Anglo settlers came, the name changed once again to Carrisa. "Carrisa Plains" was used up to the time that the current managing partners acquired the land. A decision was then made by the partners to return to the earlier name and call it the Carrizo Plain. Other information about the name and spelling came from the first post office on the Carrizo Plain which was founded in 1882 and was located at the El Saucito Ranch, which is located a couple of miles west of the Goodwin Education Center. Now let's talk a little bit about the farming and ranching history. After California earned statehood in 1850, land speculators and pioneers began acquiring parcels and settling on this arid plain. Sheep and cattle were the mainstays of these early settlers. The turn of the 20th century marked the rise of dryland farming (no irrigation) on the Carrizo Plain. In years when rainfall was sufficient, crops such as barely, wheat and oats grew well in the fertile soil of this arid climate. After the harvest, the "stubble" was grazed mostly by cattle, but also by sheep.

GEO-TOUR ROAD LOG (CONTINUED)

Miles	***(delta)***	
16.6	(1.6)	***STOP #7 (Continued):*** Because of the unpredictable weather and rainfall, some years farmers had great crops, but many years' crops were marginal. It was often described by the old ranchers as boom or bust! However, transportation to markets in the San Joaquin Valley and the Central Coast was a challenge. A road to McKittrick, built in the 1890's by local laborers solved this problem and the introduction of mechanized farm machinery in 1912 further boosted the regions grain industry. In the 1930's, large-scale farm mechanization, combined with the troubles of the Great Depression ushered in a new era. As smaller farms failed, they were consolidated into larger operations owned by absentee landlords. As a result of the intensive grain industry, the Carrizo Plain was once waypoint for large migratory populations of Sandhill Cranes which have all but disappeared with the cessation of dryland farming. In 1987, many of the big farms and ranches began to be transferred to the Bureau of Land Management, The Nature Conservancy and the California Department of Fish & Game. This was part of an effort to preserve some of California's ranching history and provide habitat for rare and endangered San Joaquin Valley wildlife. After you have examined some of the farming relics of the past at this location, I ask that you to pause for a moment, taking in the scenery around you. Think about those rugged pioneers who toiled and labored to eke out a living for themselves and their families, in this land of desolation, specters from the past in another place in another time. ***Double back to the north.***
17.2	(0.6)	Bear right through fence and turn right and follow fence line toward the Elkhorn Scarp **(35° 5.677'/-119° 38.401')**
17.9	(0.7)	Road swings left (NW) along a fence at the foot of a shutter ridge defining the southwest edge of the scarp. The San Andreas fault is on the other side of the ridge to the right. Good view of the plain and Caliente Peak, the highest point in San Luis Obispo County **(35° 6.232'/-119° 38.374')**
18.6	(0.7)	Turn right and go through fence **(35° 6.716'/-119° 38.861')**
18.7	(0.1)	***STOP #8 - Picnic Point, Lunch Break*** **(35° 6.808'/-119° 38.805')** We are now situated on the northern terminus of the Dragon's Back Pressure ridge on the San Andreas fault. Take a walk through the arroyo in the great rift where North America and Pacifica are loosely stitched together. Take time to examine the interesting rocks in the stream bed. You'll find rounded cobbles of marble, granite, sandstone along with volcanic and metamorphic clasts. What are these igneous and metamorphic rocks doing here? These are rocks that belong further south in the San Gabriel Mountains. These clasts have been transported northwestward along the fault and juxtaposed against the much younger Tertiary sedimentary rocks of the Temblor Range. For a good view of the rift and the back side of the Dragon's Back, take a short hike up the hill to the southeast. ***Return to Soda Lake Road.***

GEO-TOUR ROAD LOG (CONTINUED)

Miles	***(delta)***	
22.2	(3.5)	Junction Soda Lake Road, turn right **(35° 4.131'/-119° 38.783')**
29.0	(6.8)	About 100 yards to the left (west) is a small conical hill composed of diabase, a dark black igneous rock. This hill is all that remains of a volcano that erupted about 15 million years ago that has long since eroded away. When the vent was active, this ancient volcano was much higher than it is today, it has since tilted and the surrounding less resistant rock has eroded, leaving the cone or neck we see today. **(35° 6.665'/-119° 44.307')**
32.1	(3.1)	Panorama Road, turn right **(35° 8.784'/-119° 46.423')** To the east, scarps on the San Andreas fault are the first topographic highs between here and the Temblor Range. The Panorama Hills, located behind the scarps are composed of non-marine sediments of the Paso Robles Fm., less than 2 million years old that have been uplifted along the fault. To the west, the Washburn Ranch, lies directly below late Oligocene/early Miocene age (20-23 million years old) sandstones of the Caliente Range. The ridge that runs from the Washburn southward to the conical hill is composed primarily of sandstone and volcanic basalt. Although not visible from here, these beds dip down to the southwest and form part of a large syncline that runs along the base of the Caliente Range southward.
36.9	(4.8)	***STOP #9 – Double Scarp & Surface Fault Rupture*** **(35° 11.275'/-119° 44.233')** Pull out and park in the large clearing to the right. At this point a 400-meter hike around the ridge to the south brings you to a double scarp feature. The wide trough is unique with the higher Elkhorn scarp on the east and another younger scarplet to the west with a sag or graben (down thrown block) structure located between. Immediately adjacent to the east of the younger scarplet you'll notice a shallow trench like feature that almost has the appearance of being man-made. It is not, what you are actually looking at is the remnants of surface fault rupture from the 1857 Fort Tejon Earthquake. It is estimated that the displacement along the fault here on the Carrizo Plain was as much as 30 feet as a result of this event. Turn right out of parking area and continue east on Panorama Road.
38.5	(1.6)	Turn left onto Elkhorn Road **(35° 11.938'/-119° 43.285'**)
41.4	(2.9)	Dirt track, turn left **(35° 13.848'/-119° 45.138'**)
41.9	(0.5)	Water tank **(35° 13.532'/-119° 45.397'**)
42.4	(0.5)	Boiler tank. At this point there is a wonderful view of a line of scarps running from northwest to southeast for several miles forming porpoise structures, in reference to the similarity of how a porpoise swims through the ocean **(35° 13.291'/-119° 45.734'**)

GEO-TOUR ROAD LOG (CONTINUED)

Miles	*(delta)*	
43.0	(0.6)	***STOP #10 – Scarp City*** **(35° 13.058'/-119° 46.297')** Here the road crosses the fault. It is delineated by scarps in both directions and a beheaded stream channel with two right-lateral offsets next to the road. There are two parallel fault strands here about 50 yards apart, part of a right step-over.
43.9	(0.9)	Gate on right. Usually closed, but not locked. Pass through and leave gate as you found it. Immediately turn right to the northwest. Good view of the Temblor Range to the east with tan over gray bedding. **(35° 12.278'/-119° 46.410')**
45.9	(2.0)	Fence and gate. usually closed. Pass through and leave gate as you found it. **(35° 13.795'/-119° 47.468')**
46.7	(0.8)	Junction with Elkhorn Road, turn left. **(35° 14.377'/-119° 47.873')**
49.3	(2.6)	***STOP #11 – Wallace Creek*** **(35° 16.045'/-119° 49.635')** Although Wallace Creek is not the only creek that has been offset by the San Andreas fault, it is the most spectacular. Wallace Creek is a small stream, draining into Soda Lake, that remains dry most of the year. It drains perpendicular to the San Andreas fault, and the creek bed is currently offset by 425ft (130m) due to the movement of the fault. Researchers have determined via carbon dating of sediments deposited just before Wallace Creek cut down that the currently offset channel is 3700 years old. Two other older creek beds lay 1,560 and 1,310ft northwest along the San Andreas fault. The first creek bed was created around 13,000 years ago on a large alluvial fan. The second bed was created about 11,000 years ago. Knowing the total offset of Wallace Creek (130 m) and the age of the channel, an average rate of motion can be easily determined, giving a rate of 35 mm/yr. This is consistent with GPS and other geodetic data measuring the relative motions of monuments spanning this portion of the San Andreas fault over the last few decades. The monuments are separated by tens of kilometers and measure the broad warping that loads up the fault and which is released abruptly during an earthquake. Thus, the strain accumulation (measured by geodesy) and the strain release (measured by the offset channel) along San Andreas fault are similar at about 35 mm/yr at Wallace Creek. We do not see any motion immediately at the ground surface at Wallace Creek because the San Andreas fault on the Carrizo plain is locked. The San Andreas fault only accommodates about two-thirds of the total relative plate motion between the Pacific and North American Plates. The last ground-rupturing earthquake at Wallace Creek occurred in 1857.

GEO-TOUR ROAD LOG (CONTINUED)

Miles ***(delta)***

49.3 (2.6) ***STOP #11 – Wallace Creek (Continued)*** Thus, over 150 years later, the portion of the San Andreas fault below Wallace Creek has accumulated over 5.25 meters of slip not yet released. Early investigations of the topography and stratigraphy along the San Andreas Fault near Wallace Creek determined that the offset in 1857 (and prior earthquakes) was 8-9 m, which combined with the 35 mm/yr slip rate gave an earthquake recurrence interval of about 250 years. However, looking more closely at high resolution topography and aerial photography around Wallace Creek found evidence that slip in the last earthquakes was 5-6 m or less and thus the return period for earthquakes is closer to 140 years or less and similar to what has been determined for the dates of recent earthquakes and to the elapsed time since the 1857 earthquake. Take the short hike to the offset creek. There is an interruptive field guide located in the back of this guidebook. It will take about 45-minutes to do the entire walking tour of five stops. Turn right out of parking area and continue northwest on Elkhorn Road.

49.6 (0.3) Modern Wallace Creek crossing. **(35° 16.192'/-119° 49.807')**

49.7 (0.1) Ancient Wallace Creek crossing. The fault is about 400 yards to the right at the base of the scarp. **(35° 16.299'/-119° 49.925')**

50.7 (1.0) Junction with Simmler Road. Turn left **(35° 17.001'/-119° 50.406')**

54.7 (4.0) ***STOP #12 – "The Big Berm"*** **(35° 13.590'/-119° 51.177')**. Examine the hypersaline environment of Soda Lake. The crust of Soda Lake is composed of about 80% anhydrous sodium sulfate (Na_2SO_4) 10% sodium chloride (NaCl – table salt) and 10% miscellaneous salts. Soda Lake is the only closed basin in the Southern Coast Ranges. A lack of old shorelines indicates that, unlike other alkali lakes in the west, Soda Lake in not a remnant of a larger Pleistocene ice age lake. Instead the plain one held a meandering river. Over the last 1-3 million years, this river flowed southward toward Maricopa. Subsequent uplift and tectonic deformation associated with the San Andreas fault reversed the flow of this river to the north, into the Salinas River watershed. However, continued uplift to the north ultimately defeated the river and blocked the outlet, resulting formation of Soda Lake. A fresh to brackish water lake probably persisted through much of the Pleistocene when California was wetter and cooler than now. Diminished late Holocene precipitation led to shrinkage of the ancestral lake and associated increased salinity.

GEO-TOUR ROAD LOG (CONTINUED)

Miles	*(delta)*	
54.7	(3.0)	***STOP #12 – "The Big Berm" (Continued)*** The Soda Lake complex consists of two large basins (separated by "The Big Berm") and at least 130 smaller pans. The large L-shaped northern basin is about 4mi² in area. The remaining basins, including both those that feed the northern basin and those that have no surface outlets, comprise an area of about 1.9mi². About 30% of the basin is to the north of the lake and 70% is to the south. Water levels in the basins rise and fall seasonally. Rainfall on the Carrizo Plain is only about 7 to 8-inches in an average year but is higher on the surrounding mountains. Following exceptionally wet winters, typically El Niño years, the large northern and southern basins do not evaporate completely, although the water retreats toward the center of the basin leaving a salt crust up to 8-inches thick. From the 1880s to the 1940s, a number of enterprises intermittently mined salt and sodium sulfate. In the early 1900s, a narrow gauge railroad was used to haul salt to a refining plant on the south side of the lake. Then it was hauled to the railway at McKittrick. Sodium sulfate is used in the manufacture of textiles, soap, glass and paper. Soda Lake is one of the largest alkali wetlands remaining in a natural condition in California. It supports fairy and brine shrimp, as well as migratory and nesting birds. The Big Berm and the other low hills surrounding Soda Lake consist of clay dunes. Clay dune sediment is produced by salt efflorescence which, aggregates clay particles. The aggregates form fine sand size particles and are easily transported by wind. When the particles are deposited above lake level the salt is readily leached. The resulting mass is approximately 76% by weight clay and silt and 24% fine sand. The sand fraction consists of rounded gypsum ($CaSO_4 \cdot 2H_2O$) & quartz and plant debris. Clay dunes are very rare and only typically occur downwind on deflated pans in hypersaline environments. Most of the large and small pans are fringed by clay dunes. Continue west on Simmler Road.
56.7	(2.0)	Junction with Simmler Road. Turn left **(35° 12.108'/-119° 51.455'**)
57.5	(0.8)	Junction with road to Goodwin Education Center **(35° 11.419'/-119° 51.282'**). Tour the Goodwin Education Center and patronize the book store. You are now qualified to present a lecture to other tourists present on the geology of the San Andreas fault on the Carrizo Plain.

END OF LOG

THE SAN ANDREAS FAULT ON CARRIZO PLAIN

The Geological Society of America
Field Guide 32
2013

Field trip guide: New views on the evolution of the San Andreas fault zone in central California and the Carrizo Plain

Sinan O. Akçiz*
University of California–Irvine, Program in Public Health, Irvine, California 92697, USA

J Ramón Arrowsmith*
Arizona State University, School of Earth and Space Exploration, Tempe, Arizona 85287, USA

ABSTRACT

The San Andreas fault is arguably the best-studied strike-slip fault in the world, and our understanding of its evolution continues to improve as new data become available. This trip will take the participants to a selection of some classical as well as some new sites that will highlight a revised understanding of the San Andreas fault's recent history based on our geomorphological, paleoseismologic, and paleoclimate investigations.

OVERVIEW

On this three-day field trip, we will examine the evidence for offset along the San Andreas fault as expressed over different temporal and spatial scales. At the largest scales, we will discuss the ~320-km long-term offset of the Pinnacles-Neenach volcanic complex with a stop at Pinnacles National Monument. Working along the San Andreas fault to the southeast, we will traverse a fundamental change in strain release from the creeping section through Parkfield to the Cholame and Carrizo sections. At Parkfield, we will discuss the history of repeated M6 earthquakes and the significant monitoring instrumentation available that provides a high-resolution view of fault zone behavior and the earthquake cycle. A highlight of the trip is the examination of classic localities in the Carrizo Plain, where we will review new results from Wallace Creek, Bidart Fan, the Dragon's Back pressure ridge, and the Elkhorn Hills. We will present recent results of paleoclimate research from Soda Lake at the sink of the Carrizo Plain and their constraints on the formation of offset landforms.

E-mails: *sakciz@uci.edu; ramon.arrowsmith@asu.edu.

Akçiz, S.O., and Arrowsmith, J.R., 2013, Field trip guide: New views on the evolution of the San Andreas fault zone in central California and the Carrizo Plain, *in* Putirka, K., ed., Geologic Excursions from Fresno, California, and the Central Valley: A Tour of California's Iconic Geology: Geological Society of America Field Guide 32, p. 1–12, doi:10.1130/2013.0032(01).

INFORMATION FOR FIELD TRIP STOPS ALONG THE SOUTH-CENTRAL SAN ANDREAS FAULT

Pinnacles National Monument (36° 28′ 51.08″N, 121° 10′ 53.50″W)

The spectacular outcrops of volcanic rock that comprise the Pinnacles are key indicators of the long-term offset along the San Andreas fault. The Pinnacles-Neenach volcanic complex correlation (Matthews, 1976; Sims, 1993) along with the stratigraphic ties (Graham et al., 1989), and the basement offsets measure the long-term offsets along the San Andreas fault.

Parkfield (35° 53′ 42.52″N, 120° 26′ 05.17″W)

The Parkfield section of the San Andreas fault spans the transition from creeping to locked (Fig. 1; e.g., Allen, 1968). It is well known for a series of M6 earthquakes—the most recent being the 28 September 2004 earthquake (see special issue edited by Harris and Arrowsmith, 2006)—which were the subject of intense research (see Roeloffs, 2000, for a review). In addition, the San Andreas Fault Observatory at Depth (SAFOD) penetrated and sampled the active fault surfaces at a depth of 3 km (e.g., Zoback et al., 2011).

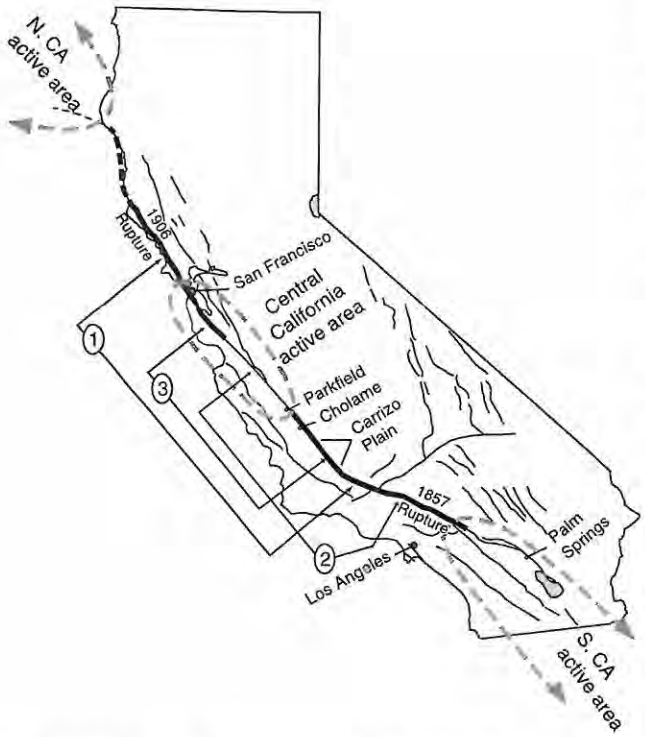

Figure 1. Areas of contrasting behavior along the San Andreas fault (modified from Allen, 1968). One of the first order features of the active fault system is the contrast between seismically quiet and active areas (which include active fault creep in central and southern California). Long-term offsets along the San Andres fault are also shown. (1) Basement offset of ~600 km, (2) Pinacles-Neenach offset (~315 km since 23.5 Ma), and (3) paleobathymetry offset (~320–330 km, post–late Oligocene–early Miocene; 320-325 km, post–early Miocene).

At the Parkfield bridge (Fig. 2), we review evidence for offset along the San Andreas fault over historic to millennial timescales (Toké and Arrowsmith, 2006; Toké et al., 2011) as well as effects of the 2004 earthquake (Toké et al., 2006). The Miller's Field site just southeast of the Parkfield bridge was the study site for the work presented by Toké et al., 2006, 2011). There, a right laterally offset channel yields a late Holocene slip rate of 26.2 +6.4/–4.3 mm/yr (1σ) for the main trace of the San Andreas fault. This is the first well-documented geologic slip rate between the Carrizo and creeping sections of the San Andreas fault. The rate is lower than Holocene measurements along the Carrizo Plain and rates implied by far-field geodetic measurements (~35 mm/yr). However, the rate is consistent with historical slip rates, measured to the northwest, along the creeping section of the San Andreas fault (<30 mm/yr). The paleoseismic exposures at the Miller's Field site reveal a pervasive fabric of clay shear bands, oriented clockwise oblique to the San Andreas fault strike and extending into the uppermost stratigraphy. This fabric is consistent with dextral aseismic creep and observations of surface slip from the 28 September 2004 M6 Parkfield earthquake. Together, this slip rate and deformation fabric suggest that the historically observed fault-slip behavior along the Parkfield section has persisted for at least a millennium, and that significant slip ~~is~~ accommodated by structures in a zone beyond the main fault trace (paragraph text modified slightly from Toké et al., 2011).

Carrizo Plain

The Carrizo Plain area, situated in the southeastern California Coast Ranges (Fig. 3), is the premier example of the San Andreas fault system in California. The area has long been regarded as a site of world-class examples of strike-slip faulting. The fault follows the northeastern side of the plain and all along it are offset, beheaded, and abandoned drainages that reflect that recent strike-slip motion. See Arrowsmith (1995) for a review of early research in the area (http://activetectonics.la.asu.edu/carrizo/cargeo_full.html). Figure 3 shows a number of stops which are described below.

Carrizo Plain Stop 1. Overview of Carrizo Plain from Big Berm of Soda Lake (35° 13′ 16.11″N, 119° 51′ 16.68″W)

The purpose of this stop is to review regional geology and geologic history and tectonic history of the San Andreas fault.

The Carrizo Plain is the only closed basin in California's southern Coast Ranges and records both climate and tectonic activity. The Plio-Pleistocene Paso Robles formation that underlies the basin indicates drainage from the Carrizo once reached Monterey Bay through the Salinas River. Alluvial fans spreading into the Carrizo from the Temblor Range are cut by the San

Figure 2. Oblique aerial photograph of Parkfield area. Parkfield bridge is just to the right (northwest) of Miller's Field. Carr Hill is headquarters for significant U.S. Geological Survey monitoring activity. Trace of San Andreas fault is dashed. View is to the southwest.

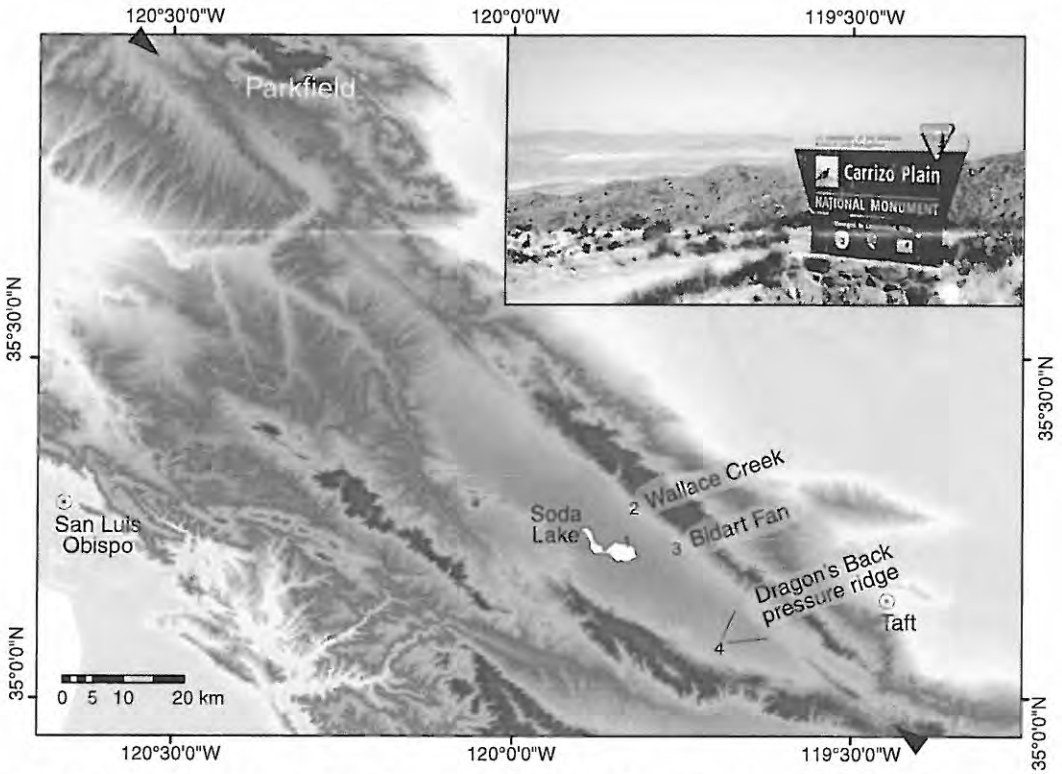

Figure 3. Digital topographic map (based on GTOPO 30 data) of the region shows field trip stops at (1) Soda Lake, (2) Wallace Creek along the San Andreas fault, (3) Bidart area, and (4) the Dragon's Back pressure ridge and northern Elkhorn Hills overview. Inset photograph shows a view of the Carrizo National Monument from the Temblor Ranges. View is to the NW.

Andreas fault. Warping of the plain associated with the fault system and tens of meters of relative uplift on the southwestern side of the basin may have severed the connection to the Salinas. Extensive clay dune remnants on the northeastern and eastern sides of the main basin and a deeply embayed southwestern shoreline are also consistent with southwest-directed tectonic tilting of the lake floor (~1 m/km) during the Holocene. Luminescence and radiocarbon dates obtained during ~~previous~~ investigations of the lacustrine and clay dune deposits accumulated in the basin have indicated a maximum age of ~10 ka for the lake. These dates and the absence of identifiable strand lines led to the conclusion that drainage from the Carrizo remained open until approximately the end of the Younger Dryas. Two exploratory core sites were sampled in May 2005. The first site is on the dry lake flat of Soda Lake's northern basin. This site was chosen to test the thickness of the lacustrine sediment by reaching coarse-grained alluvial deposits. The sediment was cored and augured to a depth of ~14 m (the limit for the equipment) without penetrating the lacustrine clay. The second core was taken in the swale between the outermost clay dune and the next lower dune, both of which fringed the retreating lake. Approximately 6 m of essentially featureless clay-rich sediment were retrieved. The top of the outer dune ridge is ~8 m above the core site and the next dune is ~4 m higher than the swale, so 10–14 m of clay dune sediment accumulated here. Taken together, the material retrieved from the cores is interpreted as evidence that the "proto–Soda Lake" that occupied the Carrizo Plain was much larger than had been suspected previously (Fig. 4), that external drainage was probably lost during the Pleistocene (which has implications for the deformation) rate, and (on the basis on an OSL date obtained from the top of the outermost dune) that the lake became saline enough for clay dunes to form before 16.7 ka ago (paragraph text modified slightly from Rhodes et al., 2005).

Carrizo Plain Stop 2. Wallace Creek Area (35° 16′ 16.04″N, 119° 49′ 37.85″W)

One of the most important reaches of the San Andreas fault is that which traverses the Carrizo Plain in south-central California. The record of faulting is of fundamental importance for testing models of earthquake physics and for constraining the significant earthquake hazard faced by southern California. The offset stream channels at Wallace Creek represent the classic measure of the millennial timescale rate of motion (released in great earthquakes).

In our recent work along the San Andreas fault at the Bidart site (~5 km southeast of Wallace Creek), we have found that recent earthquakes have occurred roughly every century concluding with the most recent in 1857 (Akçiz et al., 2009, 2010).

Measures of offset in recent earthquakes are ~5 m (Zielke et al., 2010). When combined, those ages and offsets (along with those made by Liu-Zeng et al., 2006, near Wallace Creek) yield 50–70 mm/yr short-term slip rates. We have proposed that the offset in the prior earthquakes is not constant, and that some offsets may have been smaller than 5 m (Akçiz et al., 2010; Grant Ludwig et al., 2010), and that may address the apparent inconsistency between the different rates of motion along the San Andreas fault. These results have important implications for earthquake hazards in California.

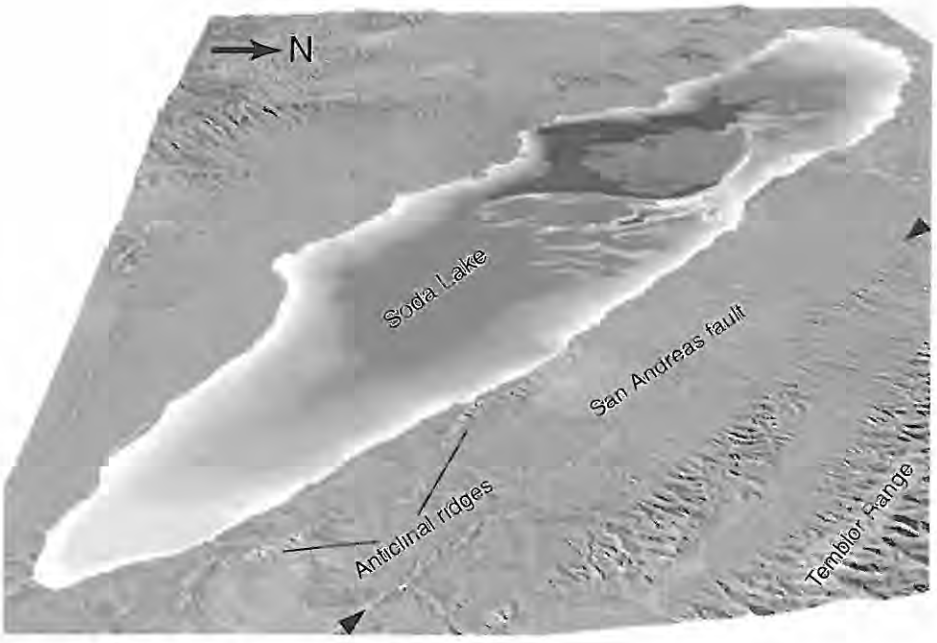

Figure 4. Overview of the Carrizo Plain showing reconstructed lake level for Soda Lake at 595 m (18 m maximum depth) water surface elevation at 16.7 ka (from Rhodes et al., 2005). Black arrows mark the location of the San Andreas fault.

At this classic location, we will review the existing data and share the results of our recent paleoseismic investigations at Wallace Creek (Fig. 5).

Optional Hike

The section of the San Andreas fault in the Carrizo Plain between Wallace Creek and Phelan Creeks is one of the most picturesque strike-slip fault sections anywhere in the world (Figs. 6 and 7). This short hike will give us an opportunity to see these spectacularly preserved geomorphological features and discuss the results of published and unpublished paleoseismic data from this stretch of the fault (e.g., Grant and Sieh, 1993, and Sims, 1994). The Wallace Creek to Phelan Creeks walk provides an overview of stream channels offset over the last 13,250 yr. The prominent features include a 350 m offset, the current 135 m and 3700 yr old offset which is used to indicate the 35 mm/yr Holocene slip rate along the San Andreas fault (Sieh and Jahns, 1984), and numerous 5–20 m offsets developed in the last several earthquakes including the most recent: the M7.8 1857 Fort Tejon earthquake (Sieh, 1978; Liu-Zeng et al., 2006; Zielke et al., 2010, 2012).

Figure 5. 2011 trench excavations along the edge of the modern Wallace Creek channel.

Carrizo Plain Stop 3. Channel Sieh 31 (35° 14′ 21.70″N, 119° 47′ 38.79″W)

Channel "Sieh 31" was identified by Sieh (1978) who measured an offset of 9 m. This is ~3 m more than the best offset estimates based on back-slipping of LiDAR topographic data (Zielke et al., 2010, 2012; see Figs. 8 and 9). This location will provide a great opportunity to investigate the morphology of the channel and to discuss (1) the discrepancy between different measurements and (2) the common criticism of geomorphic offsets as reliable coseismic displacement indicators. This discrepancy highlights the importance of using paleoseismic excavation to confirm results from similar geomorphic studies. Our 3D trenching results from a nearby channel deflected by 5 m along the trace of the San Andreas fault will also be discussed. We will not be visiting ~~this~~ deflected channel because, unlike the stops, it is on private property.

Carrizo Plain Stop 4. Bidart Fault Scarp (35° 14′ 27.58″N, 119° 47′ 22.78″W)

A short walk from the previous stop we will have a chance to investigate the southern termination of a long, linear structural anomaly subparallel to the main trace of the San Andreas fault between Wallace Creek and the Bidart Fan (Figs. 8 and 10). At this location, the newly named Bidart fault cuts late Holocene sedimentary deposits of the Bidart Fan. Two trenches opened in summer 2012 provide earthquake evidence and radiocarbon age control. Two nearby channels are offset and/or deflected along the trace of the fault scarp.

The Bidart Fan site is the only paleoseismic site along the Carrizo section of the San Andreas fault that has provided age constraints to the earthquakes that ruptured this section of the fault (Fig. 8; Grant and Sieh, 1994). Our recent paleoseismologic investigations at the Bidart Fan site indicate that the southern San Andreas fault in the Carrizo Plain has ruptured, on average, every 88 yr (45–144 yr for individual intervals) since ~A.D. 1350 (Akçiz et al., 2009, 2010). Preliminary results of our paleoseismic investigation at the Bidart scarp site will be compared to and contrasted with the rich paleoseismic data from the Bidart Fan site.

Carrizo Plain Stop 5. Dragon's Back Pressure Ridge (35° 05′ 49.35″N, 119° 37′ 33.69″W—this is the crest; note that good overviews can be had from the Soda Lake Road to the southwest)

We used high-resolution topography, geomorphic mapping of active surface processes, and geologic mapping to study the topographic and erosional response of small drainage basins to rock uplift along the Dragon's Back pressure ridge along the San Andreas fault in the Carrizo Plain (Fig. 11). We ~~infer~~ the history of deformation experienced by small drainage basins formed in poorly consolidated sedimentary rocks. A space-for-time substitution directly images the erosional and topographic responses to deformation. Progressive deformation and rock uplift are accompanied by increases in channel steepness and basin relief.

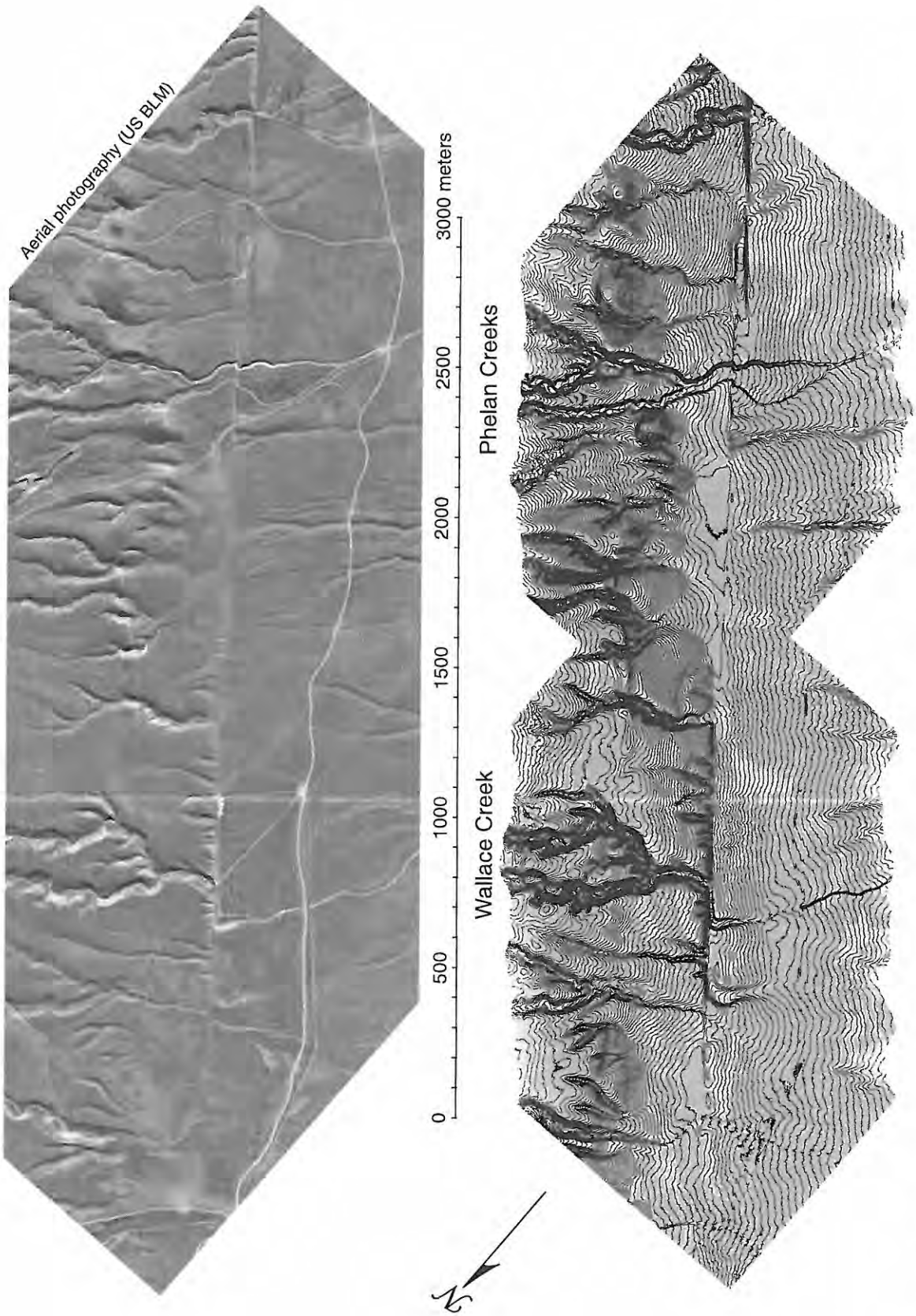

Figure 6. Aerial photography and 1 m contour map along the San Andreas fault between Wallace Creek and Phelan Creeks (see field trip guide by Sieh and Wallace, 1987). Topographic data are from the B4 project (Bevis et al., 2005).

Figure 7. View along the San Andreas fault toward the northwest near channel Sieh 31.

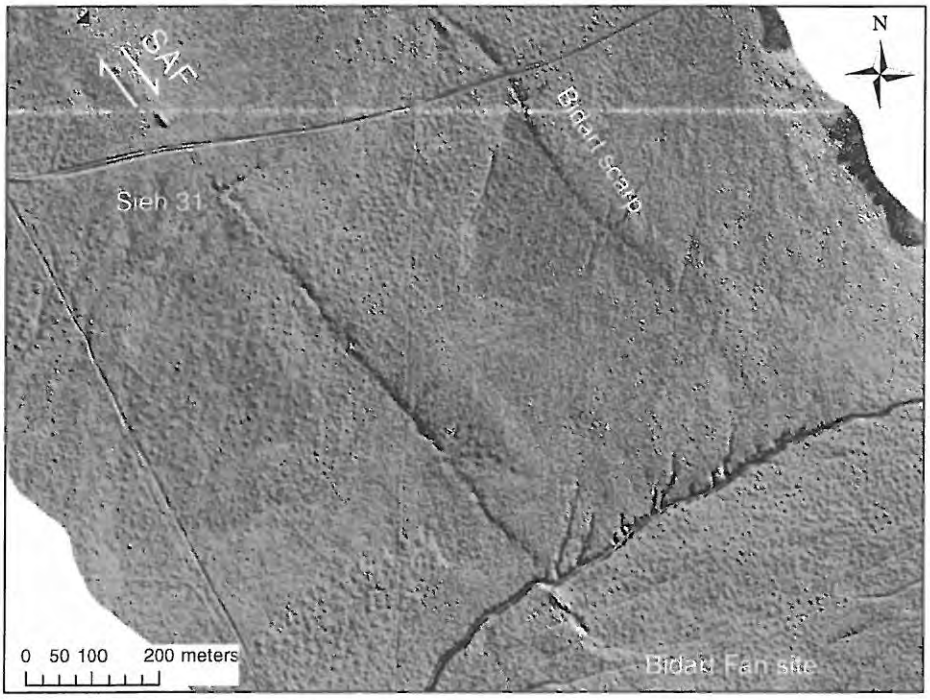

Figure 8. Hillshade topography along the San Andreas fault (SAF) showing diverse tectonic landforms for stop 3: Sieh 31 channel and Bidart scarp, as well as the area of the Bidart Fan site (Akçiz et al., 2009. 2010). B4 topographic data (Bevis et al., 2005).

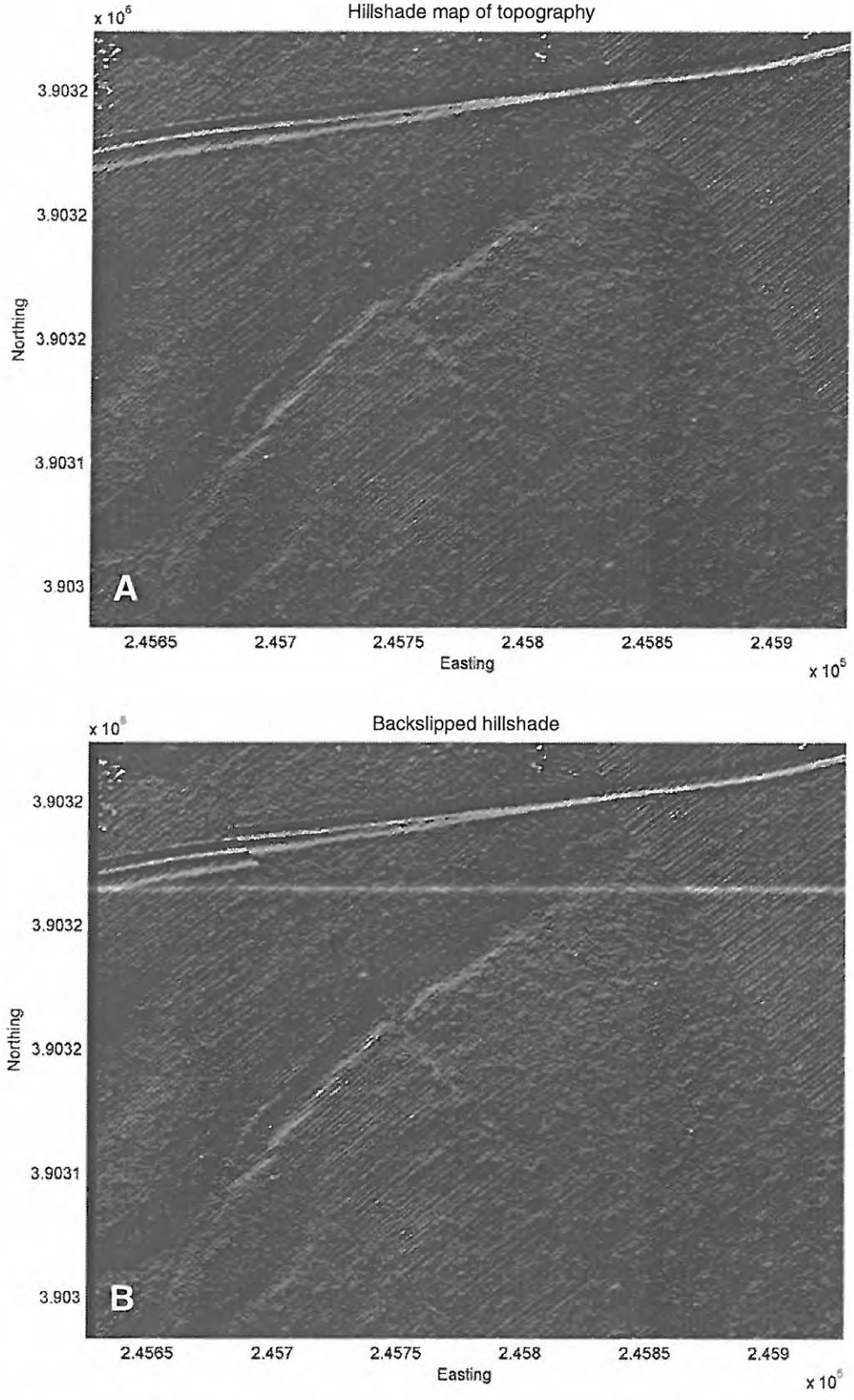

Figure 9. Current (top) and 6.0 m back-slipped shaded relief topography (bottom) of site Sieh 31 (Zielke et al., 2012; Zielke and Arrowsmith. 2012). B4 topographic data (Bevis et al., 2005).

Figure 10. Photo looking SE along the trace of the Bidart fault scarp, prior to excavation.

As uplift ceases, channel concavity rapidly increases, causing channels to undercut hillslopes—this undercutting promotes the consumption of hillslopes by landsliding. This undercutting also causes basin relief to be greatest after uplift has stopped. ~~This analysis indicates that~~ channels of the Dragon's Back pressure ridge respond to changes in rock uplift rates over thousands of years, whereas hillslope processes may take more than an order of magnitude longer to adjust to changes in rock uplift rates. Our study directly measures changes in erosional processes due to the initiation and cessation of rock uplift, which can typically only be inferred using numerical models~~, by direct field observations~~. (Paragraph text modified slightly from Hilley and Arrowsmith, 2008. See also Arrowsmith, 1995, and Hilley, 2001.)

Carrizo Plain Stop 6. Sag Ponds near Southern End of the Carrizo Plain (34° 58′ 27.58″N, 119° 27′ 35.93″W)

In this semi-arid climate, closed basins (Fig. 12) are floored by evaporates, muds, and possibly a few tens of cm of hypersaline water. Sag ponds are characteristic landforms of strike-slip fault zones and typically develop from either tectonic depression of a block (hence *sag* pond) or the juxtaposition of topography to produce the basin (see Fig. 7).

This site was photographed and investigated by H.W. Fairbanks and A.C. Lawson in January 1906. They aptly describe the fault zone: "A gentle divide separates the end of the [Carrizo] Plain from a long narrow sink extending along the Rift line toward the southeast.... This sink includes an area 6 miles long and a full 3 miles wide. Several deprest [*sic*] alkali flats, covered with water in the wet season, receive the scanty run off of this dry region. These depressions are several hundred feet wide and are bordered upon opposite sides by quite sharp bluffs, in some places 100 feet high. The phenomena suggest the sinking of long narrow blocks between two walls" (Lawson et al., 1908, p. 42).

ACKNOWLEDGMENTS

We thank Lisa Grant Ludwig, George Hilley, and Dallas Rhodes for many years of collaboration on many of these topics. Without the support of the National Science Foundation, the U.S. Geological Survey, and the Southern California Earthquake Center, we would have been unable to obtain many of the data presented here. The B4 project (http://www.earthsciences.osu.edu/b4) created an unprecedentedly accurate surface model along the San Andreas and San Jacinto faults in southern California that enabled the research and observations reported here. It was supported by the U.S. National Science Foundation and led by Ohio State University and the U.S. Geological Survey. The National Center for Airborne Laser Mapping performed the airborne data acquisition and laser data processing. Optech International generously contributed use of the ALTM3100 laser scanner system. UNAVCO and SCIGN assisted in GPS ground control and continuous high rate GPS data acquisition. A group of volunteers from USGS, UCSD, UCLA, Caltech and private industry, as well as gracious landowners along the fault zones, also made the project possible. The data and processing tools are available for download from http://www.opentopography.org. A special thank you to Keith Putirka for the encouragement to put this guide together.

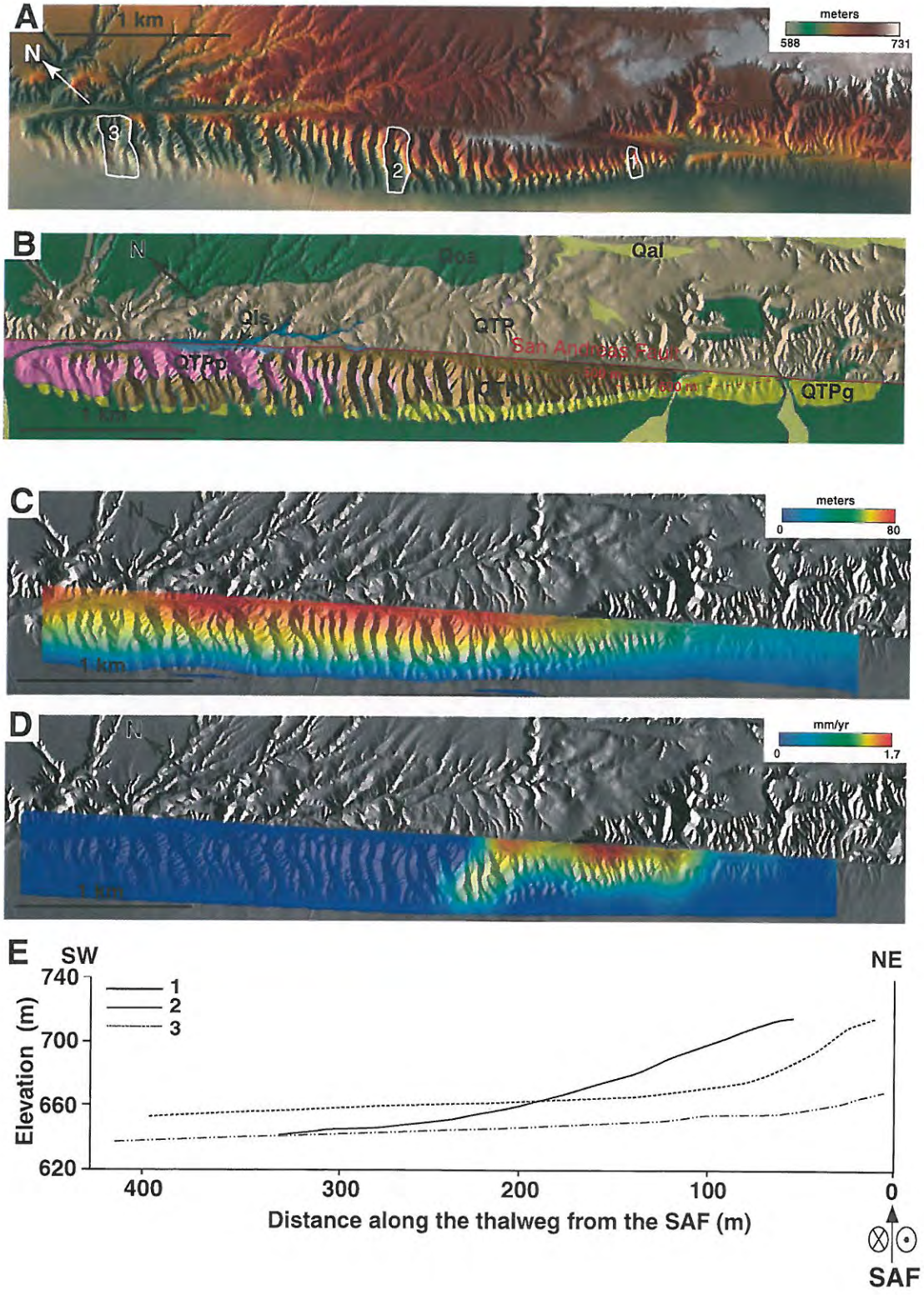
A
1 km
N
meters
588
731
3
2
1
B
N
Qos
Qal
Qls
QTR
San Andreas Fault
QTPp
QTPg
1 km
C
N
meters
0
80
1 km
D
N
mm/yr
0
1.7
1 km
E
SW
NE
740
700
660
620
Elevation (m)
1
2
3
400
300
200
100
0
Distance along the thalweg from the SAF (m)
SAF

Figure 12. Sag pond and fault traces (white) in the southern Carrizo Plain.

Figure 11. Dragon's Back pressure ridge ~~(DBPR)~~ and relatively stationary uplift zone. (A) Airborne Laser Swath Mapping ~~(ALSM)~~ topography (1 m digital elevation model ~~[DEM]~~); (B) geology (modified from Arrowsmith, 1995); (C) total rock uplift inferred from distribution of geologic contacts, assuming initially horizontal contacts; (D) instantaneous rock uplift rate (assuming 33 mm/yr of right-lateral slip along San Andreas fault ~~[SAF]~~); and (E) along-channel profiles of basin numbers referenced in panel A. In B, QTP is undifferentiated Paso Robles Formation; Qoa is Pleistocene alluvium; QTPp, QTPt, QPTg are pink, tan, and gold members of the Paso Robles Formation; Qls indicates landslide deposits; and Qal is young alluvium. Dashed contours in B show inferred location of San Andreas fault at various depths and illustrate shallow offset of San Andreas fault that produces rock uplift within southeastern portion of landform. ~~Inset in B shows location of study area and highlights surrounding features: WC—Wallace Creek, GF—Garlock fault, SB—Santa Barbara, and LA—Los Angeles.~~ Slightly modified from Hilley and Arrowsmith (2008).

REFERENCES CITED

Akçiz, S.O., Grant, L.B., and Arrowsmith, JR., 2009, Revised dates of large earthquakes along the Carrizo section of the San Andreas Fault, California, since A.D. 1310 ± 30: Journal of Geophysical Research, v. 114, B01313, doi:10.1029/2007JB005285.

Akçiz, S.O., Grant Ludwig, L., Arrowsmith, JR., and Zielke, O., 2010, Century-long average time intervals between ruptures of the San Andreas fault in the Carrizo Plain: Geology, v. 38, no. 9, p. 787–790, doi:10.1130/G30995.1.

Allen, C.R., 1968, The tectonic environments of seismically active and inactive areas along the San Andreas fault system, *in* Proceedings of a Conference on Geologic Problems of San Andreas Fault System, Stanford, California, 1967: Stanford University Publications. Geological Sciences. v. 11, p. 70–80.

Arrowsmith. JR., 1995. Coupled Tectonic Deformation and Geomorphic Degradation along the San Andreas Fault Zone [Ph.D. dissertation]: Stanford, California, Stanford University, 346 p.

Bevis, M., Hudnut, K., Sanchez, R., Toth, C., Grejner-Brzezinska, D., Kendrick, E., Caccamise, D., Raleigh, D., Zhou, H., Shan, S., Shindle, W., Yong, A., Harvey, J., Borsa, A., Ayoub, F., Shrestha, R., Carter, B., Sartori, M., Phillips, D., and Coloma, F., 2005, The B4 project: Scanning the San Andreas and San Jacinto fault zones: Eos (Transactions, American Geophysical Union), v. 86, no. 52, Fall Meeting Supplement, abstract H34B-01.

Graham, S.A., Stanley, R.G., Bent, J.V., and Carter, J.B., 1989, Oligocene and Miocene paleogeography of central California and displacement along the San Andreas fault: Geological Society of America Bulletin, v. 101, no. 7, p. 11–30, doi:10.1130/0016-7606(1989)101<0711:OAMPOC>2.3.CO;2.

Grant, L.B., and Sieh, K.E., 1993, Stratigraphic evidence for seven meters of dextral slip on the San Andreas fault during the 1857 earthquake in the Carrizo Plain: Bulletin of the Seismological Society of America. v. 83, no. 3, p. 619–634.

Grant. L.B., and Sieh. K.E., 1994, Paleoseismic evidence of clustered earthquakes on the San Andreas fault in the Carrizo Plain, California: Journal of Geophysical Research, v. 99, no. B4, p. 6819–6841, doi:10.1029/94JB00125.

Grant Ludwig, L., Akciz, S.O., Noriega, G.N., Zielke, O., and Arrowsmith, JR., 2010, Climate modulated channel incision and rupture history of the San Andreas fault in the Carrizo Plain: Science, v. 327, p. 1117–1119, doi:10.1126/science.1182837.

Harris, R.A., and Arrowsmith, JR., 2006, Introduction to the Special Issue on the 2004 Parkfield Earthquake and the Parkfield Earthquake Prediction

Experiment: Bulletin of the Seismological Society of America, v. 96, no. 4B, p. S1–S10, doi:10.1785/0120050831.

Hilley, G.E., 2001, Landscape Development of Tectonically Active Areas [Ph.D. dissertation]: Tempe, Arizona State University, 192 p.

Hilley, G.E., and Arrowsmith, JR., 2008, Geomorphic response to uplift along the Dragon's Back pressure ridge, Carrizo Plain, California: Geology, v. 36, no. 5, p. 367–370, doi:10.1130/G24517A.1.

Lawson, A.C., et al., 1908, Report of the Earthquake Investigation Commission upon the California Earthquake of April 18, 1906: Carnegie Institution of Washington, D.C., 2 vols.

Liu-Zeng, J., Klinger, Y., Sieh, K., Rubin, C., and Seitz, G., 2006, Serial ruptures of San Andreas fault, Carrizo Plain, California, revealed by three-dimensional excavations: Journal of Geophysical Research, v. 111, B02306, doi:10.1029/2004JB003601.

Matthews, V.I., 1976, Correlation of Pinnacles and Neenach volcanic formations and their bearing on San Andreas fault problem: American Association of Petroleum Geologists Bulletin, v. 60, p. 2128–2141.

Rhodes, D.D., Negrini, R.M., Arrowsmith, R., and Noriega, G., 2005, New evidence for the age and extent of lake deposits and the role of tectonic warping in late Pleistocene drainage reorganization, Carrizo Plain, California: Geological Society of America Abstracts with Programs, v. 37, no. 7, p. 225.

Roeloffs, E., 2000, The Parkfield, California earthquake experiment: An update in 2000: Current Science, v. 79, no. 9, p. 1226–1236.

Sieh, K., 1978, Slip along the San Andreas fault associated with the great 1857 earthquake: Bulletin of the Seismological Society of America, v. 68, no. 5, p. 1421–1448.

Sieh, K., and Jahns, R.H., 1984, Holocene activity of the San Andreas fault at Wallace Creek, California: Geological Society of America Bulletin, v. 95, p. 883–896, doi:10.1130/0016-7606(1984)95<883:HAOTSA>2.0.CO;2.

Sieh, K., and Wallace, R.E., 1987, The San Andreas Fault at Wallace Creek, San Luis Obispo County, California, *in* Hill, M.L., ed., Cordilleran Section of the Geological Society of America: Boulder, Colorado, Geological Society of America Centennial Field Guide 1, p. 233–238.

Sims, J.D., 1993, Chronology of displacement on the San Andreas fault in central California: evidence from reversed positions of exotic rock bodies near Parkfield, California, *in* Powell, R.E., Weldon, R.J., II, and Matti, J.C., eds., The San Andreas Fault System: Displacement, Palinspastic Reconstruction, and Geologic Evolution: Geological Society of America Memoir 178, p. 231–256.

Sims, J.D., 1994, Stream channel offset and abandonment and a 200-year average recurrence interval of earthquakes on the San Andreas fault at Phelan Creek, Carrizo Plain, California, *in* Proceedings of the Workshop on Paleoseismology: U.S. Geological Survey Open-File Report 94-568, 210 p.

Toké, N.A., and Arrowsmith, JR., 2006, Reassessment of a slip budget along the Parkfield segment of the San Andreas fault: Bulletin of the Seismological Society of America, v. 96, no. 4B, p. S339–S348, doi:10.1785/0120050829.

Toké, N.A., Arrowsmith, JR., Young, J.J., and Crosby, C., 2006, Paleoseismic and postseismic observations of surface slip along the Parkfield segment of the San Andreas Fault: Bulletin of the Seismological Society of America, v. 96, no. 4B, p. S221–S238, doi:10.1785/0120050809.

Toké, N.A., Arrowsmith, JR., Rymer, M.J., Landgraf, A., Haddad, D.E., Busch, M.M., Coyan, J., and Hannah, A., 2011, Late Holocene slip rate of the San Andreas fault and its accommodation by creep and M6 earthquakes at Parkfield: Geology, v. 39, no. 3, p. 243–246, doi:10.1130/G31498.1.

Zielke, O., Arrowsmith, JR., Grant Ludwig, L., and Akciz, S.O., 2010, Slip in the 1857 and earlier large earthquakes along the Carrizo Plain, San Andreas Fault: Science, doi:10.1126/science.1182781.

Zielke, O., and Arrowsmith, JR., 2012, LaDiCaoz and LiDARimager—MATLAB GUIs for LiDAR data handling and lateral displacement measurement: Geosphere, v. 8, no. 1, p. 206–221, doi:10.1130/GES00686.1.

Zielke, O., Arrowsmith, JR., Grant Ludwig, L., and Akciz, S.O., 2012, High resolution topography-derived offsets along the 1857 Fort Tejon earthquake rupture trace, San Andreas Fault: Bulletin of the Seismological Society of America, v. 102, no. 3, p. 1135–1154, doi:10.1785/0120110230.

Zoback, M.D., Hickman, S., and Ellsworth, W., and the SAFOD Science Team, 2011, Scientific drilling into the San Andreas Fault Zone—An overview of SAFOD's first five years: Scientific Drilling, no. 11, p. 14–28, doi:10.2204/iodp.sd.11.02.2011.

MANUSCRIPT ACCEPTED BY THE SOCIETY 28 FEBRUARY 2013

Geomorphology xxx (2009) xxx–xxx

Contents lists available at ScienceDirect

Geomorphology

journal homepage: www.elsevier.com/locate/geomorph

Tectonic geomorphology of the San Andreas Fault zone from high resolution topography: An example from the Cholame segment

J Ramón Arrowsmith *, Olaf Zielke

School of Earth and Space Exploration, Arizona State University, Tempe, AZ 85287, USA

ARTICLE INFO

Article history:
Accepted 8 January 2009
Available online xxxx

Keywords:
Tectonic geomorphology
LiDAR
San Andreas Fault
Digital Elevation Models

ABSTRACT

High resolution topographic data along fault zones are important aids in the delineation of recently active breaks. A 15 km-long portion of the south-central San Andreas Fault (SAF) along the southern Cholame segment contains well preserved tectonic landforms such as benches, troughs, scarps, and aligned ridges that indicate recurring earthquake slip. Recently acquired LiDAR topographic data along the entire southern SAF ("B4" project) have shot densities of 3–4 m^{-2}. Computed from the LiDAR returns, Digital Elevation Models (DEMs) of 0.25 to 0.5 m resolution using local binning with inverse distance weighting and 0.8 m or larger search radii depict the tectonic landforms at paleoseismic sites well enough to assess them confidently. Mapping of recently active breaks using a LiDAR-only based approach compares well with aerial photographic and field based methods. The fault zone varies in width from meters to nearly 1 km and is comprised of numerous en echelon meter to kilometer-length overlapping sub parallel fault surfaces bounding differentially moving blocks that elongate parallel to the SAF. The semantic variations of what constitutes "active" and the importance of secondary traces influence the breadth and complexity of the resulting fault trace maps.

1. Introduction

The south central San Andreas Fault (SAF; Fig. 1) is manifest at the surface by some of the most well preserved tectonic geomorphology at 10s to 1000s of meter scale in the world (Fig. 2; e.g., Wallace, 1975; Wallace and Schulz, 1983; Wallace, 1991). The troughs, ridges, sags, and offset channels along the zone have developed by the interaction of repeated slip along subparallel discontinuous roughly co-planar fault surfaces bounding the elongate blocks of the fault zone and the fluvial and hillslope processes operating on the surface (over at least the Holocene; Bryant and Hart, 2007). The features indicate a valuable record of the structural geology of the upper few kilometers of the fault zone (e.g., Lawson, 1908; Wallace, 1991; Arrowsmith, 2007) and of the history of earthquakes that have occurred along it over the last centuries to millennia (e.g., Grant and Sieh, 1994). These features are indicative of where the next earthquake is most likely to slip.

Characterizing the tectonic geomorphology of the SAF fault zone is valuable for numerous reasons. The geometry and motions of the blocks that comprise the upper few km of the fault zone inform studies of rupture dynamics, fluid flow along fault zones, fault zone strength, and evolution of fault zone fabrics (e.g., Scholz, 1991). Using landforms as markers of the horizontal and vertical motions along and across the fault zone, coupled with Quaternary geochronology, provides a measure of the strain release rate at centennial to millennial time scales—a valuable bridge between geologic strain release rates at million year time scales and the geodetically measured strain accumulation rates at decadal time scales (e.g., Sieh and Jahns, 1984; Noriega et al., 2006). The meter scale geomorphology of the fault zone guides siting and interpretation of paleoseismic sites (e.g., McCalpin, 1996). Locating the excavations must be done by interpolation between landforms indicative of the active fault location. The stratigraphy exposed in the trenches is directly related to the site geomorphology. The map geometry of the fault traces indicates the distribution of fracturing to be expected in the trench exposures and whether or not the excavations span the entire fault zone. Information on the timing and slip per event in earthquakes that comes from paleoseismic investigations is an essential ingredient in earthquake rupture forecasts (e.g., 2007 Working Group on California Earthquake Probabilities, 2008). Finally, delineating sufficiently active and well defined fault zones is of practical value for anticipating ground rupture hazard for structures (e.g., Bryant and Hart, 2007).

Airborne Laser Swath Mapping (ALSM) and LiDAR-derived measurements of topography have recently been deployed for the extensive mapping of fault zone topography at unprecedented detail and coverage (e.g., Haugerud et al., 2003; Sherrod et al., 2004; Bevis et al., 2005; Kondo et al., 2008). These data are at the appropriate scale (meters) and accuracy (decimeters) to provide useful measurements of the fine features that record repeated earthquakes in the landscape. Typically, fault zones in the USA are mapped using USGS Quadrangle topographic maps and 10 or 30 m DEMs (http://seamless.usgs.gov; Fig. 2) and aerial photography (McCalpin, 1996; Bryant and Hart,

* Corresponding author.
E-mail address: Ramon.arrowsmith@asu.edu (J.R. Arrowsmith).

0169-555X/$ – see front matter © 2009 Elsevier B.V. All rights reserved.
doi:10.1016/j.geomorph.2009.01.002

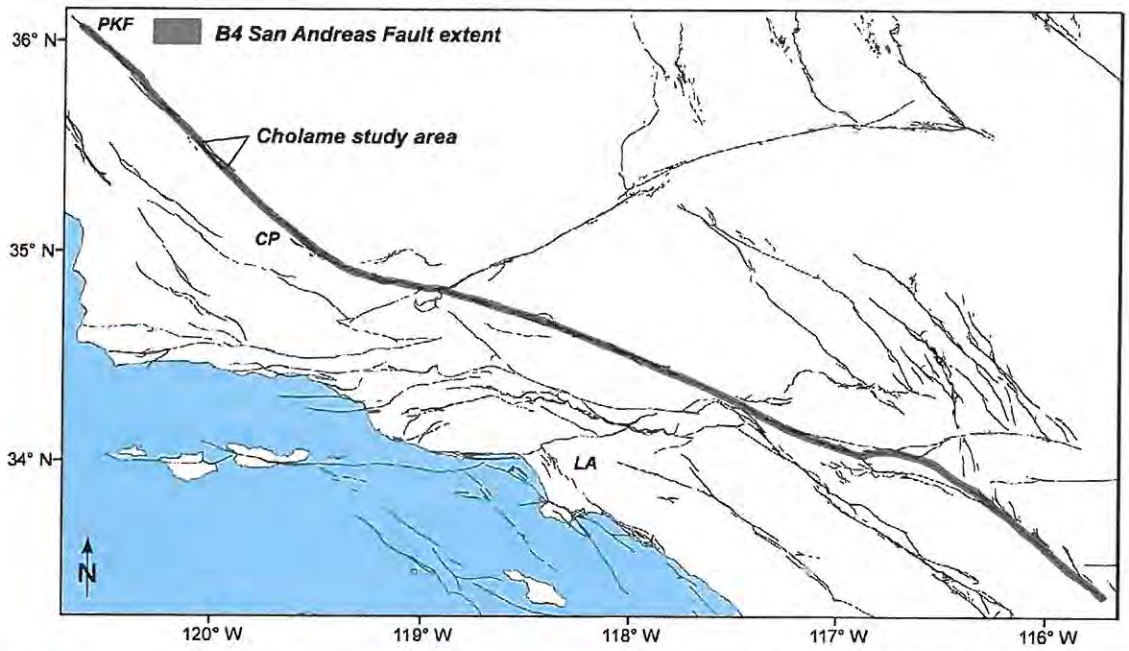

Fig. 1. Active faults of southern California (U.S. Geological Survey and California Geological Survey, 2006), the extent of the B4 San Andreas Fault (SAF) LiDAR data, and the Cholame study area along the SAF (extent of Fig. 2). LA is the location of Los Angeles, PKF is Parkfield, and CP is the Carrizo Plain.

2007). While aerial photographs certainly have meter scale resolution, and photogrammetry can be used to produce high resolution DEMs, they are typically only used in a 2-dimensional sense as base maps for locating fault traces and qualitatively in 3-dimensions for stereoscopically aided interpretation.

The recent imaging of the south-central SAF by the B4 project (Bevis et al., 2005; http://www.earthsciences.osu.edu/b4) provides many new opportunities to clarify our understanding of its structural geology, geomorphology, and recent deformation history. Examining how the new data can be optimally used for mapping recently active fault breaks, characterizing the setting of paleoseismic sites, and assessing the differences between fault trace mapping using traditional (pre-LiDAR) approaches and that done using the LiDAR topography are the major goals of this paper.

In this paper, we take our knowledge of a portion of the south-central SAF (southern Cholame segment; Figs. 1 and 2) based on prior fault trace mapping and paleoseismic work and combine it with analysis of the new LiDAR topographic data to explore its use in characterization of the SAF tectonic geomorphology. First, we examine which processing parameters produce optimal DEMs for characterizing the tectonic geomorphology. Secondly, we characterize the LY4 paleoseismic site (Stone et al., 2002; Young et al., 2002). Third, we compare "classic" field and airphoto-based mapping of recently active fault breaks along the study reach by Vedder and Wallace (1970) with representative field-based mapping done to prospect for the LY4 site (Stone et al., 1998; Stone, 1999), and new LiDAR-only mapping by co-author Zielke. The Cholame section we study presents a range of features and challenges. Results from this study have potential wide application to characterization of other faults scanned with LiDAR.

2. Previous tectonic geomorphology and paleoseismology studies

The south-central San Andreas Fault (SAF) comprises the predominantly seismogenic segments from Parkfield through the Cholame and Carrizo Plain (Fig. 1). It is notable for being the portion of the SAF with the largest total Miocene and later offset (~315 km; e.g. Sims, 1993), for the highest SAF slip rate (~35 mm year^{-1} measured over the late Holocene; e.g., Sieh and Jahns, 1984), and for having apparently steady deep slip (below about 12 km) also at about 35 mm year^{-1} (Noriega et al., 2006). It is also an iconic portion of the SAF with the well preserved tectonic geomorphology that indicates its activity. The troughs, scarps, benches, sags, and ridges that define the fault zone are readily visible from the air and now in high resolution LiDAR-derived topography.

Scientific efforts following the 1966 Parkfield earthquake included detailed mapping of the recently active fault breaks along the south-central SAF (Ross, 1969; Brown, 1970; Vedder and Wallace, 1970). The Vedder and Wallace mapping covers the Cholame and Carrizo Plain sections of the SAF. They noted that the SAF zone showed clear evidence for repeated recent fault slip (the most recent being the great 1857 earthquake). In addition, they concluded that the fault zone was comprised of more subparallel, continuous, and longer fault traces than the sections to the northwest (Brown, 1970) and southeast (Ross, 1969) and suggested that this was largely a result of the better preservation of the features because of the drier climate, but also because of possible variation in fault behavior.

Seismogenic strain release varies along the SAF with a transition from fully creeping north of Parkfield, to decreasing creep and M6 events at Parkfield (Toké and Arrowsmith, 2006), to completely locked with $M>7$ earthquakes recurring on 100–200 year time scales in the Cholame and Carrizo Plain (Grant and Sieh, 1994; Akciz et al., 2009). Slip in the 1857 earthquake was 1–2 m southeast of Parkfield, 3–5 m along the Cholame segment (Sieh, 1978; Lienkaemper, 2001; Young et al., 2002; however, it may have been higher locally, e.g., Runnerstrom et al., 2002), and up to 8 m in the Carrizo Plain (Sieh, 1978; Liu-Zeng et al., 2006; Arrowsmith and Zielke, 2008).

Given the historic precedent of the 1857 earthquake and its foreshocks, a deficit of slip of more than 4 m accumulated since 1857, and a major gap in paleoseismic sites northwest of their concentration in the Carrizo Plain, Arrowsmith and M.S. student Elizabeth Zima (neé Stone; Stone, 1999) and Ph.D. student Jeri Young (Young, 2004) focused on the southern 15 km of the Cholame segment and developed a paleoseismic site called LY4 (Fig. 2). Arrowsmith, Stone, and colleagues originally mapped the recently active faults and tectonic geomorphology along that reach to identify LY4 (see below for more discussion of this mapping). The mapping results were reported in Stone (1999), while the paleoseismic results are in Stone et al. (2002) and Young et al. (2002). Evidence for at least three

Please cite this article as: Arrowsmith, J.R., Zielke, O., Tectonic geomorphology of the San Andreas Fault zone from high resolution topography: An example from the Cholame segment, Geomorphology (2009), doi:10.1016/j.geomorph.2009.01.002

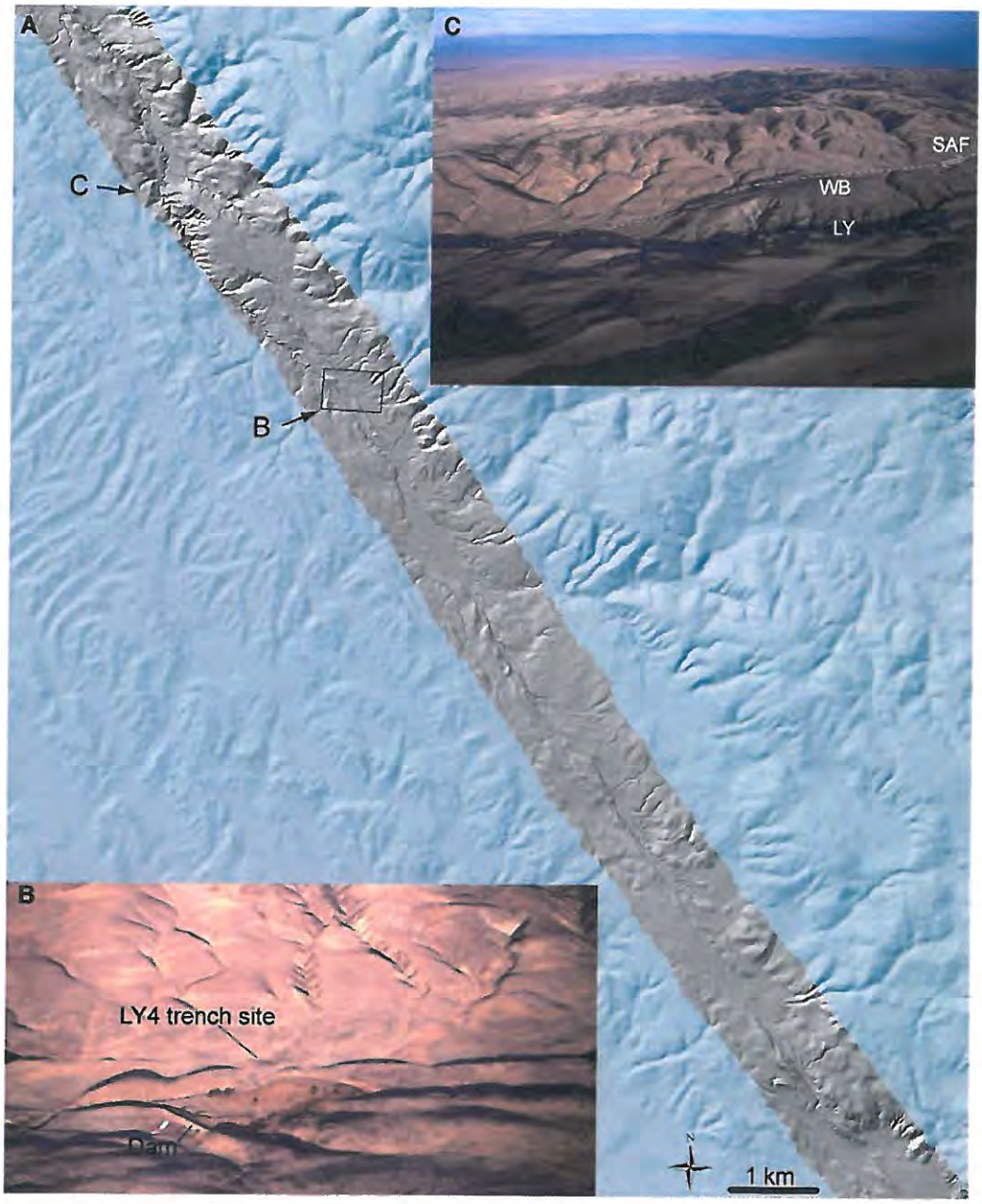

Fig. 2. A) 17 km long section of the SAF along the southern Cholame segment investigated in this study (see Fig. 1 for location; between 33 and 50 km southeast of California State Highway 46). Strip of the 0.5 m resolution hillshaded DEM from the B4 LiDAR dataset is shown in grey over the 10 m resolution NED (http://seamless.usgs.gov) hillshade in blue. The discontinuous traces of the SAF and the deflected offset and locally ponded drainages are clear in the LiDAR hillshade. Box shows location of the LY4 site (Figs. 3–6). View directions of B and C oblique aerial photographs are indicated. B) Oblique aerial photograph towards NE of the LY4 site showing the fault trace (between black triangles) and a dam that was built in the 1940s. C) Oblique aerial photograph towards ESE over the Whaleback pressure ridge (WB) and the Las Yeguas (LY) drainage where it has incised into the uplifting flank of the WB. A simplified SAF trace is dashed. (For interpretation of the references to colour in this figure legend, the reader is referred to the web version of this article.)

earthquakes since about 1030 A.D. including the 1857 event, and 3± 0.5 m of slip in 1857 across a 5 m aperture was exposed in the numerous excavations at LY4.

3. The B4 southern San Andreas Fault laser scan data set

The southern San Andreas and the San Jacinto Fault zone were scanned with LiDAR in 2005 (Bevis et al., 2005; http://www.earthsciences.osu.edu/b4; Fig. 1). The goals of the project were to gather high precision topographic (and photographic) data to characterize near fault ground deformation in a future large earthquake, to support tectonic and paleoseismic studies, and to further develop the integrated technologies and protocols (LiDAR, GPS, and IMU) necessary to routinely collect such research-grade data. An Optech ALTM 3100 was mounted in a Cessna 310 and flown at about 600 m above ground. The scanner was operated at 70 kHz with a 20° scan angle. The resulting swaths were about 430 m wide with 15 cm diameter laser spots. The stated shot spacing per swath was then 0.6 m at nadir and about 1 m at the edge of the swath. Typically, the plane made five passes to scan a total of 1–1.5 km wide zone spanning the SAF. The data were gathered by a team lead by Ohio State University that included USGS, the National Center for Airborne Laser Mapping (NCALM), and UNAVCO. The data have been made available publicly. In particular, the GEON project (http://www.geongrid.org or

Please cite this article as: Arrowsmith, J.R., Zielke, O., Tectonic geomorphology of the San Andreas Fault zone from high resolution topography: An example from the Cholame segment, Geomorphology (2009), doi:10.1016/j.geomorph.2009.01.002

http://www.opentopography.org), through the GEON LiDAR Workflow (Crosby et al., 2006; Jaeger-Frank et al., 2006), enables the scientific community access the raw point cloud and to produce Digital Elevation Models (DEMs) with user-defined resolution and other processing parameters (see below).

4. Methods and analysis

4.1. Digital Elevation Model preparation

Access to the point cloud from the B4 LiDAR scan permits us to explore the effect of the method of preparation and resolution of DEMs on their interpretability for tectonic geomorphology and earthquake geology studies. The DEM represents topography as measured by the heterogeneously distributed 3D laser returns as a two dimensional grid of elevation values spaced at a constant resolution. Computing the DEM from the scattered data is a computationally intensive, but relatively straightforward task. Many algorithms are available for these computations (e.g., El-Sheimy et al., 2005). Where the resolution is greater than the typical shot spacing, the DEM preparation method typically used is local binning (e.g., El-Sheimy et al., 2005; Kim et al., 2006) in which the value at a DEM node is a simple function (e.g., maximum, minimum, mean, and inverse distance weighted—IDW) of the points within a specified search radius (r). Increasing the search radius ensures that points will be found (otherwise a null is assigned at the grid node), but the value will represent a broader area (Fig. 3). Inverse distance weighting ($1/r^2$) partially overcomes this problem by weighting nearer points more than farther ones (e.g., El-Sheimy et al., 2005). In cases where the resolution required is smaller than the shot density, interpolation is necessary. For this case, the local binning can work with large enough search radii, but typically methods such as spline, Kriging, and Triangular Irregular Networks (TINs) are used.

The average shot density at the LY4 study site is about 3.6 ± 1.1 m^{-2}, ranging from 0 to more than 10 m^{-2} (Fig. 3E). This is a typical density for most of the B4 (Carrizo Plain and Salton Sea area as well; although we have not undertaken a systematic analysis). The density and qualitative evaluation of resulting DEMs suggests that 0.5 m DEMs are sufficiently well resolved for the local binning scheme. Four shots per square meter matches the number of nodes in a 0.5 m DEM. Using the local binning approach which we implemented including IDW (Kim et al., 2006) the question becomes, what is the optimal search radius for the favored IDW method? If there are no laser returns within the search radius, the DEM node at that location is returned as null (holes in the images in Fig. 3). As the search radius increases, the number of nulls goes down rapidly and asymptotically approach some minimum defined by anomalously large areas of no returns (water—bottom left of Fig. 3). Somewhere near that "shoulder" is an indicator of the proper

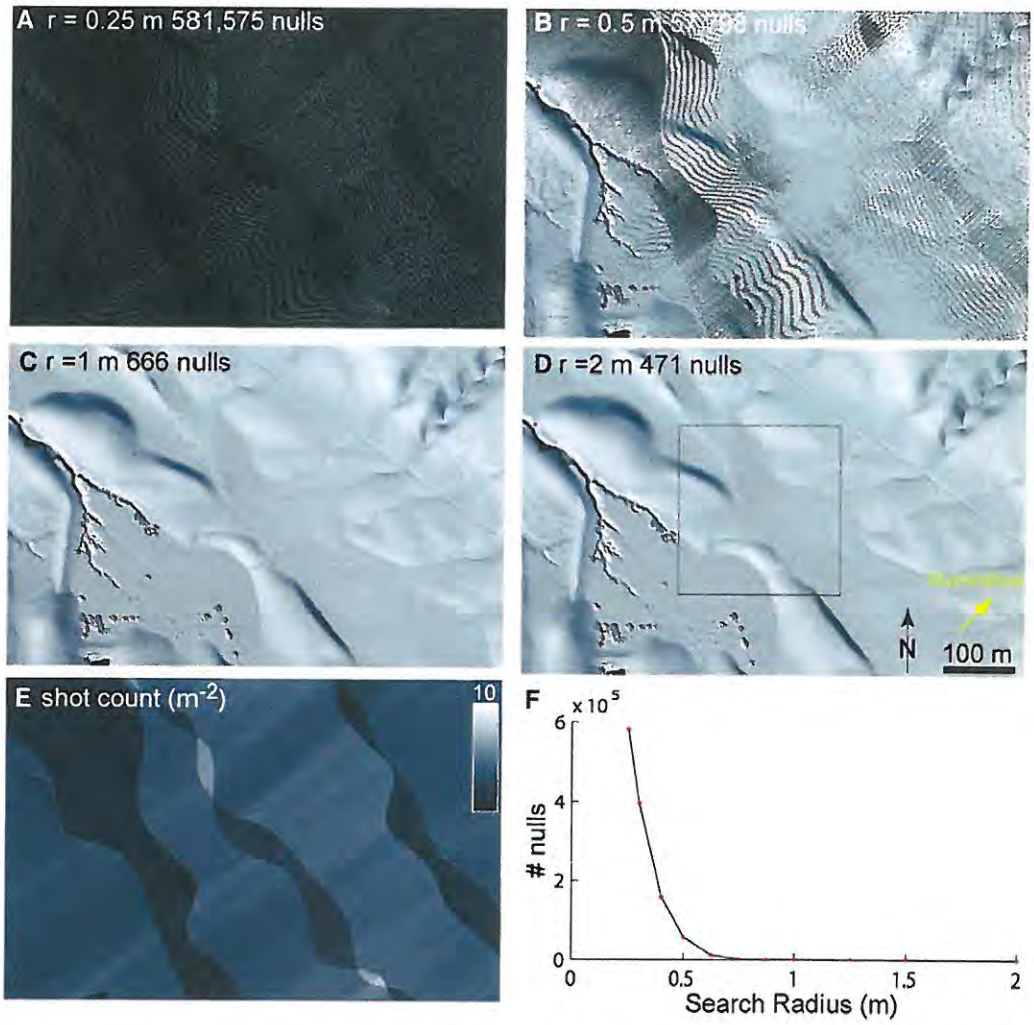

Fig. 3. Effect of search radius on local binning results in DEM production. DEMs of 0.5 m resolution are produced using inverse distance weighted local binning (Kim et al., 2006). As the search radius increases from 0.25 m (A) though 0.5 m (B), 1 m (C), and 2 m (D), the number of nulls (result from no laser returns in search radius) rapidly decreases (F). The heterogeneous shot count (m^{-2}) of the area (E) results from multiple overlapping swaths from repeat overpasses. Box in D shows location of Fig. 4.

Please cite this article as: Arrowsmith, J.R., Zielke, O., Tectonic geomorphology of the San Andreas Fault zone from high resolution topography: An example from the Cholame segment, Geomorphology (2009), doi:10.1016/j.geomorph.2009.01.002

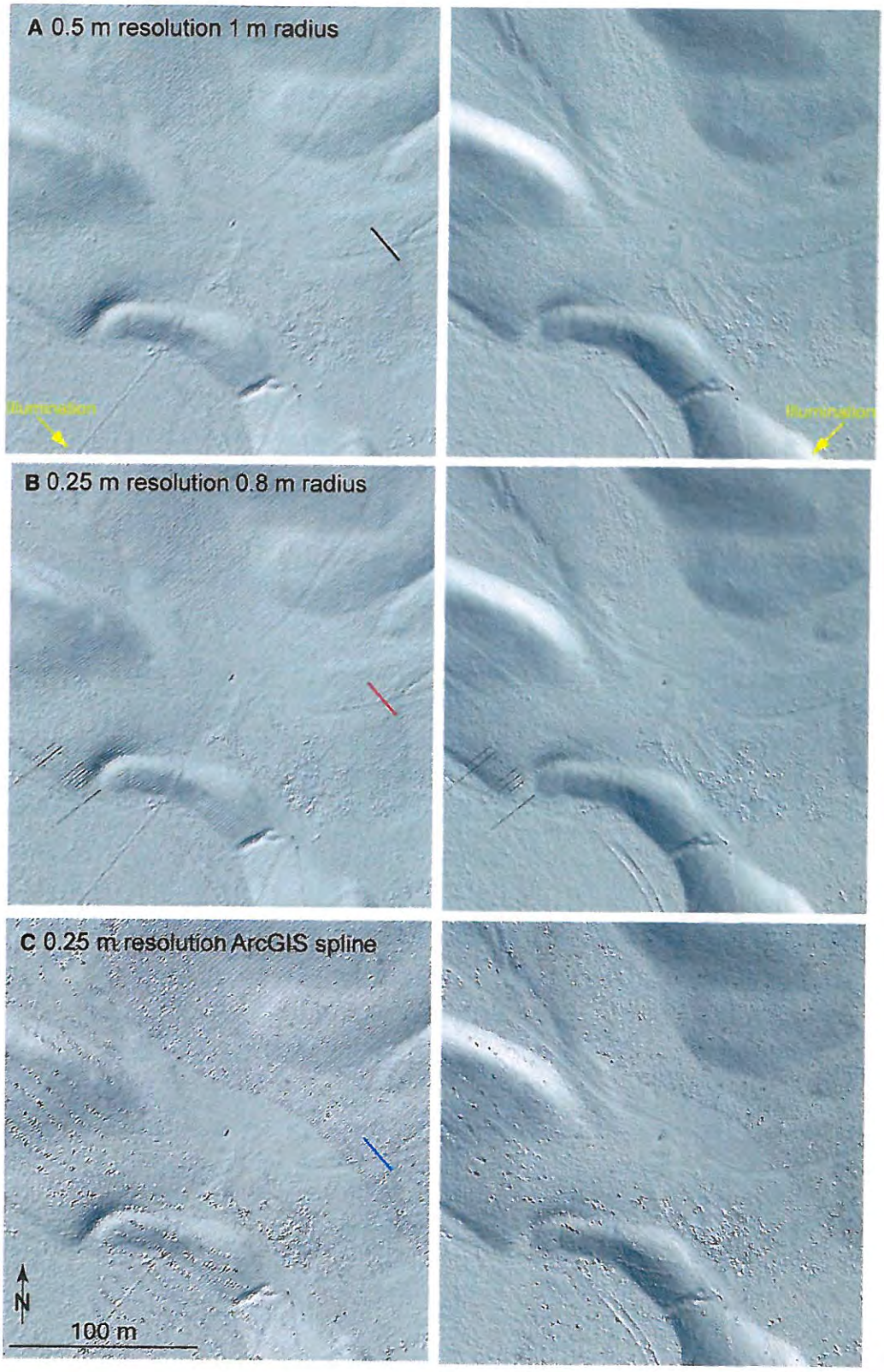

Fig. 4. Changing DEM resolution, illumination direction (N45W on left and N45E on right) and gridding algorithms at the LY4 site. A) 0.5 m IDW DEM with 1 m search radius has few nulls and is the product we typically analyze. B) 0.25 m IDW DEM with 0.8 m search radius has some nulls (NE-trending dark lineaments), and depicts the finer features slightly more clearly than A. See also Fig. 6. C) 0.25 m resolution DEM from ArcGIS spline has distracting artifacts, especially in areas of overlapping swaths. Black, red, and blue lines correspond to topographic profiles in Fig. 5. (For interpretation of the references to colour in this figure legend, the reader is referred to the web version of this article.)

Please cite this article as: Arrowsmith, J.R., Zielke, O., Tectonic geomorphology of the San Andreas Fault zone from high resolution topography: An example from the Cholame segment, Geomorphology (2009), doi:10.1016/j.geomorph.2009.01.002

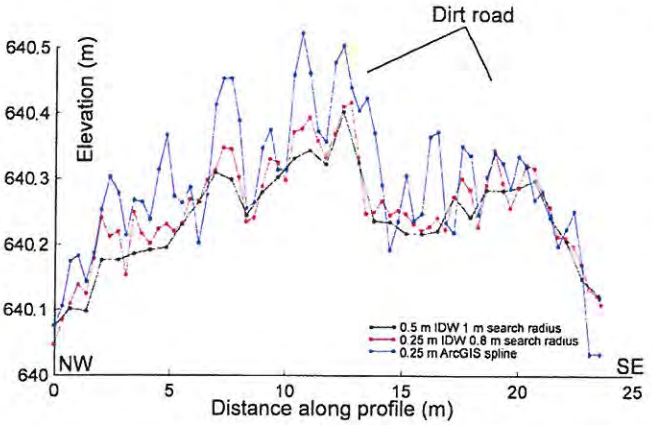

Fig. 5. Detailed topographic profiles from different DEMs (see location in Fig. 4). Each is from the same location but different data set. The convex upward alluvial fan form is evident, as is the flat dirt road, but the high frequency roughness shows the various manifestations of the "corduroy." Corduroy is highest amplitude in the spline and most subdued for the coarser resolution 0.5 m DEM.

search radius. A search radius ~0.8–1 m simultaneously minimizes the number of null cells and the search radius (Fig. 3F).

While the argument just presented that 0.5 m DEMs are probably optimal in terms of resolution, what happens if we go to a finer resolution such as 0.25 m? File sizes go up by a factor of 4. Fig. 4 presents an exploration of the difference between the reference 0.5 m with 1 m search radius IDW and finer resolution 0.25 m DEMs computed with an IDW on a 0.8 m search radius and the default spline method from ArcGIS (http://www.esri.com/software/arcgis; regularized, weight of 0.1, and number of points is 12).

The spline-based DEM highlights the "corduroy" artifacts common in many LiDAR studies (Figs. 4 and 5). The repeated passes of the aircraft have relative mislocations on the order of 0.1 m. These differences then are manifest in the point clouds and resulting DEMs as somewhat regular troughs and ridges normal to the flight direction with meter-scale wavelengths and decimeter amplitudes (Fig. 5). The spline method produces the deepest corduroy (~20 cm) while the IDW methods smooth it by a factor of two or more. With a 1 m search radius every 0.5 m, the coarser DEM has begun to average out the effects of the multiple swath mislocation. Illumination parallel to the scan direction (~N45E; right panel of Figs. 4 and 6) diminishes the distraction of the corduroy for interpretation.

4.2. Mapping of recently active breaks and tectonic geomorphology of the SAF

4.2.1. Representative mapping approaches

We chose three representative approaches to fault trace mapping for assessment. Vedder and Wallace (1970) relied on systematic review of aerial photography and topographic maps with field checking for their 1:24,000 scale mapping of recently active breaks. This "classic" method is a reference against which we compare two other approaches. The first is field-based mapping on aerial photographic base maps done to prospect for the LY4 site (Stone et al., 1998; Stone, 1999). The second is new LiDAR-only mapping (no field checking) by co-author Zielke done for this study. These different approaches are commonly employed in active fault zone mapping. Our goal in this section is to qualitatively compare their depiction of the range of tectonic landforms along the Cholame section. Results from this study should be widely applicable to other faults for which LiDAR data are available.

4.2.2. Vedder and Wallace (1970)

Vedder and Wallace (1970) present a sequence of 1:24,000 strip maps along the SAF between Cholame Valley and Tejon Pass, California. They used on-the-ground investigations and interpretation

Fig. 6. Geomorphology of the LY4 paleoseismic site on 0.25 m IDW DEM computed with 0.8 m search radius. The recently active trace of the SAF is shown in red. It broadens in places where it is defined only by geomorphology such as the moletrack in the NW. In the trenches, we know exactly where it is. The trenches were sited here because young alluvial fan deposition regularly buries fault ruptures. Cultural features such as the water tank, dams, artificial pond floor, and small truck and GPS antenna and tripod (deployed for B4 data collection) give a sense of scale and resolution. (For interpretation of the references to colour in this figure legend, the reader is referred to the web version of this article.)

Please cite this article as: Arrowsmith, J.R., Zielke, O., Tectonic geomorphology of the San Andreas Fault zone from high resolution topography: An example from the Cholame segment. Geomorphology (2009), doi:10.1016/j.geomorph.2009.01.002

of vertical aerial photographs to delineate the traces of recently active fault breaks (Fig. 7). They recognized the recently active breaks in terms of the related geomorphic features: scarps, trenches or troughs, notches, parallel ridges, offset channels, sag ponds, ponded alluvium, undrained depressions, and shutter ridges. Their mapping included recently active breaks as solid lines (certain on Fig. 7) for which field or photographic evidence of recent motion was shown by scarps, trenches, sag ponds, spring lines, or vegetation contrasts. Less obvious features, but likely fault breaks, were dashed. They also provided brief notes identifying exemplary features. The data were compiled at 1:24,000 onto topographic quadrangle maps. They claim that features large enough to represent at this scale are generally accurate to within 50 ft (15.2 m) but may be as much as 150 ft (45.7 m) off in areas of lower relief. Zielke (this study) rectified scanned versions of the original Vedder and Wallace maps to provide an equivalent to US Geological Survey Digital raster Graphic (DRG) topographic maps and then digitized the mapping without reinterpretation or relocation.

4.2.3. Stone and Arrowsmith

As part of our efforts to find a suitable paleoseismic site along the Cholame segment in the late 1990s, we (Stone, Arrowsmith, and other colleagues) mapped about 17 km of the fault zone (Stone et al., 1998; Stone, 1999; Fig. 7). This mapping included stereographic inspection of aerial photography from 1930 and field inspection and compilation on 1:10,000 printouts of the airphotos. We strictly limited the delineation of the active faults to those which showed evidence of recent motion by meter-sale topographic discontinuities. No features were mapped which were not identifiable in the field. Some alignments of features did not have clear indicators of sense of slip, but were most probably faults, so they were mapped as lineaments. This strictness results in fewer mapped features (Fig. 7) than Vedder and Wallace (1970) or Zielke (see below). We also mapped recently active landslides. The fault traces and landslide scarps and deposits were compiled and mapped onto aerial photographs rectified to the USGS DRGs (Stone, 1999). Arrowsmith (this study) re-rectified and re-digitized the relevant mapping for this study. Location accuracy for the Stone and Arrowsmith mapping is a few tens of meters.

4.2.4. Zielke (this study)

Zielke used a fully digital, GIS-based approach without any field checking and relied only on DEMs (0.5 m with a 1 m search radius for the IDW) and derivative hillshades of the B4 LiDAR survey for his mapping, the relevant portion of which is presented in Fig. 7. He mapped landslide scarps and deposits as single polygons. He looked at fault scarps, offset and deflected features (mostly drainages), and other lineaments to define the fault trace. He distinguished between main and secondary fault traces (red and blue respectively in Fig. 7). A quality rating distinguishes between 'certain,' 'uncertain,' 'inferred,' and 'queried' features. The main trace was identified as the single trace most likely active during the last earthquake in 1857. It has a well developed surface expression with clear fault scarps and drainage deflection and offsets. If multiple, parallel fault strands were present, the active trace was identified as the one that has the least degraded features. The secondary traces are clearly recognizable, but probably inactive recently or have low rates of slip. These features are typically subparallel to the main trace and are at times several hundred meters away from it, indicating the integrated width of the fault zone as a whole is larger than that is active in just the last few earthquakes. Certain features (either main or secondary) are clearly identifiable lineaments along well expressed fault scarps or offset landforms. Uncertain features are less well expressed and typically do not show evidence of offset. Uncertain is the best rating that a secondary trace will usually receive. Inferred features are those without clearly indicated recent motion, but along the extension of certain or uncertain features or buried by young alluvium. Finally, queried features are expressed only by weak lineaments sometimes beyond the ends of more certain features.

5. Results

5.1. Paleoseismic site analysis—LY4 site

Any effort to select a site for detailed paleoseismic analysis (e.g., trenching across a fault) requires an understanding of the context that comes from assessment of the topography around it. In this example, we use the B4 data to characterize the LY4 site after the fact (Stone et al., 2002; Young et al., 2002; Figs. 3–6). The two IDW DEMs (Fig. 4A, B) with illumination from the NE show the tectonic geomorphology of the site well. The 0.25 m resolution IDW DEM with the 0.8 m search radius (Fig. 4B) shows the site most clearly, even though some of the vegetation, fine topographic roughness and corduroy can be distracting. Fig. 6 takes that the 0.25 m resolution DEM with the N45E illumination, puts the similarly illuminated 0.5 m hillshade underneath to fill the nulls evident in Fig. 4B, and presents the tectonic geomorphology of the site. The trace of the SAF is clearly indicated by the en echelon troughs of the moletrack in the NW and the fault scarp to the SE (Fig. 6). The alluvial fan in the center has buried the repeated ground ruptures at the site making it a good location for paleoseismology (Stone et al., 2002; Young et al., 2002). Fine features such as the water tank and the vegetation on the alluvial fan near the trench site become clearer with the finer resolution (compare Fig. 4A and B).

5.2. Fault zone mapping

In the following subsections, we compare and contrast the Vedder and Wallace, Stone and Arrowsmith, and Zielke fault trace mapping in their depictions of the tectonic geomorphology of the SAF (Fig. 7).

5.2.1. Northwest—Fig. 7B

The northwestern 6 km of the fault zone (Fig. 7B) preserves important fault zone discontinuities, distributed deformation, and the LY4 site. Vedder and Wallace show a fault zone varying in width from a single strand to 735 m. Stone and Arrowsmith note the greater width of the stepover (~100 m) as well as nearly 200 m width near LY4 indicated by two subparallel traces (see below). Zielke's active traces are singular except for the stepover. Considering the secondary traces, the fault zone is 300–500 m wide.

The Whaleback (WB on Fig. 7B; see also Fig. 2B) is an informally named recently uplifted block bounded largely on the NE by active traces of the SAF. The drainage that crosses it (just SE of the WB label) has recently been defeated with runoff joining the main NW-flowing Las Yeguas drainage to the SE. Other subtle traces of former drainages crossing Whaleback are evident in the field and in some illuminations of the LiDAR DEMs. The uplift of the Whaleback apparently pushes the Las Yeguas creek to the SW, and promotes incision along it. The formation of numerous landslides (mapped by Stone/Arrowsmith and Zielke) attest to the recent uplift and incision. The NW end of the Whaleback is marked by a prominent left step in the active fault traces (Stone/Arrowsmith and Zielke). Stone (1999) interpreted the uplift of the Whaleback as resulting from a possibly greater fault-normal width at depth of this stepover. Vedder and Wallace and to a lesser extent Zielke delineate the fault zone to the NW of the Whaleback with discontinuous swales and scarps.

The LY4 site is located in a portion of the fault zone marked by straight and continuous overlapping traces and where the Las Yeguas Creek enters the Whaleback-driven knickpoint (see above and Fig. 6 for more details). An important concern for the LY4 paleoseismic results is the degree of recent activity along the second fault trace at the site (to the SW). Both Stone et al. (2002) and Young et al. (2002) dismissed it as not significant in terms of accommodation of slip. All three of the mapping datasets show it, but with variable activity

Please cite this article as: Arrowsmith, J.R., Zielke, O., Tectonic geomorphology of the San Andreas Fault zone from high resolution topography: An example from the Cholame segment, Geomorphology (2009), doi:10.1016/j.geomorph.2009.01.002

ratings. Young et al. (2002) determined that the main trace accommodated about 3 m of slip in 1857. Lienkaemper (2001) and Arrowsmith and Zielke (2008) conclude that this is on the lower end of the likely slip released in 1857 over this reach as indicated by offset channels and other landforms. Could the secondary trace actually have accommodated the additional 1–2 m of slip? Young et al. (2002) concluded that it has not been recently active as indicated by degraded fault scarps and undeformed inferred Holocene deposits (present west-northwest of the trench site). Review of the LiDAR-based imagery and mapping (Fig. 7B) suggests that this weakly defined trace has not undergone more than a few meters of slip during the 10s of kyr development of the landforms there (e.g., Arrowsmith et al., 1998), suggesting that it did not accommodate meter-scale slip in 1857.

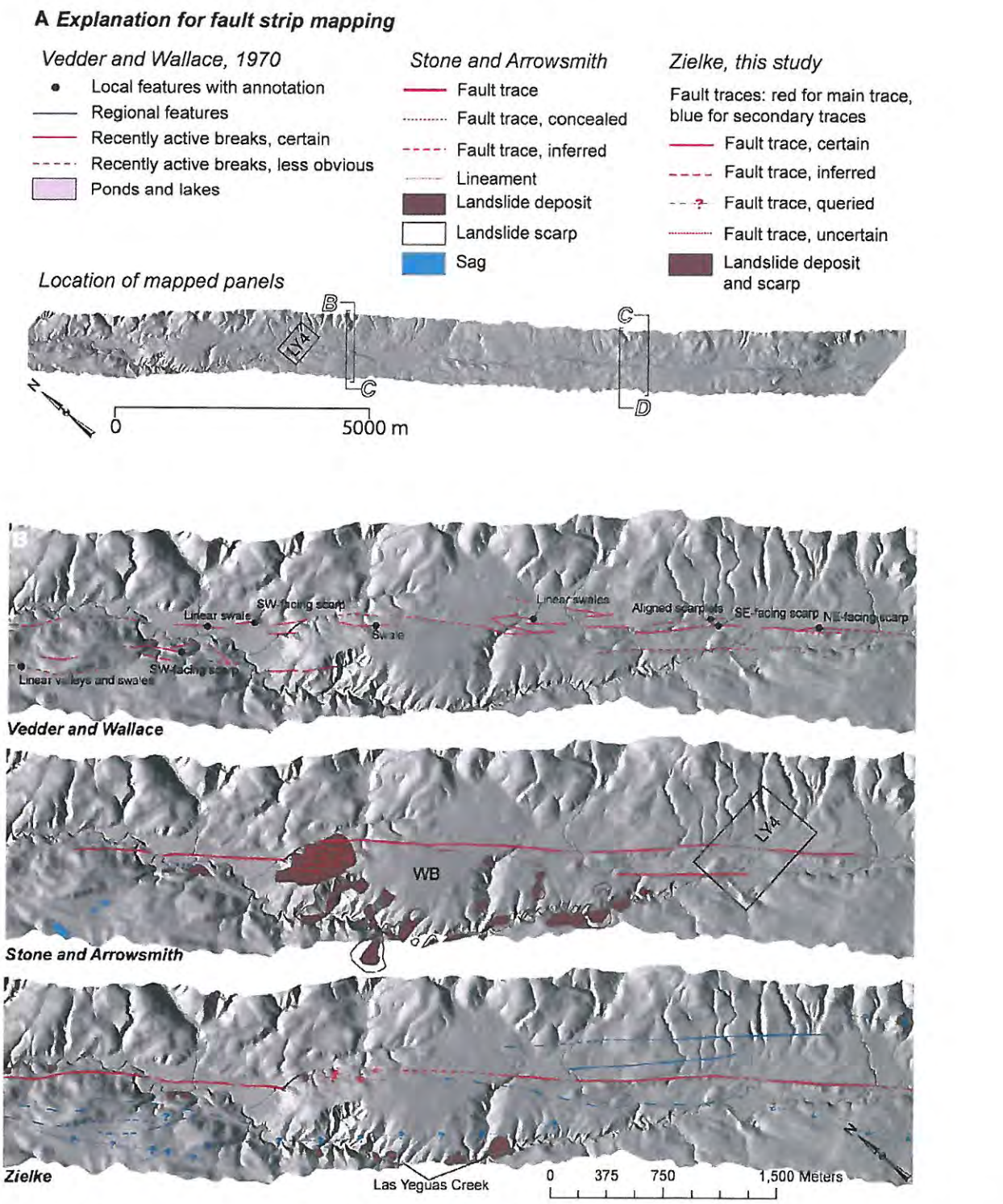

Fig. 7. Fault strip mapping by Vedder and Wallace (1970); Stone and Arrowsmith (Stone, 1999); and Zielke, this study. A) Explanation for symbology and locations of the mapped panels that follow. B) Northwestern, C) central, and D) southeastern mapped panels showing the three different mapping results overlain on 0.5 m DEMs with N45W illumination. The location of the LY4 paleoseismic site (e.g., Stone et al., 2002; Young et al., 2002; Figs. 4–6) is also indicated in A and B. See text for explanation.

Please cite this article as: Arrowsmith, J.R., Zielke, O., Tectonic geomorphology of the San Andreas Fault zone from high resolution topography: An example from the Cholame segment, Geomorphology (2009), doi:10.1016/j.geomorph.2009.01.002

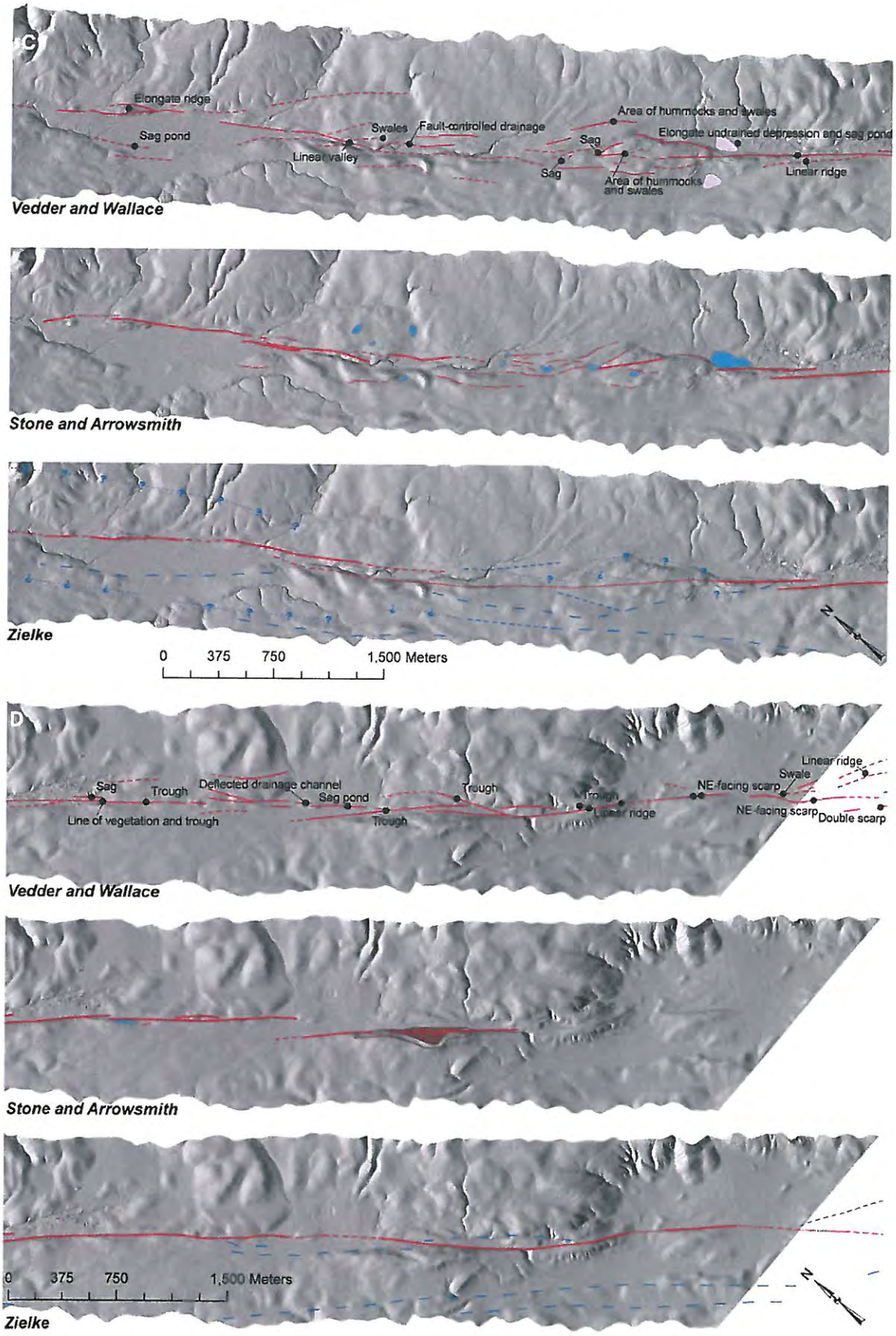

Fig. 7 (*continued*).

Please cite this article as: Arrowsmith, J.R., Zielke, O., Tectonic geomorphology of the San Andreas Fault zone from high resolution topography: An example from the Cholame segment, Geomorphology (2009), doi:10.1016/j.geomorph.2009.01.002

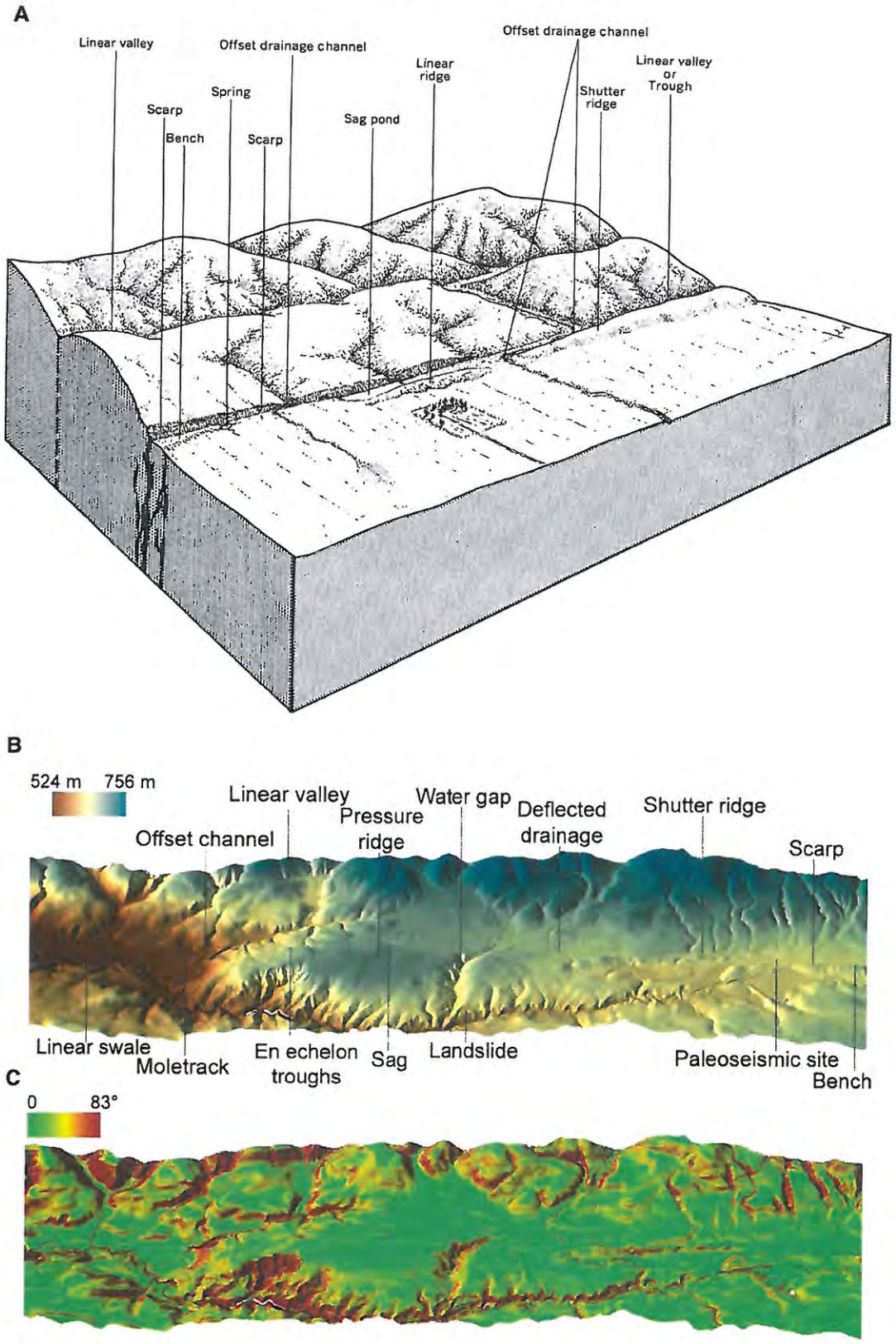

Fig. 8. Common landforms produced along recently active strike-slip faults such as the south-central San Andreas Fault. A) Classic block diagram from Vedder and Wallace (1970). B) LiDAR DEM-based oblique view (4.5 km long) of an exemplary piece of topography color-coded by elevation showing all features of A along with a few more mostly associated with the distributed deformation of the Whaleback pressure ridge (water gap and landslide in this case). C) Slope map showing the quantitative interpretative power that can come from these topographic data. B and C come from the area of Fig. 7B, but are meant to be broadly representative.

Please cite this article as: Arrowsmith, J.R., Zielke, O., Tectonic geomorphology of the San Andreas Fault zone from high resolution topography: An example from the Cholame segment, Geomorphology (2009), doi:10.1016/j.geomorph.2009.01.002

5.2.2. Central—Fig. 7C

The central 6 km of mapping is notable for a potential paleoseismic site in the northwest, important fault controlled drainage, short discontinuous and variably oriented faults in the middle, and a transition to straight and longer fault traces to the southeast. Vedder and Wallace's fault widths here are about 300 m. Stone and Arrowsmith show simple traces in the northwest and southeast bounding a ~150 m wide lineament-dominated belt. Zielke's active traces are uncertain through the central discontinuities, whereas the secondary traces show an overall fault zone with decreasing from 750 m in the NW of this section to just a single few meters wide trace in the SE.

Vedder and Wallace note the large sag pond in the NW of the map. Stone (1999) calls this the "Las Yeguas site." It is a good potential paleoseismic site (Stone et al., 1998). As all the maps show, the fault traces cross alluvial fans feeding the marshy sag from the NE.

The fault-controlled drainage identified by Vedder and Wallace confounded the field mapping by Stone and Arrowsmith. We had a hard time differentiating fluvial and fault scarps there. Just to the SE of the fault controlled drainage, the fault zone becomes even more complex. Vedder and Wallace denoted "area of hummocks and swales." Stone and Arrowsmith noted that no faults were conspicuous. Zielke can only draw an uncertain main fault through the center, while his secondary faults pick up the greater width of the fault zone. The LiDAR topography is consistent with what Stone/Arrowsmith and Vedder/Wallace maps show as sags between ridges. This zone appears to comprise ~10 discontinuous fault blocks. The blocks have moved differentially—some up and some down—to produce the notable sags and ridges. Stone (1999) interpreted this zone in 3-dimensions as one in which the fault surfaces were "petals" of a flower structure which flared upward from a more continuous through going fault surface (its buried trace perhaps delineated by Zielke). If it exists, the depth of flaring is probably on the order of the horizontal extent of the features (several hundred meters).

5.2.3. Southeast—Fig. 7D

The south easternmost 5 km of the mapped fault zone is marked by greater geometric simplicity than the portions to the NW. Vedder and Wallace show a 50–100 m wide zone of sags, troughs, and ridges. Stone and Arrowsmith show 1–2 km long stepping fault traces with a landslide-dominated 30 m high fault scarp. Zielke's gently curving traces show a ~100 m left bend heading off the map to the SE (also shown in the Vedder and Wallace mapping). Zielke's secondary traces are ~1 km long and subparallel with the main trace and delineate a ~500 m wide fault zone.

6. Discussion

The suite of landforms that indicates the recent activity of a strike-slip fault is illustrated in "textbook" form in Fig. 8A. Any landform in isolation (i.e., bench, scarp, or trough) is not sufficient to delineate the active fault. The landforms taken together in terms of their spatial association and orientation are a strong predictor of fault location (as indicated by historic earthquake surface ruptures which have occurred along such belts of topographic features and the paleoseismic trenches which have been sited accordingly and successfully exposed evidence of recent faulting). Using GIS visualization tools like ArcScene (http://www.esri.com/software/arcgis) makes it possible to update such a figure and to show a few new features (Fig. 8B). Either Fig. 8A or B is a sufficient summary of the landforms produced along recently active faults, but Fig. 8B shows them with greater realism and detail. Whether or not that makes a difference for training researchers and students to identify such features remains to be seen. But, they can use such visualization tools to interact with these data from numerous virtual view points and with different color ramps, or other manipulations.

This paper represents an early analysis of the utility of high resolution topographic data now becoming readily available along such faults as the SAF. We have applied this analysis to paleoseismic site evaluation and fault trace mapping (given the caveat that the active fault zone may be broader than the data coverage). Quantitative and systematic analysis of offset stream channels and other features (i.e., Sieh, 1978; Lienkaemper, 2001) is underway (Arrowsmith et al., 2006; Arrowsmith and Zielke, 2008).

The different mapping results show that most of the primary features are robustly manifest. We do not advocate mapping without visiting the field. Such a recommendation is not new because Vedder/Wallace and Stone/Arrowsmith inspected aerial photographs in advance of the field work. Any such inspection is an efficient step. The LiDAR DEMs provide an additional, useful, and well georeferenced dataset. Indeed, the georeferencing of the LiDAR is significantly better (probably at least an order of magnitude more accurate) than the commonly available 1 m USGS digital orthophoto quarter quadrangles. Thus, digitizing before, during, and after field inspection using LiDAR DEMs and derivatives as base maps will improve the geolocation quality of the resulting maps.

The B4 LiDAR coverage is in a largely unforested portion of Southern California. The data are not classified in terms of ground and vegetation returns. The SAF and related faults in northern California and elsewhere are spectacularly exposed in "bare earth" DEMs (e.g., Haugerud et al., 2003; Sherrod et al., 2004; Kondo et al., 2008). In such conditions, the advantage of LiDAR is even greater than discussed here.

This study is largely qualitative and subjective (as is required for siting and mapping). The eyes and mind of a geologist/geomorphologist are the most valuable tools. LiDAR analyzed within a facile GIS environment is a powerful aid. Moving beyond these "pretty pictures" will produce new understanding about rates and processes through the interaction of the hillslope, landsliding and fluvial surface processes with the faulting and distributed deformation. The high slopes along Las Yeguas Creek as it passes through the Whaleback uplift zone are clear in Fig. 8C and consistent with the mapped concentration of landslides there (Stone/Arrowsmith and Zielke mapping, Fig. 7B). Narrow swaths of higher slopes show the recently active fault traces around LY4 and NW (left) of the Whaleback. Fault scarps indicate that trace and could be morphologically dated (Arrowsmith et al., 1998). Significantly extending such musings, Hilley and Arrowsmith (2008) used the LiDAR DEMs and knowledge of the tectonic activity of a pressure ridge along the SAF in the Carrizo Plain to depict landscape development in an area of transient rock uplift.

7. Conclusions

Swaths of high resolution topographic data along fault zones are important aids in the delineation of recently active breaks. LiDAR data such as the B4 southern SAF laser scan has shot densities of 3–4 m^{-2} and can be gridded to 0.25 to 0.5 m resolution using local binning with inverse distance weighting and 0.8 m or larger search radii. Those resolutions depict the tectonic landforms at paleoseismic sites well enough to assess them confidently. Mapping of recently active breaks using a LiDAR-only based approach compares well with a combination of aerial photographic and field-based methods. But LiDAR, field, and spectral imaging (i.e., aerial photography) will give the best results. The semantic variations of what constitutes "active" and the importance of secondary traces influence the breadth and complexity of the resulting fault trace maps. The Cholame section we have studied presents a range of tectonic features and challenges. These analyses are applicable to similar kinds of studies along the SAF and other active faults for which LiDAR topography data are or may become available.

Acknowledgements

We thank Elizabeth Zima (neé Stone) for her careful Cholame segment mapping and compilation. Jeri Young's (re)consideration of

Please cite this article as: Arrowsmith, J.R., Zielke, O., Tectonic geomorphology of the San Andreas Fault zone from high resolution topography: An example from the Cholame segment, Geomorphology (2009), doi:10.1016/j.geomorph.2009.01.002

features near LY4 was valuable. Vince Matthews, George Hilley, and others made important contributions to the mapping. The Twisselmans, Sills, and Pritchards generously permitted us access to their land. We also thank Dallas Rhodes and Nathan Toké for the insightful geomorphologic and paleoseismological discussions. The B4 project is a bold concept that produced amazing data. Thanks to Mike Bevis, Ken Hudnut, and the numerous others at the Ohio State University, US Geological Survey, the National Center for Airborne Laser Mapping, and UNAVCO. This research was motivated by capabilities available through the GEON LiDAR Workflow. Thanks to Chris Crosby for sharing that vision and for numerous discussions about the tectonic geomorphology of the SAF as manifest in LiDAR topography. Reviews by Hisao Kondo, Richard Whittecar, and Takashi Oguchi were very helpful. This effort was supported partially by NSF grants (EAR-0225543, EAR-0310357, EAR-0409745, and EAR-0711282), GeoEarthscope, and the Southern California Earthquake Center (SCEC).

References

2007 Working Group on California Earthquake Probabilities, 2008. The Uniform California Earthquake Rupture Forecast, version 2 (UCERF 2). U.S. Geological Survey Open-File Report 2007-1437 and California Geological Survey Special Report 203. [http://pubs.usgs.gov/of/2007/1437/].

Akciz, S.O., Grant Ludwig, L., Arrowsmith, J.R., 2009. Revised dates of large earthquakes along the Carrizo section of the San Andreas Fault, California, since A.D. 1310±30. J. Geophys. Res 114, B01313. doi:10.1029/2007JB005285.

Arrowsmith, J.R., 2007. Structural geology, tectonic geomorphology, and recent slip history of the south-central San Andreas Fault. Geological Society of America Annual Meeting, Paper No. 155-3.

Arrowsmith, J.R., Zielke, O., 2008. Slip along the San Andreas Fault associated with the great 1857 earthquake derived from "B4" LiDAR high resolution topographic data. Eos Transactions AGU 89 (53) Fall Meet. Suppl., Abstract T44B-03.

Arrowsmith, J.R., Rhodes, D.D., Pollard, D.D., 1998. Morphologic dating of scarps formed by repeated slip events along the San Andreas Fault, Carrizo Plain, California. Journal of Geophysical Research 103, 10,141–10,160.

Arrowsmith, J.R., Campbell, B., Crosby, C., Raleigh, D., 2006. Tectonic geomorphology and earthquake geology of the 1857 reach of the San Andreas Fault: a new look from Airborne Laser Swath Mapping. Eos Transactions AGU 87 (52) Fall Meet. Suppl., Abstract G53C-0916.

Bevis, M., Hudnut, K., Sanchez, R., Toth, C., Grejner-Brzezinska, D., Kendrick, E., Caccamise, D., Raleigh, D., Zhou, H., Shan, S., Shindle, W., Yong, A., Harvey, J., Borsa, A., Ayoub, F., Elliot, B., Shrestha, R., Carter, B., Sartori, M., Phillips, D., Coloma, F., Stark, K., 2005. The B4 Project: scanning the San Andreas and San Jacinto fault zones. Eos Transactions AGU 86 (52) Fall Meet. Suppl., Abstract H34B-01.

Brown Jr., R.D., 1970. Map showing recently active breaks along the San Andreas and related faults between the northern Gabilan Range and Cholame valley, California. U.S. Geological Survey Miscellaneous Geologic Investigations Map I-575, scale 1:62,500.

Bryant, W.B., Hart, E., 2007. Fault-rupture hazards zones in California: Alquist-Priolo Earthquake Fault Zoning Act with index to earthquake fault zones. Department of Conservation, California Geological Survey, Special Publication 42.

Crosby, C.J., Arrowsmith, J.R., Frank, E., Nandigam, V., Kim, H.S., Conner, J., Memon, A., Baru, C., 2006. Enhanced access to high-resolution LiDAR topography through cyberinfrastructure-based data distribution and processing. Eos Transactions AGU 87 (52) Fall Meet. Suppl., Abstract IN41C-04.

El-Sheimy, N., Valeo, C., Habib, A., 2005. Digital Terrain Modeling: Acquisition, Manipulation, and Applications. Artech House, Boston.

Grant, L.B., Sieh, K., 1994. Paleoseismic evidence of clustered earthquakes on the San Andreas Fault in the Carrizo Plain, California. Journal of Geophysical Research 99 (B4), 6819–6841.

Haugerud, R.A., Harding, D.J., Johnson, S.Y., Harless, J.L., Weaver, C.S., Sherrod, B.L., 2003. High-resolution Lidar topography of the Puget Lowland, Washington—a bonanza for earth science. GSA Today, Geological Society of America 13 (6), 4–10.

Hilley, G.E., Arrowsmith, J.R., 2008. Geomorphic response to uplift along the Dragon's Back pressure ridge, Carrizo Plain, California. Geology 36. doi:10.1130/G24517A.1.

Jaeger-Frank, E., Crosby, C.J., Memon, A., Nandigam, V., Arrowsmith, J.R., Conner, J., Altintas, I., Baru, B., 2006. A three tier architecture for LiDAR interpolation and analysis. Lecture Notes in Computer Science 3993, 920–927.

Kim, H., Arrowsmith, J.R., Crosby, C.J., Jaeger-Frank, E., Nandigam, V., Memon, A., Conner, J., Baden, S., Baru, C., 2006. An efficient implementation of a local binning algorithm for digital elevation model generation of LiDAR/ALSM dataset. Eos Transactions AGU 87 (52) Fall Meet. Suppl., Abstract G53C-0921.

Kondo, H., Toda, S., Okamura, K., Takada, K., Chiba, T., 2008. A fault scarp in an urban area identified by LiDAR survey: a Case study on the Itoigawa–Shizuoka Tectonic Line, central Japan. Geomorphology 101, 731–739.

Lawson, A.C., 1908. Report of the Earthquake Investigation Commission upon the California Earthquake of April 18, 1906. Carnegie Institution, Washington D.C.

Lienkaemper, J.J., 2001. 1857 slip on the San Andreas fault southeast of Cholame. Bulletin of the Seismological Society of America 91, 1659–1672.

Liu-Zeng, J., Klinger, Y., Sieh, K., Rubin, C., Seitz, G., 2006. Serial ruptures of the San Andreas fault, Carrizo Plain, California, revealed by three-dimensional excavations. J. Geophys. Res. 111, B02306. doi:10.1029/2004JB003601.

McCalpin, J., 1996. Paleoseismology. Academic Press, San Diego.

Noriega, G.R., Arrowsmith, J., Grant, L.B., Young, J.J., 2006. Stream channel offset and late Holocene slip rate of the San Andreas Fault at the Van Matre Ranch site, Carrizo Plain, California. Bulletin of the Seismological Society of America 96, 33–47.

Ross, D.C., 1969. Map showing recently active breaks along the San Andreas Fault between Tejon Pass and Cajon Pass, southern California. U.S. Geological Survey Miscellaneous Geologic Investigations Map I-553, scale 1:24,000.

Runnerstrom, E.E., Grant, L.B., Arrowsmith, J.R., Rhodes, D.D., Stone, E.M., 2002. Displacement across the Cholame segment of the San Andreas Fault between 1855 and 1896 from cadastral surveys. Bulletin of the Seismological Society of America 92, 2659–2669.

Scholz, C.H., 1991. The Mechanics of Earthquakes and Faulting. Cambridge University Press, Cambridge.

Sherrod, B.L., Brocher, T.M., Weaver, C.S., Bucknam, R.C., Blakely, R.J., Kelsey, H.M., Nelson, A.R., Haugerud, R.A., 2004. Holocene fault scarps near Tacoma, Washington, USA. Geology 32, 9–12.

Sieh, K.E., 1978. Slip along the San Andreas fault associated with the great 1857 earthquake. Bulletin of the Seismological Society of America 68, 1421–1448.

Sieh, K.E., Jahns, R.H., 1984. Holocene activity of the San Andreas fault at Wallace Creek, California. Geological Society of America Bulletin 95, 883–896.

Sims, J.D., 1993. Chronology of displacement on the San Andreas fault in central California: evidence from reversed positions of exotic rock bodies near Parkfield, California. In: Powell, R.E., Weldonll II, R.J., Matti, J.C. (Eds.), The San Andreas Fault System: Displacement, Palinspastic Reconstruction, and Geologic Evolution. GSA Memoir, vol. 178. Geological Society of America, Boulder.

Stone, E.M., 1999. Geomorphology, Structure and Paleoseismology of the Central Cholame Segment, Carrizo Plain, California. M.S. Thesis, Arizona State University, Tempe.

Stone, E.M., Arrowsmith, J.R., Rhodes, D.D., Grant, L.B., 1998. Fault zone geometry and historic displacement along the Cholame segment of the San Andreas Fault, southern California. EOS Transactions AGU 79, 45 612.

Stone, E., Grant, L.B., Arrowsmith, J.R., 2002. Recent rupture history of the San Andreas fault southeast of Cholame in the northern Carrizo Plain, California. Bulletin of the Seismological Society of America 92, 983–997.

Toké, N.A., Arrowsmith, J.R., 2006. Reassessment of a slip budget along the Parkfield segment of the San Andreas Fault. Bulletin of the Seismological Society of America, Special Issue on the 2004 Parkfield Earthquake and Parkfield Experiment 96 (4B), S339–S348.

U.S. Geological Survey and California Geological Survey, 2006. Quaternary Fault and Fold Database for the United States, accessed July 20, 2008, from USGS web site: http//earthquake.usgs.gov/regional/qfaults/.

Vedder, J.G., Wallace, R.E., 1970. Map showing recently active breaks along the San Andreas and related faults between Cholame valley and Tejon Pass, California. U.S. Geological Survey Miscellaneous Geologic Investigations Map 1-574, scale 1:24,000.

Wallace, R.E., 1975. The San Andreas fault in the Carrizo Plain–Temblor Range region, California. In: Crowell, J.C. (Ed.), San Andreas Fault in Southern California: A Guide to San Andreas Fault from Mexico to Carrizo Plain. California Division of Mines and Geology Special Report, vol. 118, pp. 241–250.

Wallace, R.E., 1991. The San Andreas Fault System, California. U.S. Geological Survey, Professional Paper 1515. United States Government Printing Office, Washington D.C.

Wallace, R.E., Schulz, S.S., 1983. Aerial views in color of the San Andreas fault, California. U S Geological Survey Open File Report 83-98.

Young, J.J., 2004. Characterization of Fault Behavior Along the Central San Andreas Fault, California. Ph.D. dissertation, Arizona State University, Tempe.

Young, J.J., Arrowsmith, J.R., Colini, L., Grant, L.B., 2002. 3-D excavation and measurement of recent rupture history along the Cholame segment of the San Andreas Fault. Bulletin of the Seismological Society of America 92, 2670–2688.

Please cite this article as: Arrowsmith, J.R., Zielke, O., Tectonic geomorphology of the San Andreas Fault zone from high resolution topography: An example from the Cholame segment, Geomorphology (2009), doi:10.1016/j.geomorph.2009.01.002

The San Andreas Fault Zone in the Carrizo Plain, California: Review of Quaternary Geologic Investigations, Landforms, and Fault Activity.

Arrowsmith, J R., 1995, Appendix C, Coupled tectonic deformation and geomorphic degradation along the San Andreas Fault System, PhD. Dissertation, Stanford University, pp. 312-346.

C.1. Introduction

C.1.1. The Carrizo Plain as the Cadillac of the San Andreas fault system

Just as a Cadillac is a lavish automobile with many luxurious options, the Carrizo Plain area, situated in the southeastern California Coast Ranges (*Figure C.1*), is the premier example of the San Andreas Fault (SAF) system in California. The area has been long regarded as a site of world-class examples of strike-slip faulting. The SAF follows the northeastern side of the plain and all along it are offset, beheaded, and abandoned drainages that reflect that recent strike-slip motion. That motion apparently has been accommodated recently by great earthquakes; the most recent was the 1857 Fort Tejón earthquake [*Sieh*, 1978c]. The SAF in the Carrizo Plain has the largest accumulated post-early Miocene offset and is the oldest reach of the entire active fault system (315 km and ~15 Ma; [*Page*, 1990]). The area has provided evidence for both sides of the argument regarding the state of stress along the SAF ([*Wilcox et al.*, 1973]a strong SAF with early folding oblique to its strike; and [*Zoback et al.*, 1987]a weak SAF unable to sustain much shear traction and thus with folds, thrust faults, and the minimum horizontal stress striking nearly parallel to it).

This appendix provides descriptions of the location and setting of the Carrizo Plain; a summary of early research along the SAF zone there, and in particular, the Elkhorn Hills of the southeastern portion of the Carrizo Plain (*Figure C.1*); a review of the historic and paleoseismologic investigations along the SAF; and a discussion of the slip deficit along the Cholame segment and potential for rupture of M 7 earthquakes (prepared for the California Earthquake Prediction Evaluation Council (CEPEC) as part of its review of the Parkfield Earthquake Prediction Experiment). This appendix is meant to complement the research presented in *Chapters 3 and 4*.

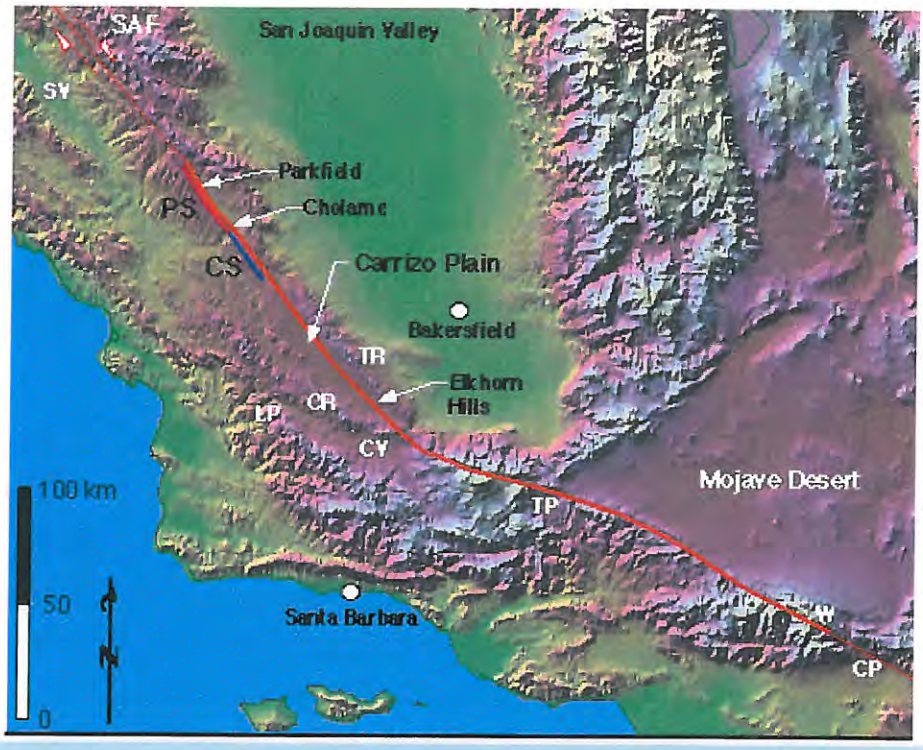

Figure C.1. Shaded relief map of central California showing the situation of the Carrizo Plain in the Coast Ranges. The orange line shows the surface trace of the SAF, and is thicker along the portion that is inferred to have ruptured in the 1857 earthquake [*Sieh*, 1978c]. TR is Temblor Range; CR is Caliente Range; CV is Cuyama Valley; LP is La Panza Range; SV is Salinas Valley; CP is Cajón Pass; TP is Tejón Pass; W is Wrightwood. Original relief map is from *Relief map of the world*: cylindrical projection; elevation data from ETOPO5 dataset; by Ray Sterner, Johns Hopkins University Applied Physics Laboratory.

C.1.2. Location and setting

The Carrizo Plain is located about 90 km west of Bakersfield and about 85 km north of Santa Barbara (*Figure C.1*). Most of it is in San Luis Obispo County, but the extreme northeastern portion is in Kern County. It is a narrow, undulating, and mostly undrained plain, about 15 km wide (NE-SW) and 75 km long (NW-SE) where elevations range from 1900' (580 m) in the alkali wetland of the Soda Lake basin to 2500' (760 m) in the Southern Elkhorn Hills of the extreme southeastern Carrizo Plain (*Figures C.1 and C.2*). The northwesternmost Carrizo Plain is dissected by the San Juan drainage which flows to the Salinas River. The ~100 km long Temblor Range separates the Carrizo Plain from the southern San Joaquin Valley on the northeast, with elevations of 3000' to 4,300' (914 to 1310 m). The Temblor Range tapers in elevation to the northwest where it merges into Table Mountain and Orchard Peak near Cholame. On its southwest side, the Carrizo Plain is separated from the Cuyama Valley by the ~80 km long Caliente Range. The maximum elevation of the Caliente Range is 5,100' (1550 m). The southern portion of the range is higher and more rugged, while the northwestern range is lower and merges with the northwestern Carrizo Plain. The La Panza Range lies west of the Cuyama Valley [*Dibblee*, 1962]. The Carrizo Plain is a perched basin, about 1000' higher than the

adjacent Cuyama Valley to the southwest, and about 1500' above the Southern San Joaquin Valley (*Dibblee*, 1962 suggested that the region was uplifted about 1000' since the late Pliocene).

The area was extensively farmed and grazed in the earlier part of this century, but now 90% of it is within the **Carrizo Plain Natural Area**: cooperatively managed by the Nature Conservancy, the United States Bureau of Land Management, and the California Department of Fish and Game. The objectives of this management include preservation of a representative sample of the historic southern San Joaquin Valley flora and fauna; conservation of threatened and endangered species and their habitat (including San Joaquin Kit Fox, San Joaquin Antelope Squirrel, Giant Kangaroo rat, short-nosed Kangaroo rat, Blunt-nosed leopard lizard, Greater and lesser Sandhill Cranes, and the California Condor); resolution of conflicts between intensive oil and gas development and endangered species habitat; provision for multiple use (including recreation and grazing); and protection and restoration of resource values (including cultural, soils, vegetation, paleontological, and geological). Indeed, the preservation of the distinctive landforms and geologic record of deformation along the San Andreas fault in the Carrizo Plain may be as important to society as the protection of endangered species.

The earliest known inhabitants of the Carrizo Plain area were the aboriginal population. Sometime 500 to 1000 years ago, a sophisticated native population flourished,

Figure C.2. Panchromatic SPOT image (courtesy of SPOT Image Corp.) of the southeastern Carrizo Plain illustrating the geography, physiography, and geomorphology of the Caliente Range foothills (at the bottom); the southeastern Carrizo Plain (center); and the Elkhorn Scarp defined in the northwest by the pressure ridges, including the Dragon's Back, and in the southeast by the southwest side of the Elkhorn Hills (northeast of the SAF, NEH is northern Elkhorn Hills, and SEH is Southern Elkhorn Hills). The

Elkhorn Plain separates the Elkhorn Hills from the Temblor Range (at the top right).

produced distinctive rock art (e. g., Painted Rock), and probably hunted the many animals attracted to the Carrizo Plain in wet times for its Soda Lake and gathered nuts and other vegetation in the surrounding mountains [*Cawley*, 1962]. The early aborigine culture that flourished in the Carrizo Plain was surely affected by great earthquakes, and may have even departed as the result of one (further research in the native descriptions of great earthquakes in this area could be interesting, similar research has been done for the coastal Indians of northwest California and their oral records of Cascadia subduction zone earthquakes). Spaniards came through the area in the 1700s and named the area "Carrizo" after the lush reeds growing there [*Cawley*, 1962].

C.2. Early geologic Investigations of the "San Andreas Rift" and the Elkhorn Hills

The Carrizo Plain area has long provided evidence for the recent right lateral motion along the fault, the amount of that slip, its diversion of drainage, and vertical motions resulting in interesting and unique topography. The recognition of the area's geomorphic and structural similarity and continuity with the SAF zone along much of its length was clear in 1906 [*Lawson and others*, 1908]. In January 1906, A. C. Lawson and H. W. Fairbanks led a field trip to the Carrizo Plain, and pictures from that trip are reproduced in the so-called Lawson Report [*Lawson and others*, 1908, volume I, plate 21]. It contains an interesting chapter entitled [3]The San Andreas Rift as a Geomorphic Feature.[2] The rift cuts across California from Humboldt County in the north to the Colorado Desert in the south and is

> a line or narrow zone characterized by peculiar geomorphic features, referable either directly to the modern deformation of the surface of the ground or to erosion controlled by the lines upon which such deformation has taken place.... The later movements on this line have given rise to minor features which subaerial and stream erosion have not yet obliterated, and it is these minor features chiefly which have attracted attention to the Rift by reason of their more striking contrast with more common geomorphic forms due to erosion. These minor features are chiefly low scarps and troughs bounded on one or both sides by low, abrupt ridges in which frequently lie ponds or swamps of quite small extent [*Lawson and others*, 1908, p. 25 - 26, V. 1].

The San Andreas Rift was recognized as the result of the interaction between geomorphic and tectonic processes. This text, written by Harold W. Fairbanks, records clear thinking about the geomorphology of the Carrizo (or Carissa) Plain:

> [In the northwestern end of the Carrizo Plain (near Simmler),] Here the width of the broken country is much greater than usual, being nearly a mile. A number of lines of displacement can be distinguished; some nearly obliterated, others comparatively fresh. This is a region of light rainfall and gentle, grass-covered slopes, presenting just such conditions as would preserve for hundreds of years the effects of moderate displacements. The Rift zone continues to be traceable along the western base of the Temblor Range, finally passing out onto the gently rolling surface of the eastern edge of the Carissa Plain. Broken and irregular slopes, cut-off ridges, blocked ravines, and hollows which are white with alkaline deposits from standing water mark the Rift.

> Carissa Plain has a length of about 30 miles. About halfway, the rift begins to be marked by a low and nearly obliterated bluff along its northeastern wall. This is at first little more than a succession of ridges or hills cut off on the side next to the level plains. These detached ridges finally become connected in a regular line of hills with a steep but deeply dissected slope toward the southwest, and long gentle slopes toward the northeast. This ridge is clearly a fault block, and now separates the southeastern arm of Carissa Plain from Elkhorn Plain. It probably originated during some earlier movements along the Rift; in fact, it is reasonable to suppose that it is of the same age as other important scarps which mark the Rift throughout its whole course, and which came into existence as a result of some mighty movement opening the earth for several hundred miles. Except for one slight bend, the ridge which we have been describing follows a straight course toward the southeast for a distance of nearly 20 miles, finally blending in a much larger mountain-like elevation. This has a height of perhaps 500 feet above the sink at its southern base. Its deeply dissected front is in line with the front of the ridge already described and the two appear to have originated together. The steeper face is deeply sculptured into gullies and sharp ridges, while the back slopes off gently toward the southern end of Elkhorn Plain. Plainly visible along the steep front of the line of hills are the lesser ridges and hollows produced during the last violent earthquake in this region, probably in 1857 (p. 41, V. 1, [*Lawson and others*, 1908]).

This clear and interesting description of the pressure ridges along the Elkhorn Scarp ([3]...deeply dissected slope toward the southwest, and long gentle slopes toward the northeast. This ridge is clearly a fault block, and now separates the southeastern arm of Carissa Plain from Elkhorn Plain[2]), and its coalescence into the Northern and Southern Elkhorn Hills (not yet so named; [3]Except for one slight bend, the ridge which we have been describing follows a straight course toward the southeast for a distance of nearly 20 miles, finally blending in a much larger mountain-like elevation.[2] These features have been investigated in detail by *Arrowsmith*, 1991b; *Arrowsmith*, 1991a; *Rhodes and Arrowsmith*, 1991; *Arrowsmith*, 1992a; *Arrowsmith*, 1992b; *Arrowsmith and Rhodes*, 1992 and *Chapter 4* of this Dissertation (Figure C.2). The conclusions of Fairbanks regarding the origin of these features are impressive in that, even in 1906 (and perhaps a realization from the 1906 earthquake), he recognized the scale of and suggested the nature of the physical deformation associated with the San Andreas Fault.

The next records of an early scientific visit to the Carrizo Plain come from *Arnold and Johnson*, 1910 who describe the area in passing, and propose names for some of the geographic elements there. Their investigation of the Carrizo Plain was peripheral to a study of the oil fields on the eastern side of the Temblor Range: the developed and well-known McKittrick, Midway, and Sunset fields. The authors spent the summer and fall of 1908 performing a detailed reconnaissance of parts of the Carrizo Plain district. Examination of their Plate I (Preliminary Geologic and Structural Map of the McKittrick-Sunset Oil Region, California), indicates that their mapping of the Carrizo Plain area was incomplete. They only covered the northern Carrizo Plain to the Caliente Range, and the western Temblor Range foothills in the central and southern Carrizo Plain. They did recognize definite evidence of horizontal offset along the SAF (including the 400'120 m offset of Wallace Creek [*Arnold and Johnson*, 1910]). They also proposed the names of some places, including the Panorama Hills, Panorama Point (in the central Carrizo Plain along the SAF), the Elkhorn Hills, the Elkhorn Scarp ([3]The name proposed for the terrace- like escarpment.... This feature is purely structural, following the great San Andreas fault or rift, and hence the application of the term 'scarp[1] (p. 20).[2] According to

their definition, the pressure ridges are only the northern portion of the escarpment separating the Carrizo Plain from the Elkhorn Hills (Figure C.2).
Arnold and Johnson's description of the topography along the San Andreas Fault in the Carrizo Plain and Elkhorn Hills region emphasizes their inference that its character resulted from the interaction of the tectonic and geomorphic processes:

> The topography produced by the latest movements in this region is unique and interesting. Low ridges on both or one side of elongated depressions, sunken areas in flat land, and great furrows along hill slopes are some of the evidences of the fracturing which occurred, as near as can be determined, in 1857. Definite evidence of horizontal movement has been found in the region, at one point of over 400 feet [Wallace Creek]. Actual measurements of between 8 and 20 feet of such displacement were made at the time of the San Francisco earthquake of 1906, which occurred at and near the northwestern end of the same zone of faulting. These latest faults are mostly of the normal type and are usually parallel or convergent at very low angles. Elkhorn Scarp is the most striking topographic evidence of the action of the San Andreas faulting. It is undoubtedly due to the dropping down of the Carrizo Plain or the elevation of the Elkhorn Valley about 200 feet. From the upper end of this scarp the fault zone extends into the Mount Pinos Mountains and thence into the San Gabriel and San Bernardino ranges.

The discussion of the Elkhorn Scarp's striking aspect followed by the description of its continuation to the south (into what is now called the Big Bend), reflects the possible structural association of the Elkhorn Hills and the beginning of the Big Bend. The Elkhorn Scarp is composed of several pressure ridges in the northwest, and a steep and incised southwest facing scarp to the southeast (see *Chapter 4 and Figure C.2*).

H. O Wood and J. P. Buwalda presented an abstract in the proceedings of the Cordilleran section of the Geological Society of America in 1931 in which they discussed the drainage patterns and other physiographic features along the SAF in the Carrizo Plain. They concluded that the drainage patterns were the result of [3]at least several thousand feet[2] of right lateral slip along the SAF, and that [3]the interpretation of the drainage patterns as merely subsequent streams is entirely inadequate as the offsets are practically without exception in the same direction[2] [*Wood and Buwalda*, 1931].
Several wells were spudded into the area of the southern Carrizo Plain during the heyday of oil exploration in the 1930s and 1940s, but none was successful [*Graff*, 1962].
In the 1950s and 1960s, Tom Dibblee mapped the region, and noted both the SAF and a southwest dipping fault parallel to the SAF in the southern Elkhorn Hills, as well as some of the grabens in the northern Elkhorn Hills. In their classic paper of 1953, Mason Hill and Dibblee noted both the offset drainages of the Carrizo Plain and [3]Recently developed trenches which trend southward into the fault have been observed on the southwest side of the Temblor Range. These are oriented correctly to be tensional in origin and due to right lateral movement along the San Andreas[2] [*Hill and Dibblee*, 1953, p. 446]. They refer to the grabens in the Elkhorn Hills that are investigated in *Chapter 4* (and are evident in *Figure C.2*). As a part of the presentation of Dibblee's work, the Carrizo Plain was the area of the 1962 field trip of the San Joaquin Geological Society and Pacific Section of AAPG and SEPM [*Dibblee*, 1962]. He comments about the geomorphology of the Carrizo Plain and vicinity:

> The Paso Robles formation was deposited as alluvial fill throughout Salinas Valley, and derived from the neighboring ranges as they rose. As the valley area became filled, the

> source areas were eventually reduced to low relief, as indicated by the old erosion surface on the crests of the Temblor and Caliente Ranges [see *Galehouse*, 1967 for details on the Paso Robles formation]. The Paso Robles formation was deposited when Carrizo Plain was being carved out by a major stream that must have meandered and flowed northwestward, as suggested by several steep-sided crescent-shaped erosional re-entrants carved into the hills at its southwestern border near Soda Lake. This episode was followed by uplift of the entire region by more than 1,000 feet. This uplift resulted in severe dissection by the San Juan drainage system, and in abandonment of Carrizo Plain by the stream that once flowed through it. The regional uplift was accompanied by lateral movement on the rift zone and associated local deformation. These movements formed the Elkhorn Hills, in which the Paso Robles gravel became anticlinally arched on the northeast side; and formed the present alignment of scarps, ridges, and trenches that extend northwesterly to and beyond Cholame Valley. Throughout this area stream washes that drain southwesterly from the Temblor Range are offset northwestward as they cross the fault, some as much as half a mile. These features clearly show that the north-eastern block on the rift zone has been shifting south-eastward relative to the southwestern block. In many places adjacent to and near the rift zone the alluvial gravel of the Paso Robles formation has been compressed into numerous minor domed folds with axes that trend slightly more west than does the rift zone. These compressive features no doubt are also the effect of right lateral distortion of the ground near the rift zone [*Dibblee*, 1962, p. 12].

Robert E. Wallace was the next geologist to turn his attention to the SAF in the Carrizo Plain area. *Wallace*, 1968 investigated the offset channels and is discussed in more detail below. The 1973 contribution was a short report on the en échelon geometry of adjacent segments of the SAF (an example of which came from the Carrizo Plain) in which he observed that the length of the longest continuous fractures was 10 to 18 km similar to the depth of the deepest earthquake foci suggesting that the fractures were roughly equidimensional [*Wallace*, 1973].

In 1975, Bob Wallace presented a less detailed description of the right laterally offset landforms than his 1968 paper, and included a discussion of the patterns of fault related stream channels in the Carrizo Plain area. He notes drainages offset right-laterally, drainages deflected by sliver ridge and pressure ridge uplift and offset, and false offsets that could result from differential uplift deflecting drainages, or en échelon fractures over the fault zone followed by subsequent streams. He included a discussion of vertical displacements that referred to sag ponds between strands of the SAF, the observation that the ratio of vertical to horizontal slip was commonly 1 to 10 or 1 to 20 (probably as a consequence of juxtaposed, horizontally offset topography), and an interesting discussion of the Elkhorn Hills:

> The Elkhorn Hills are an elongate upwarp, the crest of which is broken into a series of grabens. Some of the grabens have a sigmoid pattern..., suggestive of broad strike-slip strain. The upwarp may have formed when gouge and brecciated material in a fault zone approximately 2 km wide was squeezed upward in a semi-plastic state by regional stresses normal to the fault zone. The overlying, poorly consolidated, Paso Robles formation, once upraised, has slid laterally, producing large areas of landslides on the flanks of the upwarp and grabens at the crest. The grabens were later bowed by right-lateral strain into the sigmoid patterns now present. Large landslide blocks moved southwest, crossed the most active strand of the San Andreas fault, and were then transported northwestward from their original position ([*Wallace*, 1975, p. 244]; *Figure C.2*).

Along with Wallace's textual contributions, three maps of the area were published in the early 1970s. For the first *Vedder and Wallace*, 1970, they combined field and aerial photographic studies to produce a map of the recently active breaks along the SAF and

related faults in the Carrizo Plain area. They also commented on the locations of diverted and offset drainages, notches, cracks, depressions, benches, scarps, elongate ridges, moletracks and landslides. Associated with that work, and published in the same year, was the geologic map of the Wells Ranch and Elkhorn Hills quadrangles areas in the southeastern Carrizo Plain ranging from about the crest of the Temblor range to the crest of the Caliente Range [*Vedder*, 1970]. The map shows the structure within the uplifted and deformed Paso Robles formation of the Elkhorn Hills, as well as the locations of wells that were used to generate the geologic cross-sections presented with the map. Because the map covers two quadrangles, the Elkhorn Hills are not covered in great detail; however, it is useful in its illustration of the neighboring structures. Three things of interest are: 1) Vedder shows an area parallel to the SAF and on the northeast margin of the Elkhorn Hills as being as "Zone of Large Scale Landslides" an area whose morphology and structure is interpreted in *Chapter 4* to result from repeated slip along southwest dipping reverse faults. 2) In Vedder's cross-sections, the area underneath the SAF is described as "Zone of probable intense deformation. Lack of subsurface data precludes structural and stratigraphic interpretation." 3) The Paso Robles formation in the Elkhorn Hills is shown to overlie the Bitterwater Creek shale, an upper Miocene marine unit; the contrast in material properties between it and the Paso Robles formation may contribute to the localization of the deformation.

Another geologic map of importance is *Dibblee*, 1973. This map of the regional geology (Carrizo Plain, Temblor, Caliente, and La Panza ranges) shows the juxtaposition of different rock types across the SAF, and that the SAF truncates some of the earlier structures (e.g., the Wells Ranch Syncline in the southeastern Caliente Range).

With the suggestion and inspiration of Richard H. Jahns, Kerry Sieh carried out a detailed investigation or the chronology of large earthquakes along the SAF in southern California. Much of this work, initiated as his PhD. research, is described below in the historic and paleoseismology and Cholame segment sections. As part of the research about the 1857 earthquake, Kerry Sieh noted that along the SAF in the area of the Elkhorn Hills, right-lateral strike-slip offsets apparently formed in the 1857 earthquake abruptly decreased 10-20% (9 to 7 m; although later work has indicated that it may have been 7 to 6 m -- see *Chapter 4*; nevertheless, slip apparently decreased in this area) compared to those in the northwest. That observation led him to look to the side of the SAF for distributed deformation that might account for the decreased slip. He found good evidence for secondary faulting in the Elkhorn Hills:

> Near the southern end of the Carrizo Plain, the San Andreas fault is the southwestern boundary of the 15-km-long Elkhorn Hills.... Most of the northeastern base of the Elkhorn Hills displays scarps indicative of thrust faulting. Thus the Elkhorn Hills appear to constitute a crustal block that has risen between the San Andreas and the thrust fault, herein named the Elkhorn fault. Large linear grabens and closed depressions within the Elkhorn Hills indicate that a great deal of internal deformation has taken place also. Small scarps in Holocene (?) alluvial deposits along the Elkhorn fault are so fresh as to suggest that they may have formed during the 1857 event.... Alluviation since this event has obscured any clear indication of a lateral slip component on this fault. However, it seems very unlikely that the latest movement on the sinuous, very low-angle thrust fault could have included more than 1 m of lateral slip. Many of the faults in the Elkhorn Hills also display relatively young scarps and, in several closed depressions, many fissures and sinkholes related to "piping" are demonstrably historic. The evidence for ongoing deformation of the Elkhorn Hills suggests that substantial lateral deformation within the hills may have accompanied the 1857 event. Thus, the change form 9 to 7 m of lateral

> slip in this region may be less abrupt when measured across the entire zone of deformation. ([*Sieh*, 1978c, p. 1445]; *Figure C.2*).

Thomas and Sieh, 1981 investigated the Quaternary formation of the Elkhorn Hills as a consequence of sequential development of folds and thrusts:

> Trenching and geomorphologic mapping reveal that the welt [the Elkhorn Hills] is a product of crustal shortening which has been accomplished primarily by folding and reverse faulting. These structures have developed sequentially northwestward from the San Andreas Fault and suggest systematic enlargement of the landform normal to the fault. The most recent episodes of shortening are expressed at the margin of the hills where a young fault cuts active alluvial fans. Discrete faulting events are recorded by colluvial wedges in the fan deposits adjacent to the fault scarp. Equivalent amounts of separation between the colluvial wedges indicate that the two most recent seismic events have comparable displacements and, if the fan surface is aggrading uniformly, similar recurrence intervals. Similar but older low angle reverse faults are inferred to exist within the Elkhorn Hills. Gentle monoclines dip away from each reverse fault and towards the San Andreas Fault. Relative ages of the structures were determined by comparing drainage development, slope angle, and alluvial fan size associated in the lithologically uniform hills. The style of deformation and its sequential development are consistent with shortening perpendicular to the San Andreas Fault elsewhere along the "Big Bend" [*Thomas and Sieh*, 1981]; *Figure C.2*).

See *Chapter 4* for a discussion of detailed mapping and inferences regarding the structure and temporal development of the Elkhorn Hills.

C.3. Historic and Paleo-seismicity

The mode of strain release along the principal traces of the San Andreas fault system varies from continuous creep to infrequent large earthquakes. *Allen*, 1968 pointed out the distribution of the portions of the SAF with different modes of strain release, and discussed several effects and hypothesized causes. The two sections of the fault with the least modern seismicity were those that have recently experienced a great earthquake (the 1857 and 1906 breaks). These segments have fairly well-defined geomorphic traces (in contrast to the broader zones of creeping sections, e.g., the SAF in the Carrizo Plain versus the central creeping section that lies between San Juan Bautista and Parkfield), and both have bends in their strike. The 1906 segment has the Santa Cruz Mountains bend, and the Carrizo/Fort Tejón segment has the Big Bend.

The boundaries of the 1857 stretch were defined by investigations of felt reports and observations of the surface rupture ([Wood, 1955], and later by *Sieh*, 1977; *Agnew and Sieh*, 1978; *Sieh*, 1978b; *Sieh*, 1978c; *Figure C.3*). The southern end was correlated geologically with the increasing complexity of the SAF system as it interacts with the northernmost spreading of the Gulf of California in the Salton Trough. The transition is in the area of Cajon Pass, northwest of San Bernardino. The northern end of the rupture may be defined geologically by the 1-2 km right step in the SAF trace in the Cholame Valley. In this area, the contrast in basement types changes, with southeasternmost significant Franciscan rocks on the northeast juxtaposed against the Salinian basement [*Hanna et al.*, 1975]. However, anecdotal reports of the event suggested that it ruptured northward into the creeping section, and thus the significance of the Cholame stepover as a rupture barrier or segment boundary is still debated. The other gross structural feature of the 1857 break that may affect its style of strain release is the Big Bend in which the

SAF changes strike from ~N40W (Southern Santa Cruz Mountains to the Northern Carrizo Plain) to ~N70W near Tejon Pass [*Allen*, 1968; *Jennings and Strand*, 1969] (*Figure C.1*). *Allen*, 1968 suggested that the bend in strike and basement contrast were important controls in the style of strain release in both the 1906 and 1857 earthquakes.

C.3.1. 1857 earthquake

Investigations of the 1857 event conclude that it was part of a major earthquake sequence. These studies have included documentation of the felt effects of the earthquake sequence [*Wood*, 1955; *Agnew and Sieh*, 1978; *Sieh*, 1978c], (*Figure C.3*). The felt reports were limited by the sparse population of central California at the time (the majority of the state's population was in the area between San Francisco, Sacramento, and the North-central Sierra Nevada responding to the Gold Rush; e. g., [*Agnew and Sieh*, 1978]). At least 5 foreshocks occurred in the 9 hours before the event, including a late evening shock on January 8 of ~M¾3.5 near San Francisco; possibly 2 moderate events during the early morning and pre-dawn hours; a dawn shock; and a sunrise shock on January 9 (*Figure C.3*). The latter two events may have occurred along the Parkfield-Cholame section of the SAF, immediately northwest of the Carrizo segment, based upon comparisons of felt reports of the foreshocks with isoseismals produced by twentieth century Parkfield events (*Figure C.3*). Thus, the Parkfield-Cholame section of the SAF is

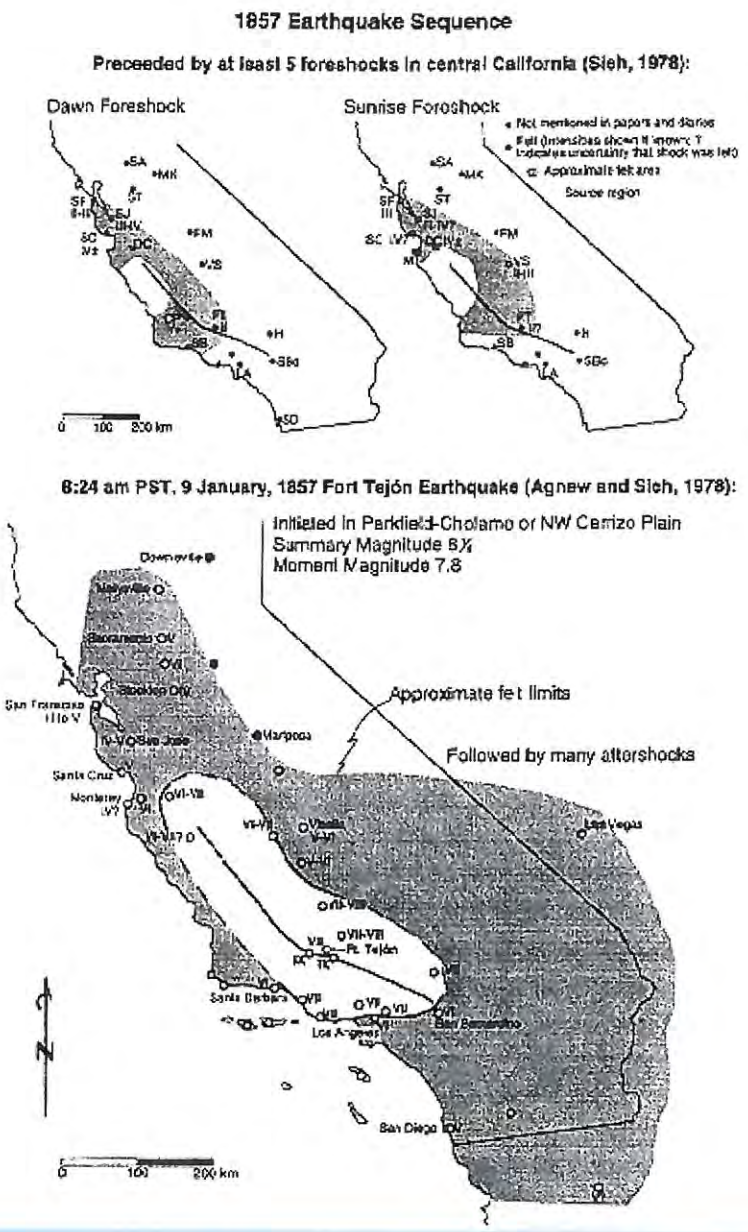

Figure C.3. Felt intensity distributions for the 1857 earthquake sequence showing the two most prominent foreshocks [*Sieh*, 1978a], and the mainshock: the Fort Tejón Earthquake [*Agnew and Sieh*, 1978].

a transitional reach with both creep and earthquake events and 1857-type events may be triggered by such a moderate earthquake [*Sieh*, 1978c; *Sieh and Jahns*, 1984].

Based upon foreshock locations, main shock isoseismals, and peak slip; the epicenter of the main event (~8:24 am PST, January 9, 1857) is inferred to be in the northwestern Carrizo Plain or along the Parkfield-Cholame section [*Agnew and Sieh*, 1978; *Sieh*, 1978c; *Goter*, 1988], and the rupture probably propagated unilaterally southeastward

([*Ellsworth*, 1990]; *Figure C.3*). Modified Mercalli Intensities of V (felt by nearly everyone, some dishes and plaster broken, and tall objects disturbed) were noted over much of California (an area approximately bounded by the Northern Sierra Nevadas; Las Vegas, Nevada; San Diego; and San Francisco). Intensities of VI (felt by all, many frightened, a few instances of damaged chimneys and fallen plaster) were felt in Los Angeles, VI-VII (slight to considerable structural damage, everybody runs outdoors) were felt in the southern San Joaquin Valley, and IX and greater (considerable to complete damage and panic) were felt along the fault. The duration of shaking was between 1 and 3 minutes which is consistent with unilateral southeastward rupture [*Ellsworth*, 1990]. Many aftershocks were felt in the weeks and months following the event, although as time from the event became greater, it is harder to differentiate the felt events from "normal" moderate California earthquakes. However, the two best identified aftershocks were: 1) A large event northwest of Tejon Pass that was felt in Cajon Pass, Los Angeles, Ventura, Visalia, and Sacramento; and caused damage at Fort Tejon (10:30 to 11 pm PST, January 9, 1857); and 2) A M~6 event located between Tejon and Cajon Passes and felt in San Diego, San Bernardino, Los Angeles, Santa Barbara, and Castaic Junction (~5 pm PST, January 16, 1857) [*Agnew and Sieh*, 1978].

Along with the investigations of the felt effects of the 1857, earthquake, abundant geomorphic evidence for the event is preserved in the Carrizo Plain (e. g., [*Arnold and Johnson*, 1910; *Dibblee*, 1962; *Wallace*, 1968; *Sieh*, 1977; *Sieh*, 1978c; *Wallace and Schulz*, 1983; *Wallace*, 1990; *Grant and Sieh*, 1993]). H. W. Fairbanks, in [*Lawson and others*, 1908, p. 41, V. 1], described the geomorphology of the SAF in the Carrizo Plain and recognized that it had "probably originated during some of the earlier movements along the Rift;" and that "Plainly visible along the steep front of the line of hills described are the lesser ridges and hollows produced during the last violent earthquake in this region, probably in 1857." [*Arnold and Johnson*, 1910], p. 20] also identified the evidence for recent offsets: "The topography produced by the latest movements in this region is unique and interesting. Low ridges on both or one side of elongated depressions, sunken areas in flat land, and great furrows along hill slopes are some of the evidences of the fracturing which occurred, as near as can be determined, in 1857." *Wallace*, 1968 presented a study on the offset streams of the Carrizo Plain: 130 streams along the SAF in the Carrizo Plain were noted to have been affected by right lateral slip. 40 of those channels were offset 20 to 50 feet, which Wallace suggested corresponded to slip from the 1857 Fort Tejón earthquake. The observation that many streams had more than 50 feet of offset suggested that recurrent earthquakes along this reach of the SAF had slipped within a narrow zone and consistently offset the drainages.

While many other geologists surely recognized the geomorphic effects of the 1857 earthquake, Kerry Sieh [*Sieh*, 1977; *Sieh*, 1978c] was the first to thoroughly investigate the distribution and extent of the smallest offsets along this reach of the SAF (although *Wood*, 1955 compiled some of the contemporary accounts of surface offsets). Sieh hypothesized that the smallest offsets of the many reference features such as stream channels, landslides, and alluvial fans along this reach were attributable to coseismic and postseismic slip in the 1857 earthquake, assuming that they were formed before that earthquake and after the penultimate one [*Sieh*, 1978c]. Features were first identified in aerial photographic studies, and then the entire reach from Parkfield to Cajón Pass was traversed and the 150 measurements of offsets were based upon at least one quarter hour

field investigation including detailed sketching and careful measurement using a tape. The resulting estimated distribution of offset was illustrated in *Sieh and Jahns*, 1984 which included data added after the publication of *Sieh*, 1978c.

With regard to the inferred 1857 slip distribution, a few points are worth mentioning.

1) The northern extent of the rupture is inferred to be at least Highway 46 in the Cholame area based upon an observation of a ~3.5±0.2 m gully 1.3 km SE of Highway 46, and contemporary accounts of the "earthquake crack" extending 80 km northwest of Cholame (into the creeping reach-[*Wood*, 1955; Sieh, 1978c]; *Figures C.3 and C.4*). This offset includes ~12 cm cumulative offset in the 1901, 1921, 1934, and 1966 Parkfield earthquake sequences. However, offsets along the SAF for ~20 km SE of Highway 46 are ambiguous, and other interpretations of this site suggest that geomorphic processes have accentuated the current offset [*Sims*, 1989]. *Lienkaemper and Sturm*, 1989 also argue that the *Sieh*, 1978c estimates for offset 21.5 km SE of Highway 46 are 2 m too low. See below for more discussion of these offsets.

2) Maximum right-lateral offsets in the 1857 earthquake are at least 7 m, and two examples of 9 m offsets are located a few hundred meters SE of Wallace Creek [*Sieh*, 1978c]. Again, the interpretation of offset gullies is difficult, and subsequent studies have argued that offsets determined geomorphically may be a maximum [*Grant and Sieh*, 1993; *Sims et al.*, 1993]; see below.

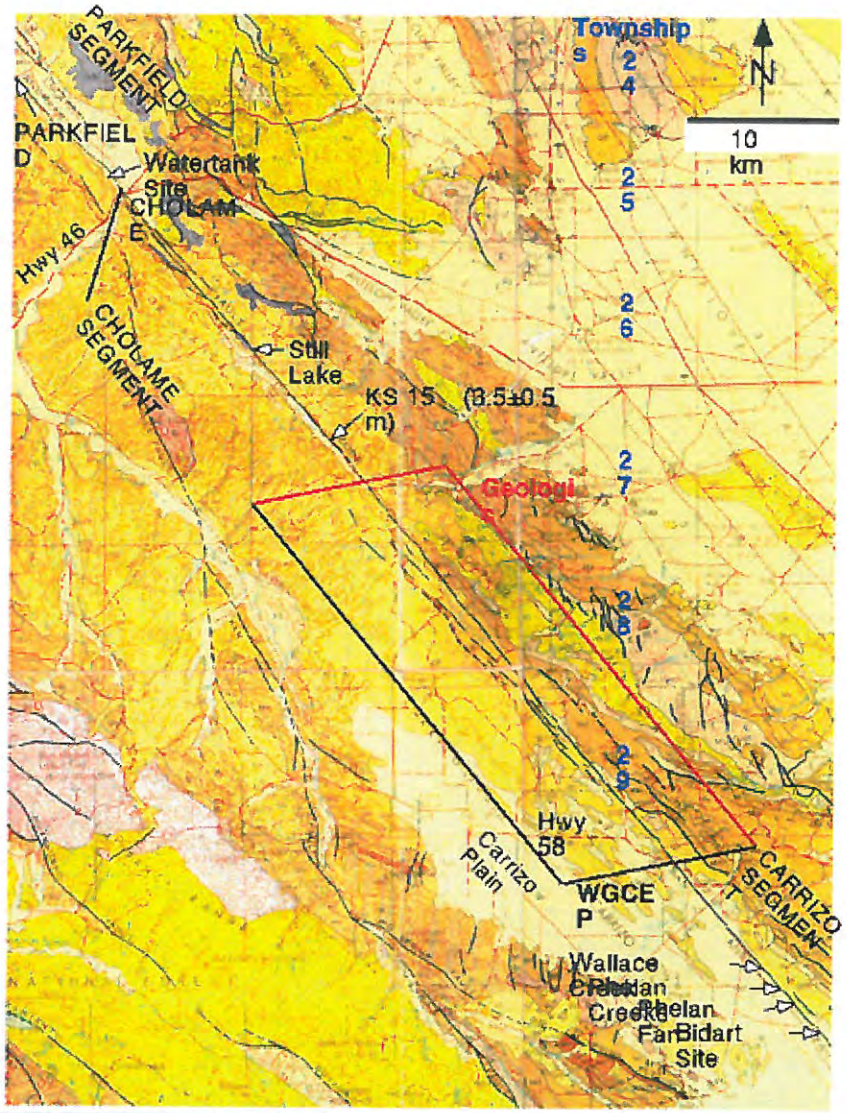

Figure C.4. Important sites around the northern portion of the Carrizo Plain and the Cholame segment of the San Andreas Fault. The definition of the segmentation of the SAF by *WGCEP*, 1988. That for the Cholame segment is illustrated along with segment boundaries suggested by geologic evidence: the 1857 slip increased by a few meters and the surface trace bends in the area of Bitterwater Canyon. The Watertank site is a paleoseismic site [*Sims*, 1987]. Still Lake is a site that has been reconnoitered and is recommended for paleoseismic investigation. Note that it is 73 km between the existing paleoseismic sites in the Carrizo Plain and the Watertank site. KS 15 and the associated number refers to offset channel #15 from *Sieh*, 1978c and L&S '89 refers to the higher offset determined for the same channel by *Lienkaemper and Sturm*, 1989. James E. Freeman surveyed township boundaries from township 24 south in 1855 and 1856, and *Grant and Donnellan*, 1994 recovered original monuments from that survey spanning the SAF in the Carrizo Plain near Wallace Creek. The background is from the 1:250,000 scale San Luis Obispo and Bakersfield sheets of the state geologic map.

3) Evidence throughout the 1857 break (and particularly in the southeastern Carrizo Plain) is consistent with a single, large offset, rather than more, smaller offsets or creep [*Sieh*, 1978c].
4) Many subsidiary faults along the SAF must have also slipped in the 1857 break, but only two areas show geomorphic evidence significant secondary deformation: the Littlerock, Nadeau, and North Branch San Andreas faults in the western Mojave desert region between Littlerock Creek and Leona Valley; and in the Elkhorn Hills (bounded on their southwest margin by the SAF) of the southeasternmost Carrizo Plain where secondary normal and reverse faults display fresh scarps [*Sieh*, 1978c], and [*Arrowsmith*, 1991b; *Arrowsmith*, 1991a; *Arrowsmith*, 1992a; *Arrowsmith*, 1992b; *Arrowsmith and Rhodes*, 1992; *Arrowsmith*, 1995]; *Figures C.2 and C.5*. Slip along the SAF adjacent to the Elkhorn Hills apparently decreased abruptly by 10-20%, and that deformation may be accommodated by distributed deformation across the Elkhorn Hills [*Sieh*, 1978c] and [*Arrowsmith*, 1991b]. Recall the discussion above.
5) The southeastern extent of the 1857 break was probably as far southeast as Wrightwood (evidence from disturbed trees [*Sieh*, 1978c; *Meisling and Sieh*, 1980]) where the smallest offsets attributable to the 1857 event are about 3 m.
6) The inferred rupture length was at least 300 km.
7) Separating the 1857 slip distribution into 4 segments of similar slip magnitude, *Sieh*, 1978c determined a seismic moment for the event (including any afterslip) of 5.3 to 8.8 x 1027 dyne-cm somewhat larger than the 1906 event (the variation results from different possibilities for the locations of the ends of the rupture, as well as its depth10 or 15 km). A moment magnitude of M = 7.9 was determined by *Hanks and Kanamori*, 1979, while M = 7.8 was determined by *Ellsworth*, 1990.

C.3.2. Slip rates along the SAF

Starting with *Wallace*, 1968, analyses of the average Holocene slip rate along the SAF have found good sites in the Carrizo Plain. *Sieh and Jahns*, 1984 used radiocarbon dating and stratigraphy to obtain time constraints for incision of downstream channel segments at Wallace Creek (the name of which was proposed by them, because it was identified and discussed by *Wallace*, 1968; *Figure C.6*). The present and previous (now beheaded and abandoned) channels at Wallace Creek were occupied 3,700 and 10,000 yr ago and are now offset ~130 m and ~350 m respectively. These data and the 475 m offset of an alluvial fan give a late Holocene slip rate for this segment of the San Andreas fault of 33.9 ± 2.9 mm/yr for the past 3,700 yr and 35.8 + 5.4/-4.1 mm/yr for the past 13,250 yr. *Wallace*, 1968 also suggested an investigation of the offset and abandoned channels of Phelan Creeks approximately 2 km southeast of Wallace Creek (*Figure C.6*). In an

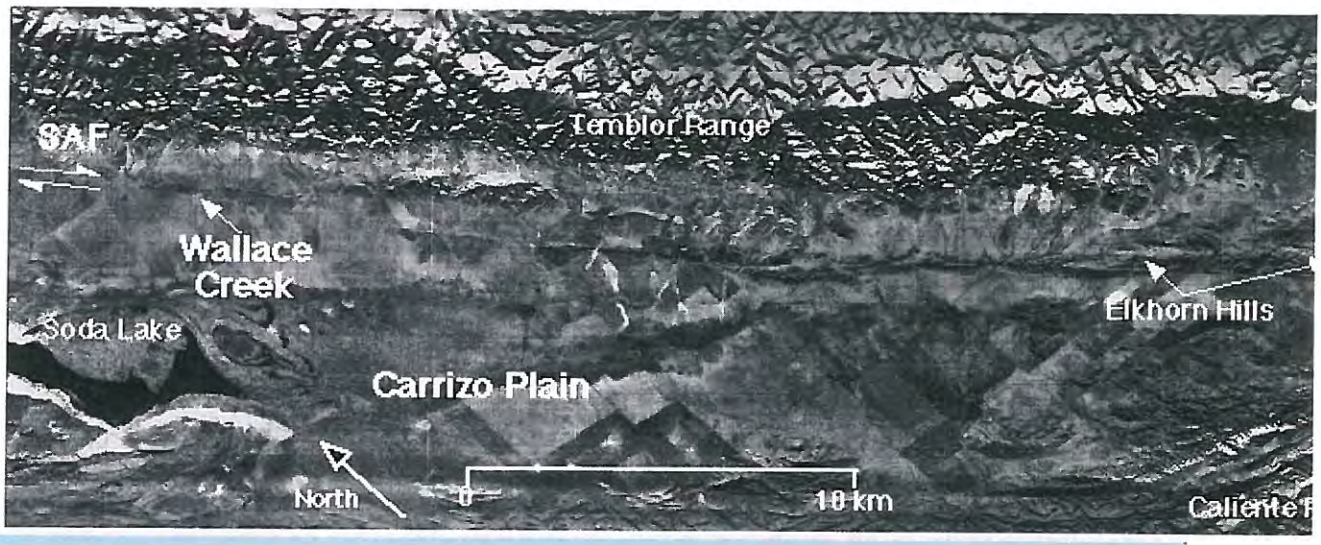

Figure C.5. Side Looking Airborne Radar image of the Carrizo Plain area. Look Direction is northeast. The rugged topography of the Temblor Range along the north side of the image is a contrast to the flatter Carrizo Plain. The patchwork texture of the Carrizo Plain results from variable grazing and farming practices on different properties. Soda Lake is the lowest portion of the Carrizo Plain (~1900' elevation). The SAF follows the southwestern foothills of the Temblor Range. Local relief along the SAF and a more westerly SAF strike increase toward the southeast. In the area of Wallace Creek in the northwest, little local relief is evident and Recent fault activity has been confined to dominantly strike-slip along a narrow fault zone. Toward the southeast in the Elkhorn Hills, on the other hand, local relief and secondary fault activity increase, possibly the result of increased contraction across the SAF zone caused by a more westerly SAF strike as it enters the Big Bend.

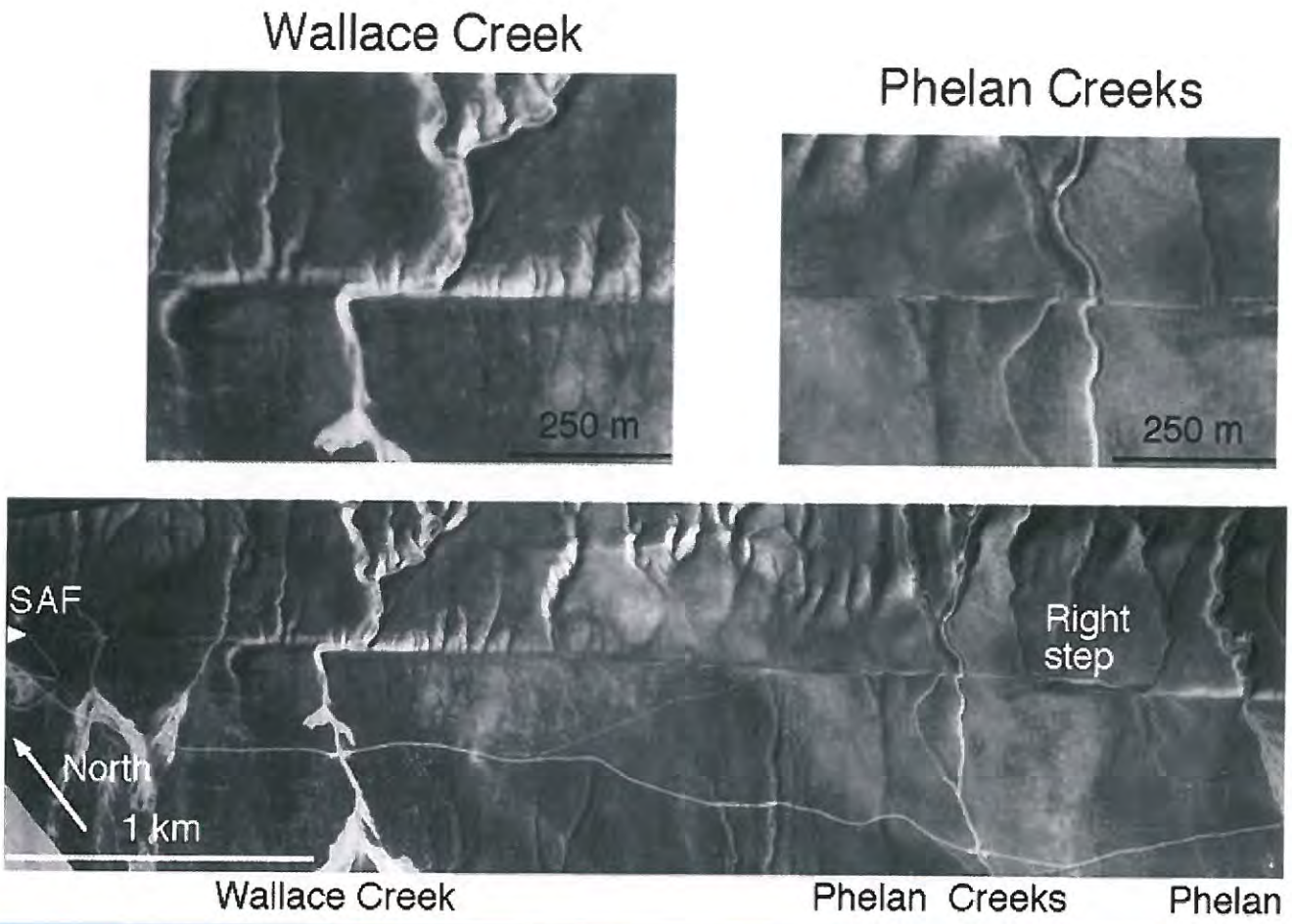

Figure C.6. Aerial photograph of the SAF zone in the central Carrizo Plain. The locations of the important landforms and paleoseismic sites of Wallace Creek [*Wallace*, 1968; *Sieh and Jahns*, 1984]; Phelan Creeks [*Sims et al.*, 1989; *Sims et al.*, 1993; *Sims et al.*, 1994]; and Phelan Fan [*Grant and Sieh*, 1993] are shown. The trace of the SAF is indicated by the triangles on the lower photo. Note the en échelon, right stepping pattern of the SAF in this area. Local extension associated with a right step in the southeastern portion of the lower photograph has produced a small graben [*Sims et al.*, 1990]. The upper two photos are blow-ups to show the detail of Wallace Creek and Phelan Creeks. Photograph courtesy of the Fairchild Aerial Photography Collection at Whittier College. Original photograph scale 1:24,000; photograph date 26 February, 1936.

extensive paleoseismic investigation of 23 trenches, *Sims et al.*, 1989; *Sims*, 1994; and *Sims et al.*, 1994 developed a chronology for the offset of the three sets of downstream channels at Phelan Creeks and determined a slip rate of 35.1 ± 2.6 mm/yr from the 238 ± 15 m offset of a channel system incised before 6778 ± 62 CAL B.P. For a channel incised a few decades after 3,764 ± 45 yr CAL BP or 3335 ± 129 yr CAL B.P. and offset 122.2 ± 1.5 m, slip rates of 32.5±2.1 mm/yr and 36.4±5.0 mm/yr are determined. *Grant and Donnellan*, 1994 recalculated the 14C dates from *Sieh and Jahns*, 1984 to determine a revised late Holocene slip rate of 33 ± 3 mm/yr. Clearly, these data are similar to that of

Sieh and Jahns, 1984, and an average late Holocene slip rate of ~33 mm/yr may be assumed.

C.3.3. Previous events slip and timing

The tectonic landforms along the 1857 reach and evidence for significant geologic offset along the SAF suggest that slip events must recur. Along much of the 1857 reach, and in particular in the Carrizo Plain, offsets of gullies are apparently clustered about integer multiples of the inferred 1857 offset and suggested that each part of the fault experienced a characteristic amount of slippage in the past few earthquakes. Around Wallace Creek, the offset has been 7 to 12.3 m during the last 3 large earthquakes [*Sieh and Jahns*, 1984]. However, with the typical dating and measurement errors and possibly variable slip distribution, it becomes difficult to differentiate between 3 7m events and 2 10.5 m events that might have caused a 21 m offset.

A re-interpretation of the offset in the last few events was presented in *Grant and Sieh*, 1993. They suggest that the 9 m offsets in the Carrizo Plain may result from either highly variable slip in 1857, or more regular 7 m 1857 slip, and 2 - 3 m slip in a previous event. Observations from the 1992 Landers, California earthquake favor a highly variable slip distribution (e.g., [*Antonellini et al.*, 1992; *Sieh and others*, 1993; *Arrowsmith and Rhodes*, 1994]); while interpretations of a complex rupture history favor different events with different magnitudes of slip ([*Grant and Sieh*, 1994], see below and *Figures C.7 and C.8*). Geodetic reoccupation of historic survey markers by *Grant and Donnellan*, 1994 favor the highly variable slip distribution because they independently determined that at least 9.5 ± 0.5 m of slip occurred along the SAF near Wallace Creek in 1857.

The conclusion of recurrence of great earthquakes and the implications for the model of characteristic earthquakes [*Schwartz and Coppersmith*, 1984], as well as the threat to the growing population of southern California, drove efforts to determine the recurrence interval for these events. Given the slip rate of ~35 mm/year, a slip predictable recurrence interval for earthquakes might be determined by assuming that the slip in 1857 would be repeated and the event would not occur until that slip had accumulated (for

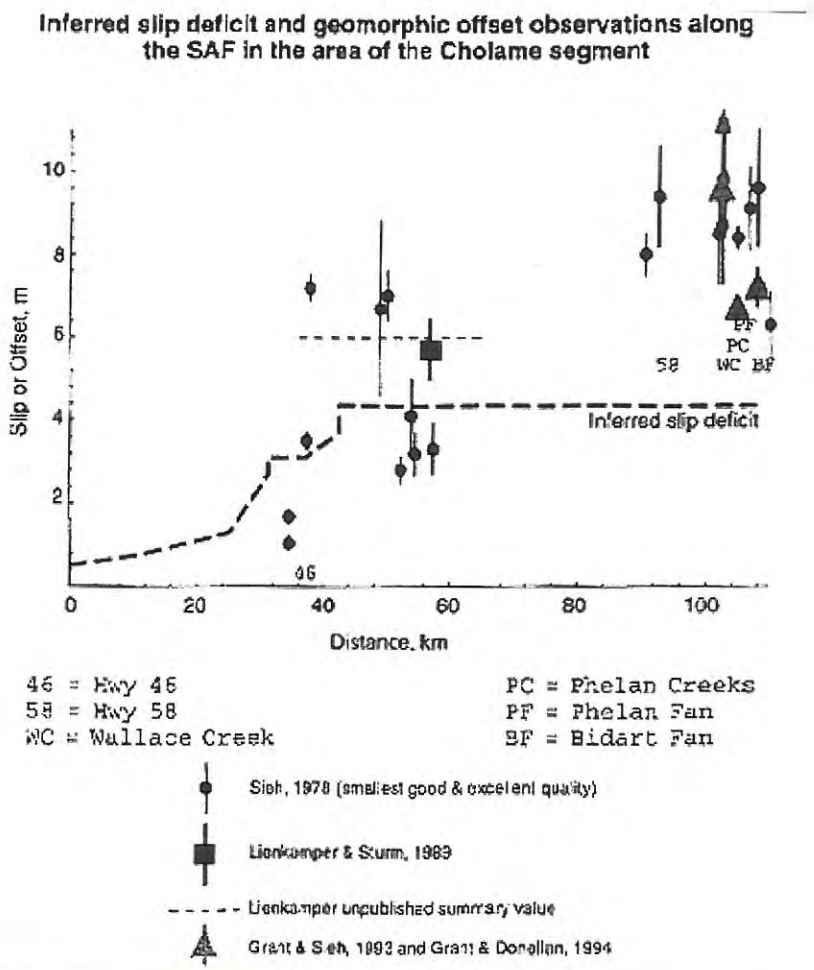

Figure C.7. Inferred slip deficit and geomorphic offset observations along the SAF in the area of the Cholame segment. The bold dashed line shows the inferred historic slip deficit assuming that all slip was released in the 1857 earthquake. The northern portion is constrained by observations of historic offset by *Lienkaemper and Prescott*, 1989, and the southern by assuming that the deficit accumulates at the long term slip rate of 33 mm/yr. Geomorphic observations are shown with error bars: circles are from Sieh, 1978c; square is from *Lienkaemper and Sturm*, 1989; the thin dashed line is the summary value from *J. Lienkamper, unpublished field notes*, 1987-1995; and the triangles show the results of *Grant and Sieh*, 1993; *Grant and Sieh*, 1994. The result from *Grant and Donnellan*, 1994 was 11 ± 2.5 m over a one mile aperture spanning the SAF.

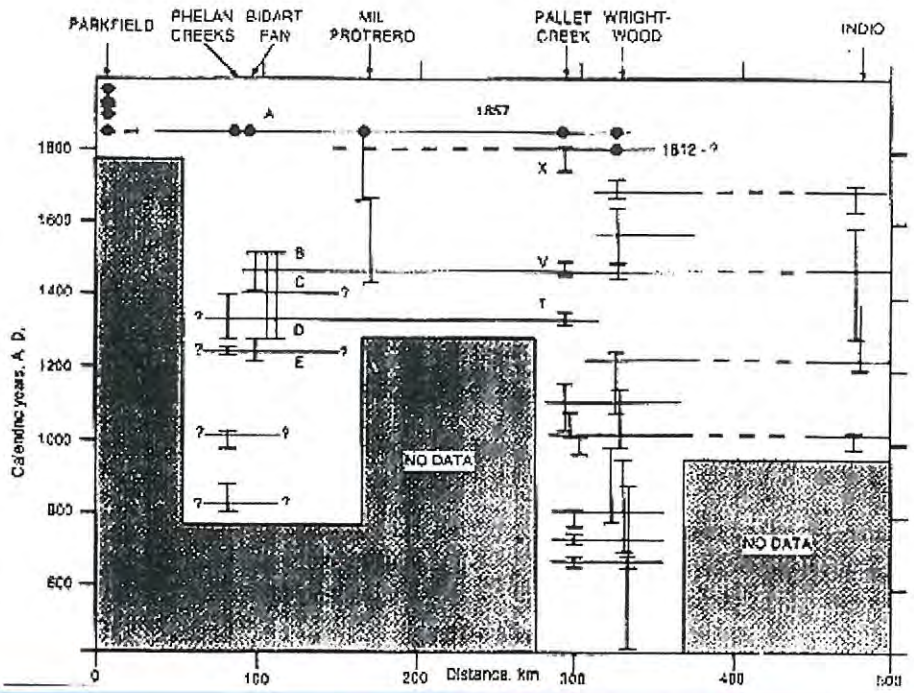

Figure C.8. Inferred temporal and spatial distribution of surface rupturing earthquakes along the SAF in central and southern California. (modified from *Grant and Sieh*, 1994 by adding inferences from *Sims et al.*, 1989; *Sims*, 1994; *Sims et al.*, 1994). Dots indicate ages of events from historic records. Vertical bars indicate possible ages within 1 s (Phelan Creeks), and 95% confidence (all others) for pre-historic events. Letters refer to events defined in individual studies. Horizontal lines indicate possible correlations of events between sites; dashes and question marks indicate greater doubt. Phelan Creeks data is from *Sims et al.*, 1989; *Sims*, 1994; *Sims et al.*, 1994; Bidart Fan data is from *Grant and Sieh*, 1994; and Wrightwood data is from *Fumal et al.*, 1993; *Weldon*, 1991. All other data is from published summaries compiled in *WGCEP*, 1988.

example, 9 m of slip would imply 257 year recurrence interval; [*Sieh and Jahns*, 1984]). Paleoseismologic studies of offset stratigraphy and landforms have provided data on the activity and applicability of simplistic recurrence models, as well as the spatial distribution of large events on the Carrizo Plain. The quality and distribution of the paleoseismologic data are dependent on the fortuity of preservation, as well as the skill and technology of interpretation. In this regard, the data are limited to several sites and have been reinterpreted. As more data becomes available, the picture of slip events along the SAF will no doubt be reinterpreted.

The current interpretation of paleoseismology along the SAF in Southern California is summarized in *Sieh et al.*, 1989; *Fumal et al.*, 1993; *Grant and Sieh*, 1994; *Sims*, 1994; *Sims et al.*, 1994 and in Figure C.8. Apparently, at least 5 large, surface-rupturing earthquakes have occurred in the Carrizo Plain since ~1218 A.D. [*Grant and Sieh*, 1994; *Sims*, 1994; *Sims et al.*, 1994]. And, at least 2 more occurred after ~200 B.C. (possibly dated by *Sims*, 1994; *Sims et al.*, 1994 at 1003±20 and 838±35). Both of these recent

studies in the Carrizo Plain have difficulties of interpretation. The events dated by *Sims*, 1994; *Sims et al.*, 1994 are based upon the assumption that a large offset rupture event perturbs the stream channels enough to trigger deposition of a coherent sediment package, or abandonment of the channel. While this may appear a difficult hypothesis, it is defensible on several accounts. 1) horizontal offsets of ~7 m can change the local slope of the channel and deposition should occur as the stream power (proportional to slope and drainage basin area[*Horton*, 1945]) decreases during the offset event. 2) the deposition may not occur immediately, but the moderate frequency storms that must do much of the geomorphic work have recurrence intervals on the order of tens of years an order of magnitude less than that of the earthquakes and thus the event dated may be only within a few tens of years of the earthquake (similar as the 14C dating precision). 3) The offset to cause abandonment occurs when the stream is nearly ready to abandon itself because of the flow processes around the bends in the channel, so it is plausible that a large slip event could easily push the channel across that threshold, as well as possibly juxtaposing a new low across the fault from the upstream channel [*Sims et al.*, 1993].
The investigation of *Grant and Sieh*, 1994 relies upon more typical paleoseismic analysis of fracture terminations and stratigraphic disruptions. However, it suffered from relatively poor radiocarbon control, as well as a depositional hiatus between 200 B.C. and 1218 A.D. possibly concealing earthquake events. Despite these caveats, these studies have provided control on the late Holocene record of faulting in the Carrizo Plain. Their data may be correlated with that from further southeast and two conclusions drawn. 1) the Carrizo segment may rupture independently, in conjunction with the Parkfield-Cholame segments to the northwest (see below), or in conjunction with the Mojave segment to the southwest (e. g., 1857) and 2) the occurrence of these events may not be regular [*Grant and Sieh*, 1994]. Different ruptures from the northwest and southeast may explain the discrepancy in the interpretation of the offset in the last two events [*Grant and Sieh*, 1993].

C.4. Slip deficit along the Cholame segment and potential for rupture of M 7 earthquakes

The Parkfield segment of the SAF stretches from the southern end of the central creeping section (at about Middle Mountain) 30 km southward to the apparently locked Cholame segment that begins near State Highway 46 [*WGCEP*, 1988] (*Figure C.3*). The Cholame segment extends about 55 km SE to near State Highway 58 in the north central Carrizo Plain. Assuming that all of the accumulated elastic strain along the SAF in the Cholame segment was released in the 1857 earthquake, and assuming a long term slip (and thus loading) rate of ~35 mm/yr, *Sieh and Jahns*, 1984 suggested that a surface slip deficit of ~4 m (accumulated since the 1857 earthquake) exists along the Cholame segment (this was also suggested by *Harris and Archuleta*, 1987; *WGCEP*, 1988; *Lienkaemper and Prescott*, 1989). *Harris and Archuleta*, 1987 investigated data from geodetic networks spanning this segment and determined that it is probably locked to a depth of 15 km and thus accumulating elastic energy. From Parkfield northwestward, the surface slip deficit (since 1857) is small (accommodated by creep and the previous Parkfield earthquakes), while along the Cholame segment, very little (near Highway 46) to no historic slip since

1857 has been observed [*Lienkaemper and Prescott*, 1989] (*Figure C.7*). If we assume that a fault segment will be ready to slip again once the slip deficit accumulates to the same magnitude as the slip released in the last earthquake. Therefore, depending on the amount of slip in the 1857 earthquake along the Cholame segment, the area may or may not be ready to slip again.

The essential piece of ambiguous data is the slip magnitude along the Cholame segment in 1857. Several interpretations vary from 1 to 6 m. For the northern portion of the segment, John Sims suggests that only about 1 m of slip occurred in 1857 (*personal communications*, 1993-1995). The *Sieh*, 1978c survey of offset landforms along the SAF concluded that there was about 4 m of slip along this segment in 1857 and in the penultimate event. The *Sieh*, 1978c observations of ~9 m in the Carrizo Plain near Wallace Creek have been corroborated by *Grant and Donnellan*, 1994, although the slip in that area varied from ~9 m at Wallace Creek to ~7 m at Phelan Fan 2.6 km SE [*Grant and Sieh*, 1993]. *Lienkaemper and Sturm*, 1989 made a careful investigation of an offset stream channel along the Cholame segment and inferred that it was offset ~6 m in the 1857 earthquake. In spring 1987, a *blue ribbon committee* of USGS geologists visited the area and "discussed the evidence with Sieh. They concluded that the geomorphic features recorded major fault slip, but differed among themselves in their interpretations, emphasizing the ambiguous nature of the geomorphic data" [*WGCEP*, 1988, p. 33].

C.4.1. Recommendations for future research: paleoseismology, continued geomorphic investigations, and investigation of historic land surveys

While there are many possible avenues of research concerning the segmentation and seismic rupture potential of the central SAF, I recommend the following as potentially fruitful avenues of research that may help determine the timing of slip events and the slip in the 1857 earthquake along the Cholame segment.

C.4.1.1. Paleoseismology

The Cholame segment has not received much attention in paleoseismic investigations. The Watertank site, *Sims*, 1987 is about 3 km NW of Highway 46 (*Figure C.4*). The next paleoseismic sites are on the Carrizo Plain at Phelan Creeks [*Sims et al.*, 1994], Phelan Fan [*Grant and Sieh*, 1993], and the Bidart site [*Grant and Sieh*, 1994], about 70 km SE of Highway 46. Within those ~73 km, there are candidate sites for paleoseismic investigations. For example, the area around Still Lake (~11 km SE of Highway 46) has been surveyed by John Sims and colleagues (*Figure C.4*).

C.4.1.2. Continued geomorphic investigations

Between Highways 46 and 58, *Sieh*, 1978 observed 19 offset landforms. *Lienkaemper and Sturm* , 1989 investigated one of them in great detail by generating detailed topographic maps from repeated aerial photography. That type of thorough geomorphic and sedimentologic investigation should be continued, and further work accompanied by paleoseismic investigations may begin to eliminate the ambiguity associated with the geomorphic offset indicators.

C.4.1.3. Investigation of historic land surveys

This is an intriguing possibility. In 1855 and 1856, James E. Freeman surveyed Township and Range lines in the region of the Carrizo Plain and possibly northward. *Grant and Donnellan*, 1994 recovered original monuments from that survey spanning the SAF in the Carrizo Plain near Wallace Creek and determined that the 1857 slip along the SAF between those monuments was 9.5 ± 0.5 m. While most of the monuments have been

moved, destroyed, or otherwise lost, the possibility of recovering a few more along the Cholame segment is interesting. Based upon the work of *Grant and Donnellan*, 1994 (whose errors were ~1-2 m), we could differentiate between offsets of 1 and 6 m along the Cholame segment in the 1857 earthquake.

C.5. Acknowledgments

Kerry Sieh reviewed an early version of this manuscript, and his comments (especially with regard to the history of the scientific research in the Carrizo Plain) are appreciated. Ron Lyon provided the radar image shown in Figure C.5. I am grateful to Mark Zoback, Bill Ellsworth, and Steve Hickman for their invitation to participate in the San Andreas Fault Zone Deep Drilling Project Workshop, and to the California Earthquake Prediction Evaluation Council (CEPEC) and the California State Geologist, Jim Davis, for the invitation to comment on the geologic and geomorphic observations along the Cholame segment. These invitations encouraged me to summarize the research presented in this appendix.

C.6. References

The Working Group on California Earthquake Probabilities (WGCEP), *Probabilities of large earthquakes occurring in California along the San Andreas fault; USGS Open File Report 88-398*, 1988.

Agnew, D. C. and K. E. Sieh, A documentary study of the felt effects of the great California earthquake of 1857, *Bulletin of the Seismological Society of America, 68*, 1717-1729, 1978.

Allen, C. R., The tectonic environments of seismically active and inactive areas along the San Andreas Fault system, in *Proceedings of conference on geologic problems of San Andreas fault system*, (edited by W. R. Dickinson and A. Grantz), Stanford University Publications in the Geological Sciences, 70-82, 1968.

Antonellini, M., R. Arrowsmith, A. Aydin, P. P. Christiansen, M. Cooke, K. Cruikshank, Y. Du and H. Wu, Complex surface rupture associated with the North Emerson Lake fault zone, caused by the 1992 Landers, CA earthquake: results of detailed mapping, *EOS Transactions AGU, 73*, 362, 1992.

Arnold, R. and H. R. Johnson, *Preliminary report on the McKittrick-Sunset oil region, Kern and San Luis Obispo counties, California*, U. S. Geological Survey Bulletin 406, 1910.

Arrowsmith, J. R., Coupled tectonic deformation and geomorphic degradation along the San Andreas Fault system, PhD. Dissertation thesis, Stanford University, 1995.

Arrowsmith, R., Coupled tectonic deformation and landform development along the San Andreas fault, in *Proceedings of The Rock Fracture Project*, (edited by D. D. Pollard and A. Aydin), The Rock Fracture Project, II, H-1 to H-7, 1991a.

Arrowsmith, R., The Northern Elkhorn Hills: A 2 km wide deformation zone near the Big Bend of the San Andreas fault, *Geological Society of America Abstracts with Programs, 23*, 4, 1991b.

Arrowsmith, R., Fault zone structure and geomorphology along the San Andreas fault, in *Proceedings of The Rock Fracture Project*, (edited by D. D. Pollard and A. Aydin), The Rock Fracture Project, III, J-1 to J-7, 1992a.

Arrowsmith, R., Progressive deformation and degradation along the northern portion of the Big Bend of the San Andreas fault, *Geological Society of America Abstracts with Programs, 24*, A147, 1992b.

Arrowsmith, R. and D. D. Rhodes, Kinematics, structure, and degradation of pressure ridges along the San Andreas fault in the Carrizo Plain, San Luis Obispo County, California, *Geological Society of America Abstracts with Programs, 24*, 3, 1992.

Arrowsmith, R. and D. D. Rhodes, Original forms and initial modifications of the Galway Lake Road scarp formed along the Emerson Fault during the June 28, 1992 Landers, California earthquake, *Bulletin of the Seismological Society of America Special Issue on the Landers Earthquake Sequence, 84*, 511-527, 1994.

Cawley, J. J., Aborigines of the Carrizo Plain, in *Guidebook: geology of Carrizo Plains and San Andreas fault*, (edited by O. Hackell), San Joaquin Geological Society and Pacific section, AAPG and SEPM, 36, 1962.

Dibblee, T. W., Displacements on the San Andreas rift zone and related structures in Carrizo Plain and vicinity, in *Guidebook: geology of Carrizo Plains and San Andreas fault*, (edited by O. Hackell), San Joaquin Geological Society and Pacific Section, AAPG and SEPM, 5-12, 1962.

Dibblee, T. W., Regional geologic map of the San Andreas and related faults in Carrizo Plain, Temblor, Caliente, and La Panza ranges and vicinity, California, United States Geological Survey Miscellaneous Geologic Investigations Map I-757, 1973.

Ellsworth, W. L., Earthquake history, 1769-1989, in *The San Andreas fault system*, (edited by R. E. Wallace), United States Geological Survey, 153-181, 1990.

Fumal, T. E., S. K. W. I. Pezzopane, R. J. and D. P. Schwartz, A 100-year average recurrence interval for the San Andreas fault at Wrightwood, California, *Science, 259*, 199-203, 1993.

Galehouse, J. S., Provenance and paleocurrents of the Paso Robles formation, California, *Geological Society of America Bulletin, 78*, 951-978, 1967.

Goter, S., Seismicity of California, 1808-1987, *United States Geological Survey National Earthquake Information Center, Open File Report 88-286*, 1988.

Graff, L. B., Exploration drilling in the Carrizo Plain, in *Guidebook: geology of Carrizo Plains and San Andreas fault*, (edited by O. Hackell), San Joaquin Geological Society and Pacific Section, AAPG and SEPM, 21 - 23, 1962.

Grant, L. B. and A. Donnellan, 1855 and 1991 surveys of the San Andreas Fault; implications for fault mechanics, *Bulletin of the Seismological Society of America, 84*, 241-246, 1994.

Grant, L. B. and K. E. Sieh, Stratigraphic evidence for several meters of dextral slip on the San Andreas fault during the 1857 earthquake in the Carrizo Plain, *Bulletin of the Seismological Society of America, 83*, 619-635, 1993.

Grant, L. B. and K. E. Sieh, Paleoseismic evidence of clustered earthquakes on the San Andreas Fault in the Carrizo Plain, California, *Journal of Geophysical Research*, v. 99, pp. 6819-6841, 1994.

Hanks, T. C. and H. Kanamori, A moment magnitude scale, *Journal of Geophysical Research, 84*, 2348-2350, 1979.

Hanna, W. F., H. W. Oliver, R. F. Sikora and S. L. Robbins, Bouguer Gravity Map of California, Bakersfield Sheet: California Division of Mines and Geology, 7 p., 1 sheet, scale 1:250,000., 1975.

Harris, R. A. and R. J. Archuleta, Slip budget and potential for a M7 earthquake in Central California, *Geophysical Research Letters, 15*, No. 11 pp. 1215-1218, 1987.

Hill, M. L. and T. W. Dibblee, San Andreas, Garlock, and Big Pine faults, California a study of the character, history, and tectonic significance of their displacements, *Bulletin of the Geological Society of America, 64*, 443-458, 1953.

Horton, R. E., Erosional development of streams and their drainage basins, hydrophysical approach to quantitative morphology, *Geological Society of America Bulletin, 56*, 275-370, 1945.

Jennings, C. W. and R. G. Strand, Geologic map of California: Los Angeles Sheet, California Division of Mines and Geology, Sacramento, California, 1969.

Lawson, A. C. and others, *Report of the earthquake investigation commission upon the California earthquake of April 18, 1906*, Carnegie Institution of Washington, D. C., 1908.

Lienkaemper, J. J. and W. H. Prescott, Historic surface slip along the San Andreas Fault near Parkfield, California, *Journal of Geophysical Research, B, Solid Earth and Planets*, 94, 17,647-17,670, 1989.

Lienkaemper, J. J. and T. A. Sturm, Reconstruction of a channel offset in 1857(?) by the San Andreas Fault near Cholame, California, *Bulletin of the Seismological Society of America, 79*, 901-909, 1989.

Meisling, K. E. and K. E. Sieh, Disturbance of trees by the 1857 Fort Tejon earthquake, California, *Journal of Geophysical Research, 85*, 3225-3238, 1980.

Page, B. M., Evolution and complexities of the transform system in California, U. S. A., *Annales Tectonicae*, 4, 53-69, 1990.

Rhodes, D. D. and R. Arrowsmith, Variation and evolution of gullies formed on a pressure ridge adjacent to the San Andreas Fault, Carrizo Plain, California, *Abstracts with Programs - Geological Society of America, 23*, 91, 1991.

Schwartz, D. P. and K. J. Coppersmith, Fault behavior and characteristic earthquakes; examples from the Wasatch and San Andreas fault zones, *Journal of geophysical research, 89*, 5681-5698, 1984.

Sieh, K. E., A study of Holocene displacement history along the south-central reach of the San Andreas fault, PhD. thesis, Stanford University.

Sieh, K. E., Central California foreshocks of the great 1857 earthquake, *Bulletin of the Seismological Society of America, 68*, 1731-1749., 1978a.

Sieh, K. E., Prehistoric large earthquakes produced by slip on the San Andreas fault at Pallet Creek, California, *Journal of Geophysical Research, 83*, 3907-3939, 1978b.

Sieh, K. E., Slip along the San Andreas fault associated with the great 1957 earthquake, *Bulletin of the Seismological Society of America, 68*, 1421-1448, 1978c.

Sieh, K. E. and R. H. Jahns, Holocene activity of the San Andreas Fault at Wallace Creek, California, *Geological Society of America Bulletin, 95*, 883-896, 1984.

Sieh, K. E. and others, Near-field investigations of the Landers earthquake sequence, April to July 1992, *Science, 260*, 171-176, 1993.

Sieh, K. E., M. Stuiver and D. Brillinger, A more precise chronology of earthquakes produced by the San Andreas fault in southern California, *Journal of Geophysical Research, 94*, 603-623, 1989.

Sims, J. D., Late Holocene slip rate along the San Andreas Fault near Cholame, California, Geological Society of America, Cordilleran Section, 83rd annual meeting; with the Paleontological Society of America, Pacific Coast Section, 451, 1987.

Sims, J. D., Field guide to the Parkfield-Cholame segment of the San Andreas fault, central California, in *The San Andreas Transform Belt*, (edited by A. G. Sylvester and J. C. Crowell), American Geophysical Union, 98-103, 1989.

Sims, J. D., Stream channel offset and abandonment and a 200-year average recurrence interval of earthquakes on the San Andreas fault at Phelan Creeks, Carrizo Plain, California, in *Proceedings of the workshop on paleoseismology, US Geological Survey Open-File Report 94-568*, (edited by C. S. Prentice, D. P. Schwartz and R. S. Yeats), 170-172, 1994.

Sims, J. D., J. C. Hamilton and R. Arrowsmith, Geomorphic study of earthquake offsets and subsequent landform response along the San Andreas fault, Carrizo Plain, California, *EOS Transactions AGU, 74*, 612, 1993.

Sims, J. D., T. Ito and C. D. Garvin, Holocene deposits in a right step-over on the San Andreas Fault as an example of development and propagation of strike-dip pull-apart basins, American Geophysical Union 1990 fall meeting, 1632, 1990.

Sims, J. D., T. Ito, J. Hamilton, A. J. Foss, C. D. Garvin and D. B. Meier, A 200-year average recurrence interval of earthquakes on the San Andreas fault at Phelan Creeks, Carrizo Plain, California: reconstruction from paired offset paleochannels, *unpublished manuscript*, 1994.

Sims, J. D., T. Ito, J. C. Hamilton and D. B. Meier, Late Holocene record of earthquakes and slip along the San Andreas fault in excavations on the Carrizo Plain, Central California, *EOS, Transactions of the American Geophysical Union, 70*, 1349, 1989.

Thomas, E. A. H. and K. E. Sieh, Quaternary development of the Elkhorn Hills along the San Andreas fault: sequential development of folds and thrusts along a strike-slip fault, *Geological Society of America Abstracts with Programs, 13*, 566, 1981.

Vedder, J. G., Geologic map of the Wells Ranch and Elkhorn Hills quadrangles, San Luis Obispo and Kern counties, California, U.S. Geological Survey, 1970.

Vedder, J. G. and R. E. Wallace, Map showing recently active breaks along the San Andreas and related faults between Cholame Valley and Tejon Pass, California, U.S. Geol. Survey Misc. Geol. Inv. Map I-574, 1970.

Wallace, R. E., Notes on stream channels offset by the San Andreas fault, in *Proceedings of conference on geologic problems of the San Andreas fault*, (edited by W. R. Dickinson and A. Grantz), Stanford University Publications in the Geological Sciences, 11, 1968.

Wallace, R. E., Surface fracture patterns along the San Andreas fault, in *Proceedings of the Conference on Tectonic Problems of the San Andreas fault system*, (edited by R. L. Kovach and A. Nur), Stanford University Publications in the Geological Sciences, 13, 248-250, 1973.

Wallace, R. E., The San Andreas fault in the Carrizo Plain Temblor Range region, California, in *The San Andreas fault in southern California*, (edited by J. C. Crowell), California Division of Mines and Geology, Special report 118, 241-250, 1975.

Wallace, R. E., *The San Andreas Fault System, California*, 283 pp., United States Government Printing Office, Washington, D. C., 1990.

Wallace, R. E. and S. S. Schulz, *Aerial views in color of the San Andreas fault, California, USGS OFR 83-98*, U S Geological Survey, 1983.

Weldon, R. J., II, Active tectonic studies in the United States, 1987-1990, U. S. Natl. Rep. Int. Union Geod. Geophys. 1987-1990, *Rev. Geophys., 29*, 890-906, 1991.

Wilcox, R. E., T. P. Harding and D. R. Seely, Basic wrench tectonics, *American Association of Petroleum Geologists Bulletin*, 57, 74-96, 1973.

Wood, H. O., The 1857 earthquake in California, *Seismological Society of America Bulletin, 45*, 47-67, 1955.

Wood, H. O. and J. P. Buwalda, Horizontal displacement along the San Andreas fault in the Carrizo Plain, California, *Geological Society of America Bulletin, 42*, 298-299, 1931.

Zoback, M. D., M. L. Zoback, V. S. Mount, J. Suppe, J. P. Eaton, D. Oppenheimer, P. Reasenberg, L. Jones, C. B. Raleigh, I. G. Wong, O. Scotti and C. Wentworth, New evidence on the state of stress of the San Andreas fault system, *Science, 238*, 1105- 1111, 1987.

 Return to Tectonogeomorphology Project Home Page

 Go to ASU Geology Home Page

---

1857 FORT TEJON EARTHQUAKE

THE CAMELS ARE COMING!

SEE THE U.S. CAMEL CORPS!

Fort Tejon Earthquake

Type of Faulting: right-lateral strike-slip

Time: January 9, 1857 / about 8:20 am PST

Location: 35° 43' N, 120° 19' W about 72 km (45 miles) northeast of San Luis Obispo, about 120 km (75 miles) northwest of Bakersfield, as shown on the map (epicenter location uncertain).
Magnitude: M_W 7.9 (approx.)
Length of Surface Rupture: about 360 km (225 miles)
Maximum Surface Offset: about 9 meters (30 feet)

The Fort Tejon earthquake of 1857 was one of the greatest earthquakes ever recorded in the U.S., and left an amazing surface rupture scar over 350 kilometers in length along the San Andreas fault. Yet, despite the immense scale of this quake, only two people were reported killed by the effects of the shock -- a woman at Reed's Ranch near Fort Tejon was killed by the collapse of an adobe house, and an elderly man fell dead in a plaza in the Los Angeles area (?).

The fact that only two lives were lost was primarily due to the nature of the quake's setting; California in 1857 was sparsely populated, especially in the regions of strongest shaking, and this fact, along with good fortune, kept the loss of life to a minimum. The effects of the quake were quite dramatic, even frightening. Were the Fort Tejon shock to happen today, the damage would easily run into billions of dollars, and the loss of life would likely be substantial, as the present day communities of Wrightwood, Palmdale, Frazier Park, and Taft (among others) all lie upon or near the 1857 rupture area.

As a result of the shaking, the current of the Kern River was turned upstream, and water ran four feet deep over its banks. The waters of Tulare Lake were thrown upon its shores, stranding fish miles from the original lake bed. The waters of the Mokelumne River were thrown upon its banks, reportedly leaving the bed dry in places. The Los Angeles River was reportedly flung out of its bed, too. Cracks appeared in the ground near San Bernadino and in the San Gabriel Valley. Some of the artesian wells in Santa Clara Valley ceased to flow, and others increased in output. New springs were formed near Santa Barbara and San Fernando. Ridges (moletracks) several meters wide and over a meter high were formed in several places. In Ventura, the mission sustained considerable damage, and part of the church tower collapsed. At Fort Tejon, where shaking was greatest, damage was severe. All around southern and central California, the strong

shaking caused by the 1857 shock was reported to have lasted for at least one minute, possibly two or three!

The surface rupture caused by the quake was extensive. The San Andreas fault broke the surface continuously for at least 350 km (220 miles), possibly as much as 400 km (250 miles), with an average slip of 4.5 meters (15 feet), and a maximum displacement of about 9 meters (30 feet) (possibly greater) in the Carrizo Plain area. Kerry Sieh (1978) noted that the **Elkhorn Thrust**, a low-angle thrust fault near the San Andreas, may have slipped simultaneously in the 1857 quake -- an observation that a team of researchers (1996) have recently used to support the idea that future movements along the San Andreas fault zone might produce simultaneous rupture on thrust faults in and near the Los Angeles area, causing a terrible "double earthquake".

The location of the epicenter of the Fort Tejon earthquake is not known. As the name suggests, one idea is to locate it near the area of strongest reported shaking -- Fort Tejon. However, because there is evidence that foreshocks to the 1857 earthquake may have occurred in the Parkfield area, it is located on this map near the northwestern end of the surface rupture, just southeast of Parkfield, near Cholame. (Note: locating it near Fort Tejon would also have caused interference on the map between this quake's symbol and that of the 1952 Kern County quake. Hence, for both these reasons, the Cholame location was chosen.)

Below is a map of southern California with various place names marked, and the surface traces of major faults drawn in blue-green. The theoretical "Cholame" epicenter of the 1857 earthquake is marked with the large red dot -- Fort Tejon is shown by a white "x" on black -- and that part of the San Andreas fault which exhibited surface rupture during the earthquake is shown in red.

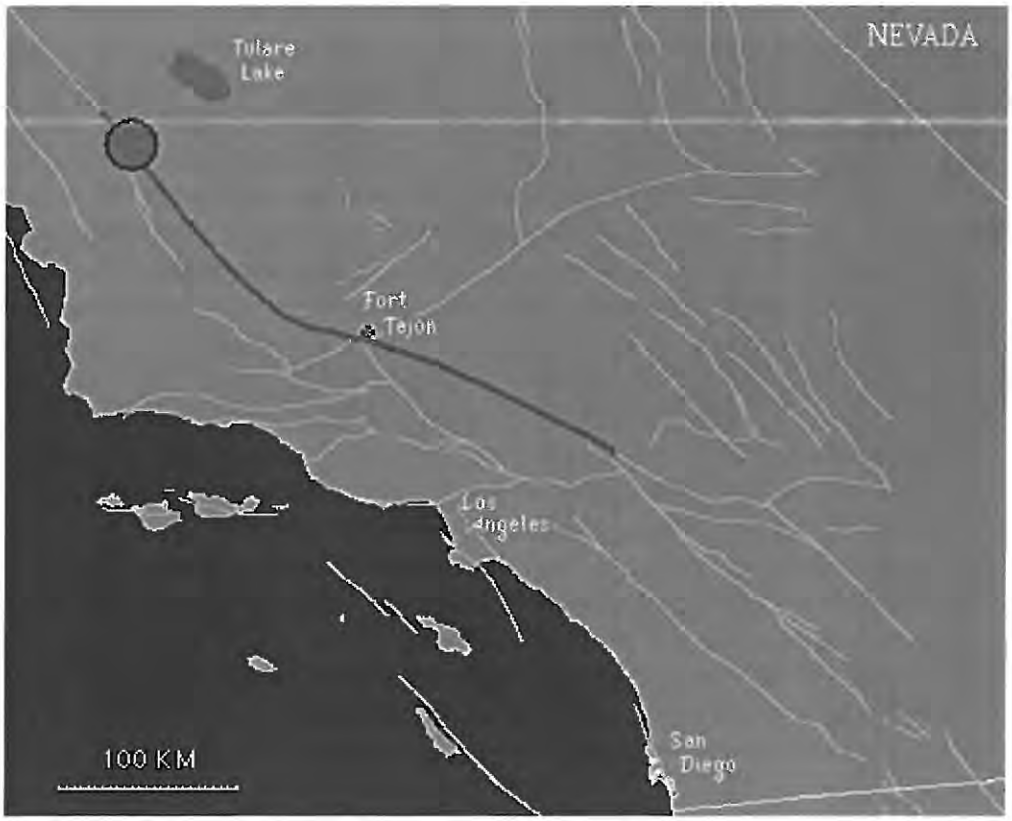

From California Geology, August 1972, Vol. 25, No. 8.

Eye-witness geology

Dust from Antelope

The Fort Tejon Earthquake of 1857

Donald B. Eisman

A story about an earthquake that turned a quiet lake into a raging sea and snapped branches from trees appears in a curious book, Historic facts and fancies, a collection of tales of 19th century California printed by the California Federated Women's Clubs. The book is undated, but, to judge by references in the stories, it must have been printed in 1913 or shortly thereafter.

The earthquake is probably the southern California Earthquake of 1857, sometimes called the Fort Tejon Earthquake. All authorities agree this was one of the biggest quakes within California's recorded history, and at least one expert thought it was the biggest, even larger than the massive event that wrecked San Francisco in 1906.

The story in Facts and fancies is apparently a transcript of remarks by one J. M. Barker before the Bakersfield Women's Club, date also not given. Barker says that in 1857, when he was 25, he lived on a cattle ranch on the Kings Kiver near Tulare Lake. He continues:

One morning in the month of November, 1857, l started out on horseback in company with an old Englishman, my nearest neighbor, to search for some horses of ours that had strayed away. We shaped our course to skirt the shores of Tulare Lake, between what is known as Cross Creek and Kings River. At this time Tulare Lake was a very large sheet of water, about one hundred miles in length by thirty miles in width at its widest place. For a couple of miles from the shore, the waters in the shallows were covered with burnt tules and other refuse matter unfit for use for man or beast, until a distance of two miles from the shore was reached.

We knew that our horses would not drink from the lake, but there were sloughs and holes of water in depressions outside of the lake, where the water was clear and fit for use.

To one of these water-holes, which was surrounded by a fringe of tall willows, we directed our course in order to look for tracks of our missing stock. As several of them were shod, we knew if we found the shod tracks that we were on the right trail.

There was a keen frost, and when we reached the water-hole a thin film of ice was seen upon the water. l dismounted and led my horse by the bridle, and walked to the edge of the water. Just as l reached it, the ground seemed to be violently swayed from east to west. The water splashed up to my knees; the trees whipped about, and limbs fell on and all around me. I was affected by a fearful nausea, my horse snorted and in terror struggled violently to get away from me, but l hung to him, having as great a fear as he had himself. Of course, all this occupied but a few seconds, but it seemed a long time to me. The lake commenced to roar like the ocean in a storm, and, staggering and bewildered, I vaulted into the saddle and my terrified horse started, as eager as I was to get out of the vicinity. I found my friend, who had not dismounted, almost in a state of collapse. He eagerly inquired, while our horses were on the run and the lake was roaring

behind us, "What is this?" I replied, "An earthquake! Put the steel to your horse and let us get out of this!" and we ran at the top of our speed for about five miles.

We observed several hundred antelopes in a state of the wildest confusion and terror. They ran hither and thither, creating a great dust, stumbling and falling over each other in mortal fear. It is their habit at this season of the year, while rearing their young, to congregate in great numbers for mutual protection from coyotes and other vermin; the males also herding in bands by themselves until the new grass starts.

We returned the next day and found that the lake had run up on the land for about three miles. Fish were stranded in every direction and could have been gathered by the wagon-load. The air was olive with buzzards and vultures eager for the feast, but the earth had acquired its normal condition.

We can only imagine what the consequences would have been if a great city had stood upon the eastern shore of the lake.

The San Andreas fault has been the subject of much investigation in the past and will undoubtedly continue to be so in the future. As the map shows, the fault zone is underwater near San Francisco, between Bodega Bay and Fort Ross, and once more between Point Arena and Point Delgada. At Cape Mendocino the fault zone veers to the west and apparently joins the Mendocino Escarpment under the Pacific Ocean. From San Gorgonio southward, a number of roughly parallel faults are collectively called the San Andreas fault zone. Prior to 1906 none of these geological phenomena were an issue. After that date, earthquakes and the role of faults became more clearly understood, but there is still much to learn.

In 1857, Tulare Lake may not have been as big as Barker said it was, but it certainly was much bigger then than it is today. The depth of water in the lake and the size of the lake varied annually, depending on the amount of runoff carried by the Kings, Kaweah, and Tule Rivers. The flood control and irrigation dams that have been built upstream, and the many levees and drainage canals constructed since then divert the water that used to flow uncontrolled into the lake.

Barker's last comment is an interesting example of how a layman came to an appreciation of the difference between an earthquake as an event in nature and an earthquake as a destroyer of manmade objects. Each has to be measured separately, and this, in general, is what the magnitude scale does for the natural event and the intensity scale for effects. It's possible for a big earthquake to do only a modicum of damage because population and construction are sparse; conversely, a small quake can cause a great deal of local damage if it is centered in a densely settled area. To argue that a city on the east shore of Tulare Lake would be earthquake-safe simply because no city has ever been destroyed there over-looks the fact that no city has existed there during a local major earthquake.

Unfortunately, no one knows the magnitude of the 1857 quake, and the reason is simple: the seismograph had not yet been invented. Attempts to estimate its magnitude are hampered by the fact that what little is known of the event comes from unscientific sources.

One could question whether Barker's account does in fact refer to the big quake of 1857. He says the commotion occurred in the morning, the same time of day as the big quake. But his date is wrong. The big earthquake occurred on January 9, whereas Barker speaks of November. However, the man must have been close to 80 when he told his story and could have confused

the end-of-the-year rainy season with the beginning-of-the-year wet season. In fact, one of the most frequently cited accounts of the big shake was written by a man who placed it in 1856.

That account was by Stephen Barton, editor of the Visalia Iron Age, who, in 1876, described the quake in a "History of Tulare County," which ran serially in that newspaper. Barton's description of ground displacement along what would later be named the San Andreas fault figures in nearly every attempt to estimate the size of the quake. In the 1950s, two highly respected earth scientists, evaluating Barton's story and other evidence, came to somewhat different conclusions on the size of the earthquake.

Harry O. Wood, in an article in the January 1955 issue of the Bulletin of the Seismological Society of America (BSSA), was not inclined to doubt Barton's statement that fault displacement occured as far southeast as the Colorado Desert. Wood put the extent of fault displacement at a minimum of 275 miles (p. 60, 64). Elsewhere, he had described the shock as "outstanding," a classification that would mean a magnitude of at least 7.75. He called it "one of the five largest and strongest on record" in California (p. 47).

"While relatively few matters can now be *demonstrated*," Wood wrote (p. 65), "it is the judgment of the writer, long and carefully considered, strengthened by studies in the field along the affected part of the outcrop of the fault zone, that this 1857 earthquake was definitely stronger and probably larger than the similar shock in 1906, possibly considerably larger. That there are also strong suggestions of still greater shocks at earlier times along this segment of the fault should not be overlooked.....

Seismologist Charles F. Richter, in his Elementary Seismology (W. H. Freeman and Company, San Francisco, 1955), was somewhat more conservative than Wood had been. Richter, inclined to doubt displacement into the Colorado Desert, said Barton had probably not clearly distinguished "the actual displacement of 1857 . . . from the topographic features of the San Andreas Rift" (p. 475). Richter continued (p. 451- 52):

"In 1906 actual strike-slip was observed along 190 miles of the Rift from Point Arena southeastward. It is probable that in 1857 there was a nearly equal extent of faulting, presumably terminating at San Gorgonio Pass; Allen's findings cast further doubt on the questionable references to displacements on that occasion extending farther east."

Richter felt the 1857 and 1906 events were similar in other ways and concluded: "The magnitudes of the two events cannot have differed greatly" (p. 475).

Whatever its magnitude, the 1857 earthquake produced extremely high intensities. Sidney D. Townley and Maxwell W. Allen, in an earthquake catalog in the January 1939 BSSA, stated (p. 34) that, if Barton's description of fault movement was accurate, "the intensity could not have been less than X" on the Rossi-Forel Intensity Scale, the maximum on that scale.

In the San Joaquin Valley northeast of the Tulare Lake basin, Barton wrote, houses and trees vibrated furiously, the earth itself rolled like the sea and animals and birds fled in terror. Farther south, at Kern Lake, according to the Stockton Argus, the water in the river was forced back and rose over the banks about four feet.

Damage was apparently most severe at Fort Tejon, some 100 miles southeast of where Barker was. Adobe buildings were badly damaged; plaster, walls and chimneys fell. The Pasadena Star News, in a biographical item published in 1933, quoted Benjamin D. Wilson, who had been mayor of Los Angeles in 1851, as saying that "not a structure at the fort was left standing intact."

Other reports said the ground opened in a wide rent for 30 or 40 miles, large trees were broken off near the ground, cattle rolled down hillsides and the road to Los Angeles was blocked by immense landslides.

An interesting effect was noted at the southeast end of the Carrizo Plain, where a round corral, which apparently straddled the fault trace, became an s-shaped non-corral. The size of the conal and the amount of displacement there are, unfortunately, not known exactly. The displacement has been estimated at 30 feet (Robert Wallace, Proceedings of the Conference on the San Andrea: fault, 1965, pJ4).

The big shock was accompanied by foreshocks and after-shocks. Wilson wrote: "A chimney at John Reed's, at La Puente, killed one of his domestics, a woman who was planning to steal away because of the earthquakes then fresh in the memory of every one. Wilson said "at least one aged person in Los Angeles alone was killed." (Wood, p. 49)

It was reported that houses toppled in Los Angeles, the Los Angeles River overflowed, the ground opened in the beds of the San Gabriel and Santa Clara Rivers, hot gas billowed out of a mountain near San Fernando and, in several places streams began flowing where no water had run before.

The quake was even felt severely in San Francisco. In fact, Wood seemed to think shaking must have been perceptible in virtually all of California and well into Mexico. He based his argument on the fact that Edward S. Holden, director of the Lick Observatory when he published an earthquake catalog in 1595, assigned a Rossi-Forel intensity of IX to Fort Yuma, Arizona and VI to Sacramento. Wood argued (p. 64): "Even if, as may be possible or even likely, these estimates should be reduced considerably, it is obvious that the shock must have been perceptible far to the southeast and to the northwest of these places."

The area of southern California most severely affected in 1857 has earthquakes with some degree of regularity. A recent one that got a press notice came on February 27, 1969. On the San Andreas fault near the Palmdale Reservoir, it had a magnitude variously reported at between 3.2 and 4.3. It pales to insignificance beside the 1857 event, yet it got a lot of people excited. The area has had many little earthquakes, but Wood wrote that "there can be no doubt that this 1857 earthquake was the largest and strongest shock which has occurred in south-central and southern California since the occupation of this region by white men" (p. 65). Writing 15 years ago, he concluded, somewhat ominously, "It is nearly one hundred years since its occurrence."

WALLACE CREEK

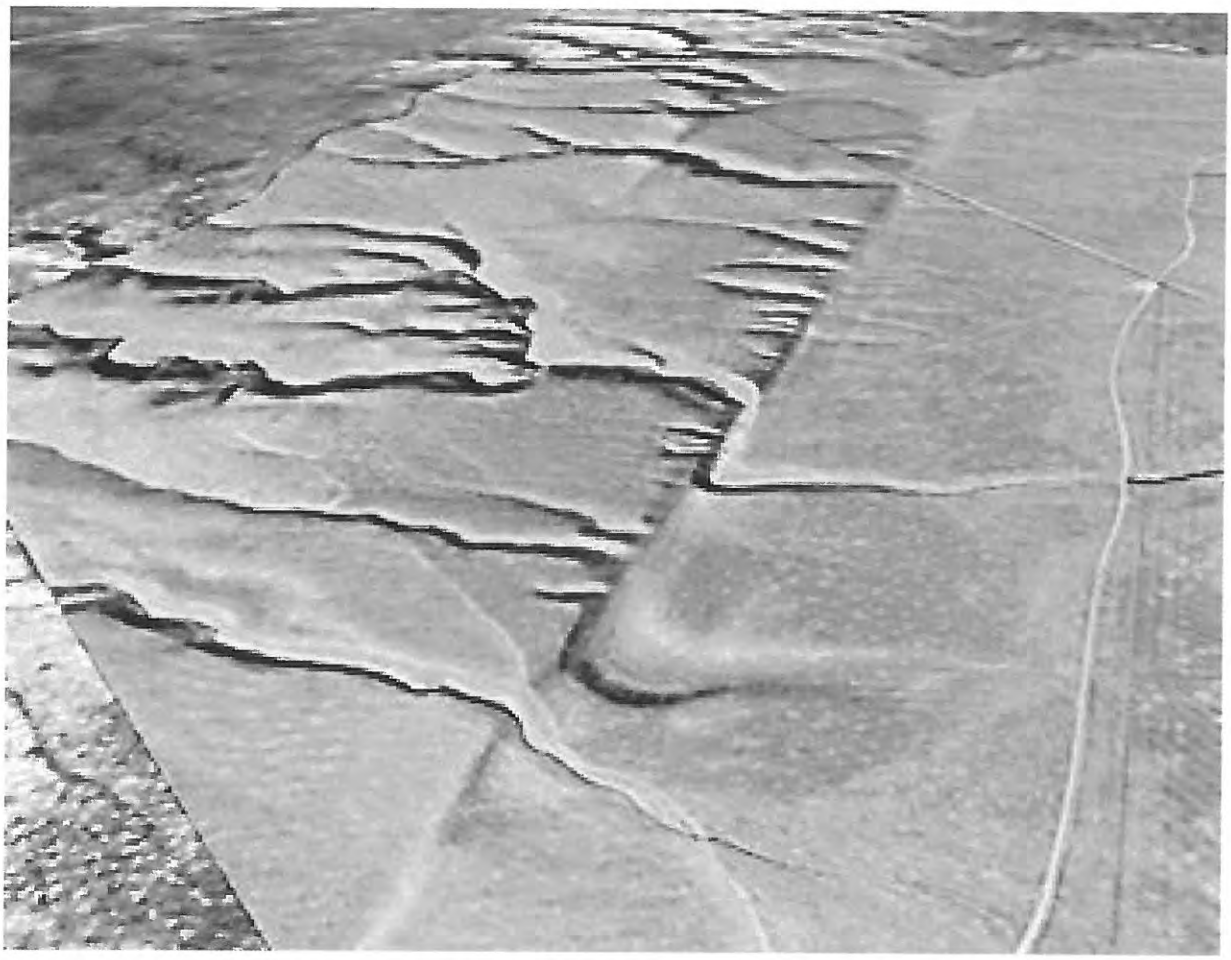

Geological Society of America Centennial Field Guide—Cordilleran Section, 1987

55

The San Andreas fault at Wallace Creek, San Luis Obispo County, California

Kerry Sieh, Division of Geological and Planetary Sciences, California Institute of Technology, Pasadena, California 91125
Robert E. Wallace, U.S. Geological Survey, 345 Middlefield Road, Menlo Park, California 94025

LOCATION

From either the coast or the interior, Wallace Creek is most easily reached by way of California 58 (Fig. 1). Precisely at the southwestern base of the Temblor Range, leave California 58 and drive southwest on an unmarked paved road about 0.2 mi (0.3 km) to a junction with an unpaved road (Fig. 2). Turn left (south) on this road and follow the San Andreas fault to Wallace Creek.

The unpaved road leading to Wallace Creek is impassable to all vehicles during and immediately following major storms. At all other times, two-wheel- or four-wheel-drive vehicles can be easily driven to within 1,300 ft (400 m) of the site. To avoid the gradual destruction of fragile tectonic landforms, park vehicles along the road near the section 33/34 boundary fence and walk the short distance north to the fault. During the dry season, be careful not to park on dry, flammable vegetation.

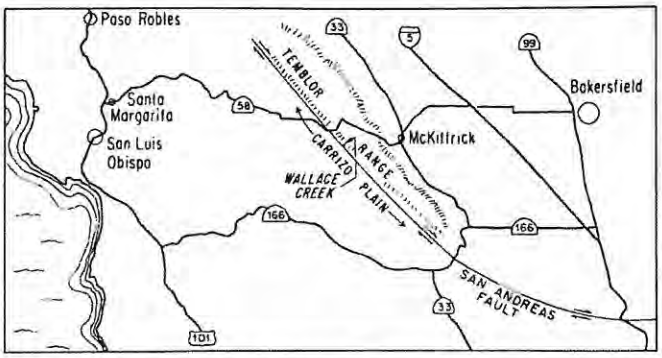

Figure 1. Location of Wallace Creek area. Wallace Creek drains southwestward out of Temblor Range and crosses San Andreas fault as it passes into Carrizo Plain.

SIGNIFICANCE OF THE SITE

Rarely are tectonic landforms as well expressed and as well dated as they are at Wallace Creek. Along this 1.5 mi (2.5 km) length of the San Andreas fault are examples of most of the classic geomorphic features of strike-slip faults, including offset and beheaded channels, shutter ridges, and sags. The smallest features, including right-lateral offsets measuring about 33 ft (10 m), formed in association with the great Fort Tejon earthquake of 1857 (Sieh, 1978). The offsets of larger features, including a 3,700-year-old channel offset 430 ft (130 m), have grown by successive episodes of deformation (Sieh and Jahns, 1984; Wallace, 1968).

Radiometric dating of offset features at this locality demonstrates that the San Andreas fault has been slipping at an average rate of about 1.4 in/yr (34 mm/yr) for at least the past 13,000 years. This rate is only 60 percent of the total relative velocity between the North American and Pacific plates of 2.2 in/yr (56 mm/yr) determined by Minster and Jordan (1978). Hence, a significant fraction of the relative plate motion must be accommodated on other structures, and, contrary to popular belief, the plate boundary cannot be straddled by standing astride the San Andreas fault.

Division of this rate into the amount of offset accumulated during the past three large earthquakes yields recurrence interval estimates ranging between 240 and 450 years. These values are far greater than the current period of dormancy that began following the 1857 earthquake, and a great earthquake will probably not be produced by rupture involving this segment of the fault until at least 2100 A.D.

SITE INFORMATION

The San Andreas fault is perhaps the most famous of all transform faults; certainly it is one of the most accessible. At this locality, features of the surficial trace of this major crustal structure are especially well displayed.

Tectonic Landforms

Figure 3 depicts landforms associated with the fault. Traces of the fault and mappable geologic units have been excluded from this topographic map in order to avoid obscuring the landforms. The location of the fault trace is indicated by small block triangles on the left and right margins of the map. Features discussed in the text are referenced to a 100-m grid marked from left to right on the upper and lower edge of the map.

Offset channels are one of the tectonic landforms most apparent on Figure 3. Between the 300- and 500-m marks is the channel of Wallace Creek, which is offset 430 ft (130 m) along the fault. Farther to the southeast, at the 2,250-m mark, is a younger channel, offset about 65 ft (20 m). Between the 690- and 900-m marks are four very small gullies that are offset about 30 ft (9.5 m).

At the 1,050-m mark is another small gully incised about 1.5 ft (0.5 m) into an alluvial fan. The portion of this gully upstream from the fault is no longer visible in the field. It was buried during a severe storm in February 1978. Prior to its burial, the gully displayed a measurable offset of about 30 ft (9.5 m).

Excellent examples of beheaded channels are at the 100-, 2,800-, 2,000-, and 2,100-m marks. Each of these has been displaced several hundred ft (m) from its source. The history of the

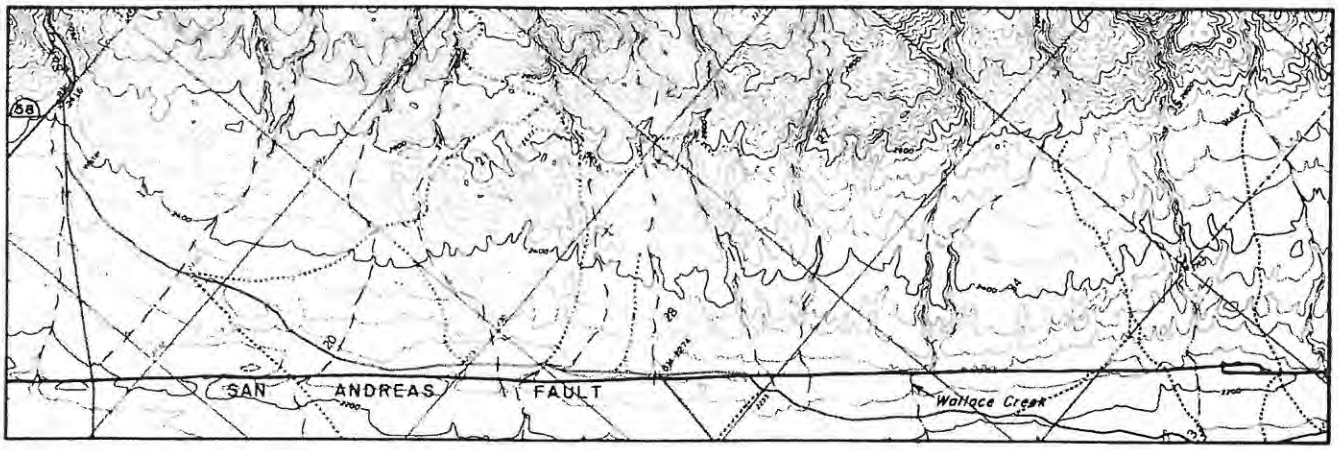

Figure 2. Topographic map of Wallace Creek area showing access roads and San Andreas fault. Location of San Andreas fault mostly from Vedder and Wallace (1970).

TABLE 1. SMALLEST STREAM OFFSETS NEAR WALLACE CREEK AND PROPOSED INTERVALS BETWEEN GREAT EARTHQUAKES (FROM SIEH AND JAHNS, 1984)

Stream Offsets (m)	Number of Measurements	Produced by	Slip associated with earthquake (m)	Proposed Interval Between Events (yr)
9.5 ± 0.5(± 1σ)	5	1857 event	9.5 ± 0.5(± 1σ)	240-320 §
21.8 ± 1.1	4**	1857 plus last prehistoric event	12.3 ± 1.2*	300-440 §
32.8 or 33.5 ± 1.9	3**	1857 plus latest 2 prehistoric events	11.0 or 11.7 ± 2.2†	240-450 §

*$21.8 - 9.5 \pm (0.5^2 + 1.1^2)^{1/2}$.
†$32.8 - 21.8 \pm (1.1^2 + 1.9^2)^{1/2}$ or $33.5 - 21.8 \pm (1.1^2 + 1.9^2)^{1/2}$.
§Slip during following earthquake in column 4 divided by average late Holocene slip rate (33.9 ± 2.9 mm/yr).
**Offset gullies are all between Wallace Creek and gully at 900-m mark in Figure 1.

latter two channels is discussed in more detail by Wallace (1968, p.17–18). A smaller, but very distinct, beheaded channel is visible at the 960-m mark. Very probably it was cut by streams that now flow out of the canyon at the 1,040-m mark. Much smaller beheaded gullies are present between the 570- and 870-m marks. These are barely visible in Figure 3, and some are difficult to see and interpret in the field because the channel segments near the fault are choked with debris that has been washed off the fault scarp.

These smallest beheaded and offset channels provide an important clue to the behavior of the San Andreas fault. The smallest measurable dislocations within the map area are small gullies offset about 30 ft (9.5 m). These dislocations probably formed during the great 1857 earthquake, which was produced by fault rupture along a 220-mi (360-km) or somewhat longer segment of the fault in southern California (Sieh, 1978; Agnew and Sieh, 1978). It appears that none of the 30 ft (9.5 m) has accumulated during the 20th century, because fences built across the fault in the Carrizo Plain at about the turn of the century display no offset whatsoever (Brown and Wallace, 1968). Also, the 30-ft (9.5-m) dislocations probably do not represent smaller offsets accumulated during two or more large earthquakes, because small gullies form very frequently in the Carrizo Plain. For example, a new gully formed at the 1,950-m mark in February 1978. It and many older post-1857 gullies in the Carrizo Plain display no offset at all (Sieh, 1978; Wallace, 1968). If large dislocations are produced at intervals of several decades or more, discrete populations of offsets should be observable.

In fact, larger dislocations in this area are rough multiples of the 30-ft (9.5-m) offset (Sieh and Jahns, 1984, Table 1). Several gullies are offset about 80 ft (22 m), and several more are offset about 100 ft (33 m). A logical conclusion is that the 1857 earth-

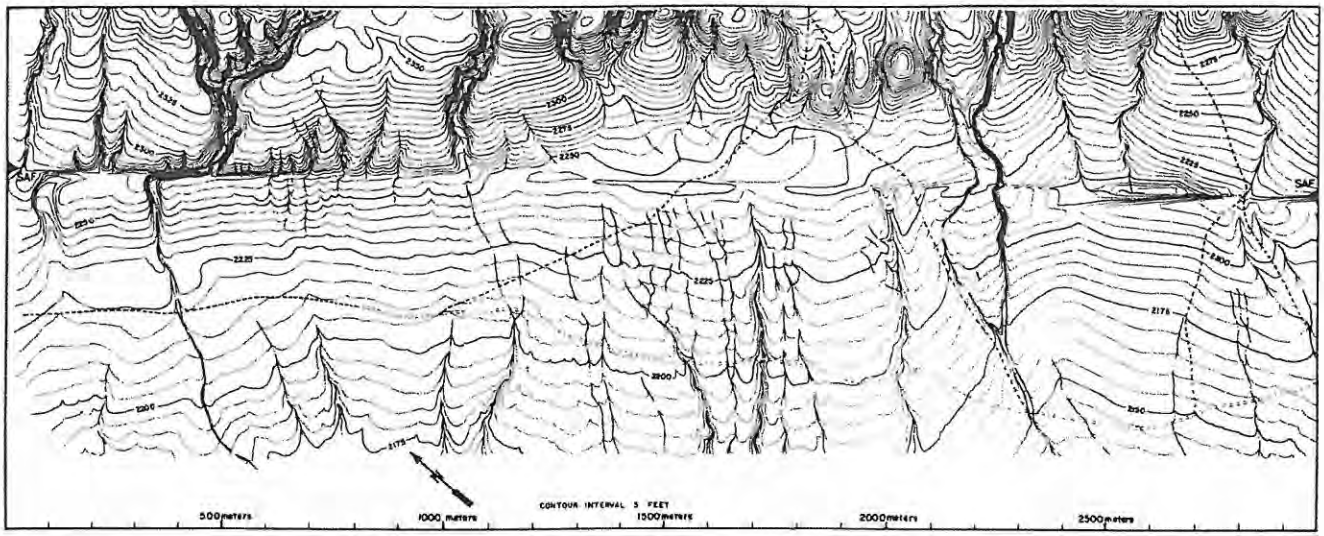

Figure 3. Topographic map of Wallace Creek area illustrates offset and beheaded channels, sag depressions, shutter ridges, and other tectonic landforms produced by recurring strike-slip movement along San Andreas fault. Elevations approximate the National Geodetic Vertical Datum (NGVD 29). Triangles (SAF) at left and right margins mark location of San Andreas fault.

quake was accompanied by about 30 ft (9.5 m) of slip and that its two predecessors were accompanied by about 40 and 36 ft (12.5 and 11 m) of slip.

Shutter ridges of various sizes are well represented along this segment of the fault. The term "shutter ridge" was originally employed by Buwalda (1936, p. 307) to describe topographic highs that had been moved across drainage courses along strike-slip faults. He envisioned these highs or ridges to have been carried by lateral fault slip into positions immediately downstream from existing drainages. The largest shutter ridge at this site can be found between the 1,100- and 1900-m marks. We are uncertain as to the origin of this shutter ridge: It may well represent a broad alluvial fan offset from a source southeast of the 2,300-m mark. Alternatively, it may be a more dynamic feature—perhaps an anticline with a southwest-plunging axial trace that has risen incrementally while being moved laterally over the past several thousand or more years. Smaller shutter ridges, composed of displaced alluvial and colluvial aprons, block the offset gullies between the 620- and 890-m marks.

Sediment is commonly "ponded" behind shutter ridges. A large region of active deposition currently exists upslope of the shutter ridge between the 1,100- and 1,900-m marks. Streams flowing into this region of topographic closure lose their carrying capacity on reaching this area of low gradient and drop their bed load. Three small alluvial fans are clearly visible on the northeastern margin of the depression. Although we have never witnessed it, water may, at times of high discharge, actually pond in this area of topographic closure behind the shutter ridge. This would enable deposition of silty and clayey suspended load as well. Eventually, alluvial fans building southwestward or quiet-water silts and clays filling the basin may be able to overtop the shutter ridge, enabling reestablishment of a fault-crossing drainage there. This drainage would probably cross the fault at the low point in the shutter ridge at the 1,670-m mark, reoccupying the ancient beheaded drainge there. Smaller examples of "ponded" sediment occur immediately upstream from the fault in most of the small drainages between the 680- and 890-m marks. The small right-lateral jogs between the 680- and 890-m marks must result in lesser competence of these ephemeral streams immediately upstream from the fault. Perhaps this is because several meters of length, but virtually no height, are added to the long profile at the time of dislocation. Thus, dislocations add a section of shallower gradient at the fault. Alternatively, substantial losses in stream- or debris-flow velocity may occur at the fault, because the flow must abruptly bend to the right, around the small shutter ridges.

Between the 2,350- and 2700-m marks, two fault traces are arranged en echelon. Dextral slip has resulted in an increase in volume between the overlapping parts of these two faults, and a "sag" or depression has formed as the surface has dropped between the two fault planes. Spectacular evidence of this was evident immediately following a severe storm in mid-February 1978. During that storm, the three major channels that terminate in the sag delivered enough water to form an ephemeral sag pond about 12 ft (3.5 m) deep. Substantial erosion of the northwestern and southeastern channel beds also occurred at that time, and alluvial fans with deltaic fronts formed on the margins of the pond. Along the long margins of the pond, many large, elongate pits, some as much as 10 ft (3 m) deep and long, formed as the ponded water catastrophically drained into open fractures along both fault planes. Fresh pond-facing fault scarplets, up to about 6 in (15 cm) in height, formed along both long margins of the lake as near-surface debris was carried to greater depths by these

waters and surficial blocks slumped in to fill the voids. Remnants of the delta fronts, collapse fissures, and fault scarps are still visible at the time of this writing (1985).

Fault scarps of several ages and degrees of activity are present within the area of Figure 3. The continuous high scarp that extends the full length of Figure 3 between zero and 300 m northeast of the fault trace is 30 ft (10 m) high and is still growing between the 490- and 650-m marks. The trace of the fault lies very near its base, and its lower slopes are much steeper than its upper slopes (about 35° versus about 5°). Sieh and Jahns (1984) demonstrated that this scarp has been growing since about 13,000 years ago, when the alluvial fan in which it formed ceased accumulating. The scarp has risen 10 ft (3 m) in the past 3,700 yrs, at an average rate of 0.03 in/yr (0.8 mm/yr). Between the 650- and 1,900-m marks, the fault scarp has either ceased growth or transforms into a broad monocline. This is indicated by several lines of evidence. First, the fault trace at the 1,900-m marks is farther away from the base of the scarp than at the 650-m mark. Second, the scarp is buried by greater volumes of debris toward the southeast (note the large alluvial fans between the 1,320- and 1,900-m marks). Third, the steepness of the lower portion of the scarp diminishes toward the southeast. Thus, this scarp appears to be growing in height northwest of and decreasing in height southeast of the 650-m mark. Thus, the block upstream from the fault appears now to be bulging upward in the northwest and subsiding in the southeast.

The scarps immediately adjacent to the fault trace alternate along strike from northeast-facing to southwest-facing: a common feature of strike-slip faults termed "scissoring." In some localities, scissoring is clearly a result of purely strike-slip offset of a nonplanar ground surface. In the field, for example, scissoring of the fault scarp can be readily observed across the alluvial fan between the 960- and 1,100-m marks. On the northwestern half of the fan the fault scarp faces uphill, whereas on the southeastern half it faces downslope. This is best explained as strike-slip offset of the convex surface of the alluvial fan.

Wallace Creek

The geomorphology and stratigraphy of Wallace Creek, the large, prominent channel between the zero- and 700-m marks has been studied in detail by Sieh and Jahns (1984). By employing surficial geologic mapping, trenching, and radiocarbon dating, they were able to determine the age and evolution of Wallace Creek, and thereby determined a long-term slip-rate for the fault and made estimates of recurrence intervals for large earthquakes there. Between about 19,000 and about 13,000 years ago, the San Andreas fault at Wallace Creek traversed a broad, active alluvial fan (Fig. 4a). The fan surface was aggrading at a rate sufficient to bury fresh fault scarplets soon after their formation. About 13,000 years ago, perhaps due to climatic changes, Wallace Creek cut a channel into the fan and the fan surface ceased aggrading (Fig. 4b).

Subsequently, the fault has progressively offset the channel several hundred ft (m). Twice the channel segment downstream from the fault has been abandoned, and a new downstream segment cut straight across the fault from the upstream segment (Fig. 4c, e). The oldest downstream segment now resides at the minus 10-m mark about 1,500 ft (475 m) away from its upstream continuation and just off the northwest edge of the map of Figure 3. Another former channel of Wallace Creek now lies beheaded at the 100-m mark. It was first cut by Wallace Creek about 10,000 years ago (Fig. 4c). Between 11,000 and 3,700 years ago this channel was offset about 250 m but was able to avoid beheading by maintaining a deep channel segment along to the fault, analogous to the segment of the presently active channel that follows the fault (Fig. 4d). During a period of merely a century or so, alluvium choked this segment of the channel. A terrace 23 ft (7 m) above the modern channel floor near the fault-crossing and between the 450- and 480-m marks is a remnant of the surface of this 3,700-year-old channel filling. This channel aggradation led to abandonment of the old channel and entrenchment of a new channel straight across the fault (Fig. 4e). In the past 3,700 years, this new channel has been offset 430 ft (130 m) to its present configuration (Fig. 4f).

SLIP RATE DURING THE LATE HOLOCENE AND ESTIMATION OF RECURRENCE INTERVALS

Knowing the date of the most recent entrenchment of Wallace Creek and the offset that accumulated since that entrenchment, one can calculate rather precisely a slip rate of 33.9 ±2.9 mm/yr (±2σ) for the San Andreas fault. The latest prehistoric dislocation of 40.6 ft (12.3 m) is estimated to have occurred between 1540 and 1630 A.D. The previous dislocation of about 36 ft (11 m) may have occurred between 1120 and 1300 A.D. If the interval between large events is indeed as long as is indicated by these estimates, the next event at Wallace Creek should not be anticipated until about 2100 A.D. or even later.

IMPLICATIONS OF THIS SITE FOR KINEMATICS OF SOUTHERN CALIFORNIA

Minster and Jordan (1978) determined from a circumglobal data set that the relative motion of the Pacific and North American plates has averaged about 2.2 in/yr (56 mm/yr) during the past 3 m.y. The geologic record at Wallace Creek shows that, at least during the past 13,000 yr, only about 1.4 in/yr (34 mm/yr) of this has been accommodated by slip along the San Andreas fault. If the 3-m.y. average is assumed to represent the Holocene average rate across the plate boundary as well, then clearly the San Andreas fault is accommodating only 60 percent of the relative plate motion. The reminder of the deformation must be accomplished elsewhere within a broader plate boundary. The San Gregorio–Hosgri fault system, which traverses the coast of central California, may have a late Pleistocene–Holocene slip rate of 0.2 to 0.5 in/yr (6 to 13 mm/yr) (Weber and Lajoie, 1977), and the Basin Ranges, to the east of the San Andreas fault, may

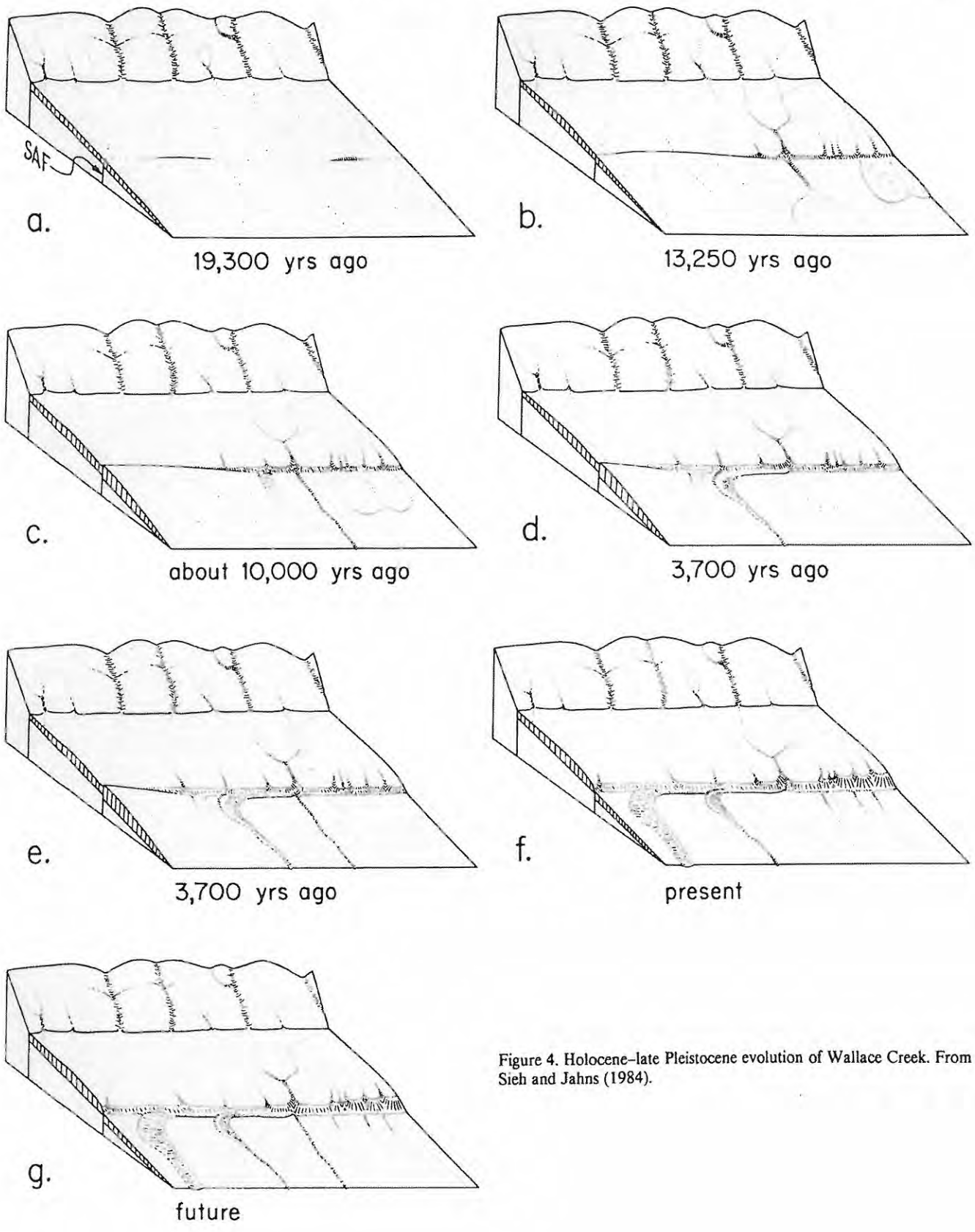

Figure 4. Holocene–late Pleistocene evolution of Wallace Creek. From Sieh and Jahns (1984).

be opening N.35°W. on oblique normal faults at a late Pleistocene–Holocene rate of about 0.3 in/yr (7 mm/yr) (Thompson and Burke, 1973). Most of the 2.24-in/yr (56-mm/yr) plate rate may thus be attributed to the San Andreas, San Gregorio-Hosgri, and Basin Range faults.

REFERENCES CITED

Agnew, D., and Sieh, K. E., 1978, A documentary study of the felt effects of the great California earthquake of 1857: Seismological Society of America Bulletin, v. 68, p. 1717–1729.

Brown, R. D., and Wallace, R. E., 1968, Current and historic fault movement along the San Andreas fault between Paicines and Camp Dix, California, *in* Dickinson, W. R., and Grantz, A., eds., Conference on Geologic Problems of San Andreas Fault System, Proceedings: Stanford, California, Stanford University Publications in the Geological Sciences, v. 11, p. 22–41.

Buwalda, J. P., 1936, Shutterridges, characteristic physiographic features of active faults [abs.]: Geological Society of America Proceedings 1936, p. 307.

Minster, J. B., and Jordan, T. H., 1978, Present-day plate motions: Journal of Geophysical Research, v. 83, p. 5331–5354.

Sieh, K., 1978, Slip along the San Andreas fault associated with the great 1857 earthquake: Seismological Society of America Bulletin, v. 68, p. 1731–1749.

Sieh, K. E., and Jahns, R. H., 1984, Holocene activity of the San Andreas Fault at Wallace Creek, California: Geological Society of America Bulletin, v. 95, p. 883–896.

Thompson, G. A., and Burke, D. B., 1973, Rate and direction of spreading in Dixie Valley, Basin and Range Province, Nevada: Geological Society of America Bulletin, v. 84, p. 627–632.

Wallace, R. E., 1968, Notes on steam channels offset by the San Andreas fault, southern Coast Ranges, California, *in* Dickinson, W. R., and Grantz, A., eds., Conference on Geologic Problems of the San Andreas Fault System, Proceedings: Stanford, California, Stanford University Publications in the Geological Sciences, v. 11, p. 6–21.

Weber, G. E., and Lajoie, K. R., 1977, Late Pleistocene and Holcene tectonics of the San Gregorio fault zone between Moss Beach and Point Ano Nuevo, San Mateo County, California [abs.]: Geological Society of America, Abstracts with Programs, v. 9, no. 4, p. 524.

Vedder, J. G., and Wallace, R. E., 1970, Map showing recently active breaks along the San Andreas and related faults between Cholame Valley and Tejon Pass, California: U.S. Geological Survey Miscellaneous Investigations Map I-574.

Holocene activity of the San Andreas fault at Wallace Creek, California

KERRY E. SIEH *Division of Geological and Planetary Sciences, 170-25 California Institute of Technology, Pasadena, California 91125*
RICHARD H. JAHNS* *School of Earth Sciences, Stanford University, Stanford, California 94305*

ABSTRACT

Wallace Creek is an ephemeral stream in central California, the present channel of which displays an offset of 128 m along the San Andreas fault. Geological investigations have elucidated the relatively simple evolution of this channel and related landforms and deposits. This history requires that the average rate of slip along the San Andreas fault has been 33.9 ± 2.9 mm/yr for the past 3,700 yr and 35.8 + 5.4/-4.1 mm/yr for the past 13,250 yr. Small gullies near Wallace Creek record evidence for the amount of dextral slip during the past three great earthquakes. Slip during these great earthquakes ranged from 9.5 to 12.3 m. Using these values and the average rate of slip during the late Holocene, we estimate that the period of dormancy preceding each of the past 3 great earthquakes was between 240 and 450 yr. This is in marked contrast to the shorter intervals (~150 yr) documented at sites 100 to 300 km to the southeast. These lengthy intervals suggest that a major portion of the San Andreas fault represented by the Wallace Creek site will not generate a great earthquake for at least another 100 yr. The slip rate determined at Wallace Creek enables us to argue, however, that rupture of a 90-km-long segment northwest of Wallace Creek, which sustained as much as 3.5 m of slip in 1857, is likely to generate a major earthquake by the turn of the century.

In addition, we note that the long-term rates of slip at Wallace Creek are indistinguishable from maximum fault-slip rates estimated from geodetic data along the creeping segment of the fault farther north. These historical rates of slip along the creeping reach thus do represent the long-term—that is, millennial—average, and no appreciable elastic strain is accumulating there.

Finally, we note that the Wallace Creek slip rate is appreciably lower than the average rate of slip (56 mm/yr) between the Pacific and North American plates determined for the interval of the past 3 m.y. The discrepancy is due principally to slippage along faults other than the San Andreas, but a slightly lower rate of plate motion during the Holocene epoch cannot be ruled out.

INTRODUCTION

California has experienced many episodes of tectonic activity during the past 200 m.y. During the past 15 m.y. horizontal deformations due to the relative motion of the Pacific and North American plates have been dominant. On land, the major actor in this most recent plate-tectonic drama has been the San Andreas fault, across which ~300 km of right-lateral dislocation has accumulated since the middle Miocene (Hill and Dibblee, 1953; Crowell, 1962, 1981; Nilsen and Link, 1975).

The San Andreas fault traverses most of coastal California, running close to the populous Los Angeles and San Francisco Bay regions (Fig. 1a). Its historical record of occasional great earthquakes (Lawson and others, 1908; Agnew and Sieh, 1978) amply demonstrates that it poses a major natural hazard to inhabitants of these regions. The future behavior of the San Andreas fault thus has long been a topic of great interest to Californians. Interpretations of historical, geodetic, and geologic data have yielded estimates of one century to several centuries for the time between great earthquakes along the fault in the San Francisco Bay region (Reid, 1910; Thatcher, 1975). Geologic data indicate that similar recurrence intervals apply in southern California (Sieh, 1978b, and in press).

The behavior of the San Andreas fault during the past few thousands of years is one of the best clues to its future behavior. Useful forecasts concerning the likelihood or imminence of a great earthquake along the fault will be much more difficult without greater understanding of its behavior during the past several millennia.

In this paper, we present and discuss the geologic history of Wallace Creek, a locality about halfway between San Francisco and Los Angeles that contains much information about the Holocene behavior of the San Andreas fault (Fig. 1a). For the purpose of determining rates of slip in Holocene time, the channel of Wallace Creek offers excellent possibilities. The channel crosses and is offset along a well-defined linear trace of the San Andreas fault in the Carrizo Plain of central California (Fig. 1b). It is relatively isolated from other large drainages, and, therefore, its history is not complicated by involvement with remnants of other drainages that have been brought into juxtaposition.

The simple geometry of Wallace Creek suggests a simple history of development. Arnold and Johnson (1909) inferred 120 m of offset on the San Andreas fault, because the modern channel of the creek runs along the fault for about that distance. Wallace (1968) also inferred a simple history of offset involving incision of a channel into an alluvial plain, offset of ~250 m, then channel filling and new incision across the fault. The latest dextral offset of 128 m then accumulated. These interpretations are verified and quantified by us in this paper.

STRATIGRAPHY AND GEOMORPHOLOGY

Figure 2 is a geologic map of the Wallace Creek area that is based upon surficial mapping and study of sediments encountered in numerous excavations. The map shows four main geologic units: older fan alluvium (uncolored), younger fan alluvium (green), high-channel alluvium (dark orange), and low-channel alluvium (light orange). A mantle of slope wash and local alluvium, which is extensively burrowed by rodents, overlies most of the deposits. This unit has been mapped (brown) only where it is thicker than ~1 m and does not cover units and relationships that need to be shown on the map.

*Deceased.

Geological Society of America Bulletin, v. 95, p. 883–896, 11 figs., 3 tables, August 1984.

Figure 1. a. Wallace Creek (WC) is along the San Andreas fault (SAF) between Los Angeles (LA) and San Francisco (SF), in the Carrizo Plain of central California. b. This oblique aerial photograph shows the modern channel, which has been offset ~130 m, and an abandoned channel that has been offset ~380 m. An older abandoned channel, indicated by white arrow at left, has been offset ~475 m. Photograph by R. E. Wallace, 17 September 1974. View is northeastward.

a

b

Older Fan Alluvium

Underlying all other units exposed at the site, there is a late Pleistocene alluvial fan deposit derived from the Temblor Range to the northeast. This deposit, here termed the "older fan alluvium," consists of thin sheets, lenses, and stringers of indurate silty clay, pebbly sandy clay, and sandy gravel. Most of the trenches (Figs. 2 and 3) exposed this unit. Southwest of the fault, the older fan alluvium is covered by various deposits, but northeast of the fault, the deformed fan surface is incised.

Charcoal disseminated within the older fan alluvium 4 m below the surface of the fan in trench 5 (Fig. 3), yielded an age of 19,340 ± 1,000 yr B.P. (Table 1). The lack of major unconformities and paleosols in the older fan alluvium below or above this dated horizon implies that all of the exposed 13 m of the unit formed during the late Pleistocene epoch. Evidence discussed below supports a conclusion that the fan surface on the northeast side of the fault had become inactive by about 13,000 yr B.P.

FIGURE 2 EXPLANATION

UNITS

- Hl — Low-channel alluvium
- Hh — High-channel alluvium
- Hs — Slope wash (mantles most of area, but mapped only where boundaries are distinct)
- Py — Younger-fan alluvium (dots indicate edges of individual lobes)
- Po — Older-fan alluvium

SYMBOLS

- Contacts (solid where geomorphically apparent or exposed in trench, dotted where buried, dashed where inferred
- 0.3 — Faults (as above; hachures on downthrown side; numbers indicate height of scarp)
- Selected small gullies offset ~9m in 1857
- 5 / 10 — Trenches: backhoe / bulldozer
- Crests of small fans and source gullies offset ~9m in 1857
- 0.3 — Landslide, showing headscarp, scarp height, and direction of movement

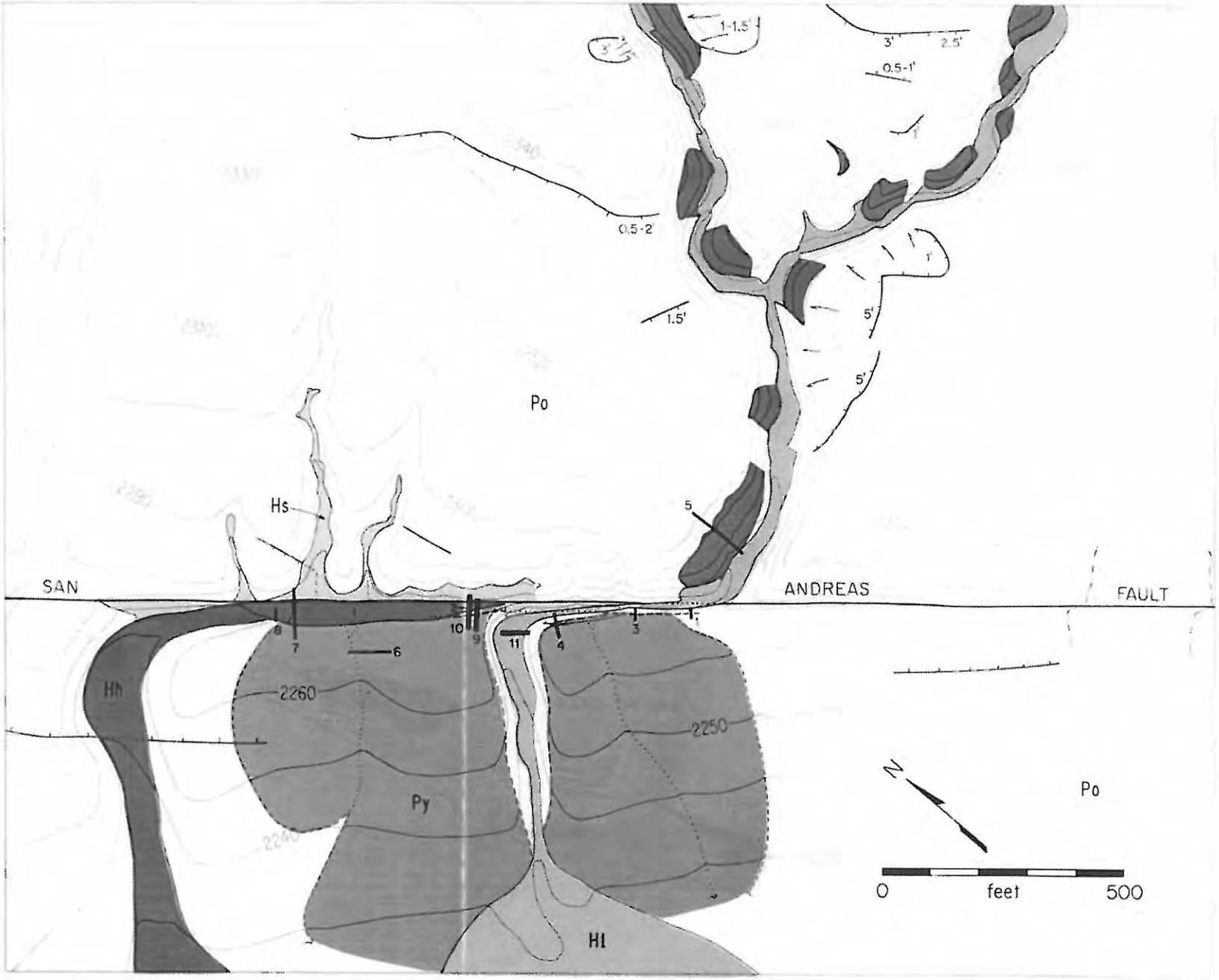

Figure 2. Geologic map of Wallace Creek. Contours of topographic base map show elevation (in feet) above sea level.

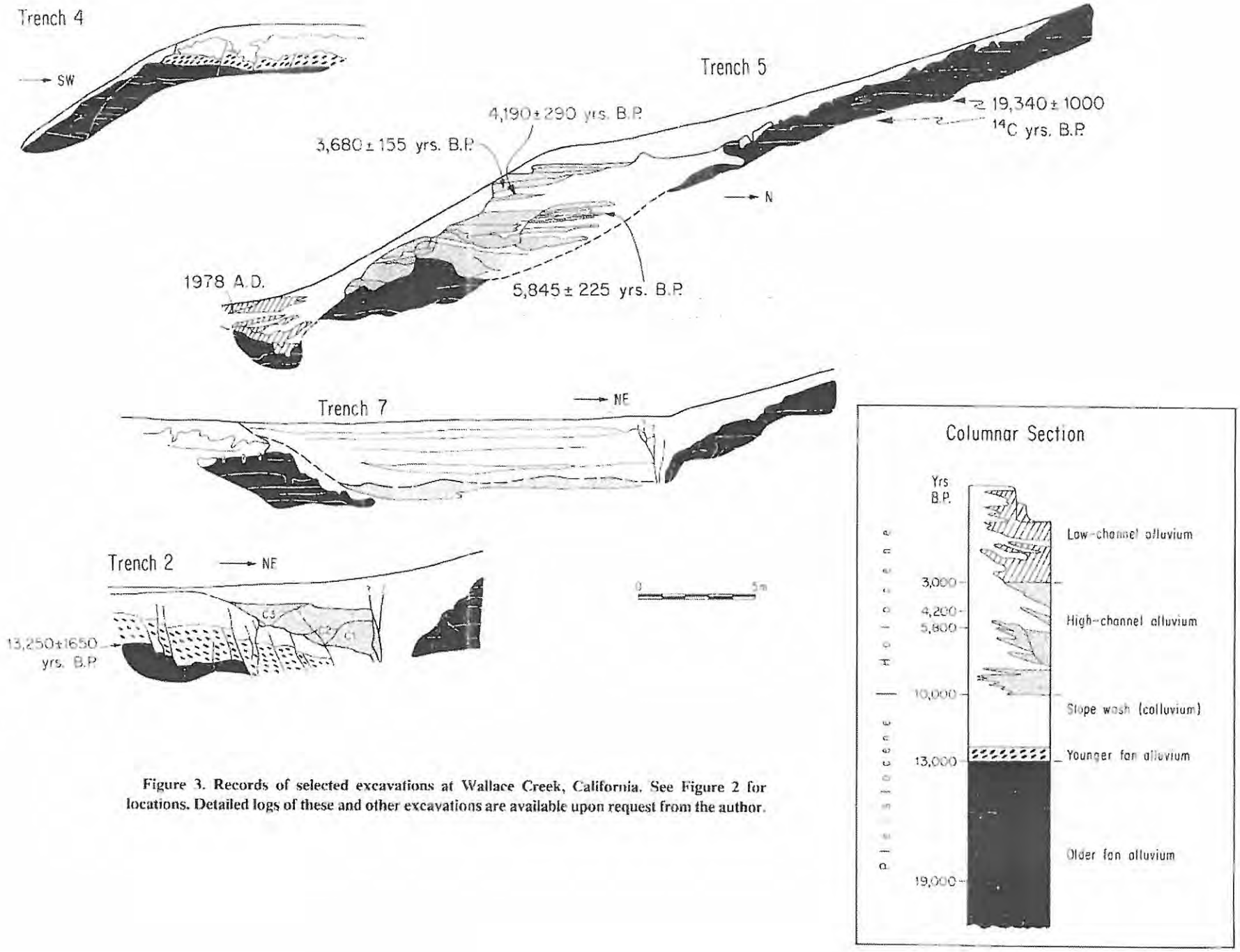

Figure 3. Records of selected excavations at Wallace Creek, California. See Figure 2 for locations. Detailed logs of these and other excavations are available upon request from the author.

TABLE 1. RADIOCARBON ANALYSES

Sample no.		Conventional ^{14}C age* (yr B.P.)	$\delta^{13}C$	Reservoir corrected age†	Calendric age (yr B.P.)
WC-5	UW-567	18,750 ± 450	22.37	18,782 ± 450	19,340 ± 1080**
WC-2	UW-572	12,865 ± 1650			13,250 ± 1650**
WC-6	UW-564	5,040 ± 180	21.51	5,096	5,845 ± 225§
WC-7	UW-565	3,730 ± 170	−22.40	3,752	4,190 ± 290§
WC-9-2	UW-566	3,920 ± 140	10.5	3,956	4,480 ± 270§
WC-3	UW-563	3,495 ± 110	19.71	3,580	3,680 ± 155§
WC-3	UW-563b	3,295 ± 100	19.71	3,270	
MWBS-1	UW-358	3,340 ± 130			
WC-10-2	UW-342	3,320 ± 100	13.4	3,476	3760 ± 155§
WC-11	UW-745	1,110 ± 180	10.5	1,341	1,035 ± 235§

Note: all date uncertainties in the table are at 95% confidence level.
*As quoted by Stuiver and Pearson (1977, p. 356).
†As explained in Stuiver and Pearson (1977), conventional ages must be corrected for isotopic fractionation.
‡Computed using half-life of 5,730 yr, uncertainty estimated following suggestion of Klein and others (1982, p. 137).
§From Klein and others (1982, Table 2).
**From Stuiver, 1982.

Younger Fan Alluvium

Southwest of the fault (Fig. 2), there is a lobate deposit that we have termed the "younger fan alluvium." This deposit overlies and is less indurated than the older fan alluvium. It is a well-sorted gravelly sand with a distinctive imbrication of pebbles that indicates southwestward current flow. The unit is thickest near trenches 2, 9, and 10 and thins to the northwest, southeast, and southwest. The boundary of this composite alluvial fan is inferred from the topography and the trench exposures. A radiocarbon date from charcoal in the upper centimetre of the older fan alluvium (trench 2) indicates that the younger fan alluvium began to accumulate 13,250 ± 1,650 yr B.P. (Table 1).

High-Channel Alluvium

Nestled within the channel of Wallace Creek above the modern stream bed, there are numerous remnants of an ancient terrace (Fig. 2). This surface is referred to as the "high terrace," and it is underlain by sand and gravel beds characterized by scour-and-fill structures, which we refer to as the "high-channel alluvium" (trench 5 in Fig. 3). The massive and poorly sorted nature of some of these "high-channel" beds indicates that they are debris-flow deposits. Other beds that are well sorted and laminated must have been transported as bedload in the waters of Wallace Creek.

Radiocarbon analyses (3) of charcoal from within the high-channel deposits in trench 5 demonstrate that these beds were accumulating through a period from 5845 ± 225 yr B.P. to 3680 ± 155 yr B.P. (samples WC-3, WC-6, and WC-7 in Table 1).

Southwest of the San Andreas fault, the high-channel deposits occur in the abandoned channel of Wallace Creek (Figs. 1 and 2). Trenches 2, 7, and 8 (Fig. 3) and 9 and 10 (Fig. 4) show these sands and gravels residing in a 3- to 4-m-deep channel cut into colluvium. Like their correlatives northeast of the fault, these beds exhibit major episodes of scour and fill. A radiocarbon analysis of organic matter from trench 10 yielded an age of 3,780 ± 155 yr B.P. This sample was collected from a colluvial wedge in the middle of the deposits in the abandoned channel, and its age indicates that the abandoned-channel deposits are contemporaneous with the high-channel deposits across the fault and upstream.

Figure 5 includes a profile of the high terrace. The height of the high terrace above the modern channel is greatest at the fault; the terrace merges with a low terrace ~1 km upstream from the fault. Judging from the elevation difference of the high terrace across the fault, vertical slip during the past 3,800 yr is 3 m, which is a mere 2.3% of the horizontal slip during that time period. It is worth noting that within 1 km to the northwest and to the southeast, this vertical slip diminishes to zero and reverses sense.

Modern-Channel Alluvium

Younger sand and gravel beds very similar to the high-channel alluvium have been deposited in the modern channel of Wallace Creek (Fig. 2, and trench 5 in Fig. 3). Like the high-channel alluvium, this "modern-channel alluvium" also exhibits scour-and-fill structures and interfingers with debris derived from the channel walls.

In trench 5, the base of the modern-channel alluvium is ~2.5 m beneath the creek bed, and along the entire channel, there is a low terrace that occurs 1.5 m above the modern creek bed (Fig. 5). This terrace represents the highest level reached by the modern-channel deposits; it formed and was incised within the past 1,000 yr, as indicated by the radiocarbon date of 1035 ± 235 yr B.P. on charcoal 2.5 m below the terrace surface in trench 11 (Fig. 6). An early photograph of the channel shows that the low terrace was incised by the creek prior to A.D. 1908 (Sieh, 1977, p. 61).

GEOLOGIC HISTORY

The evolution of Wallace Creek has been rather simple. It is divisible into four periods, each of which ends in a sudden change of channel configuration.

Accumulation of Older Fan Alluvium and Initial Entrenchment of a Channel

Prior to initial incision of Wallace Creek, during the late Pleistocene epoch, the older fan alluvium gradually accumulated as broad, thin beds on an alluvial fan or apron that extended southwestward from the Temblor Range across the San Andreas fault (Fig. 7a). The lack of small channels within the older fan alluvium indicates either that any scarps that formed along the fault during this interval were buried before they accumulated even 1 m of height, or that they faced mountainward and served to pond the older fan alluvium on the upstream side of the fault. About 13,000 yr B.P., the first major entrenchment of the older fan alluvium occurred (Fig. 7b). Several small gullies were eroded into the fault scarp, and their debris, the younger fan alluvium shown in Figure 2, was deposited at the foot of the scarp. At about the same time, the initial entrenchment of Wallace Creek occurred. The downstream segment of this initial channel now lies outside the mapped area, ~475 m northwest of Wallace Creek (beneath the white arrow at left margin of Fig. 1b).

Initial Offset of Wallace Creek and Re-entrenchment

After ~100 m of right-lateral slip had been registered by the features formed ~13,000 yr B.P., the initial downstream segment of Wallace Creek was abandoned, and a new segment was cut, so that a straight-channel configuration was restored across the fault (Fig. 7c). This new segment is the one labeled "abandoned channel" in Figure 1.

More Offset and Re-entrenchment of the Channel

For several millennia the newly re-entrenched Wallace Creek served as a narrow conduit for materials being transported fluvially out of the nearby Temblor Range. The depth of initial incision of this channel is poorly constrained, but it cannot have been more than 12 m, which is the depth of the base of the high-channel deposits below the surface of the old alluvium in trench 5. As slip accumulated along the San

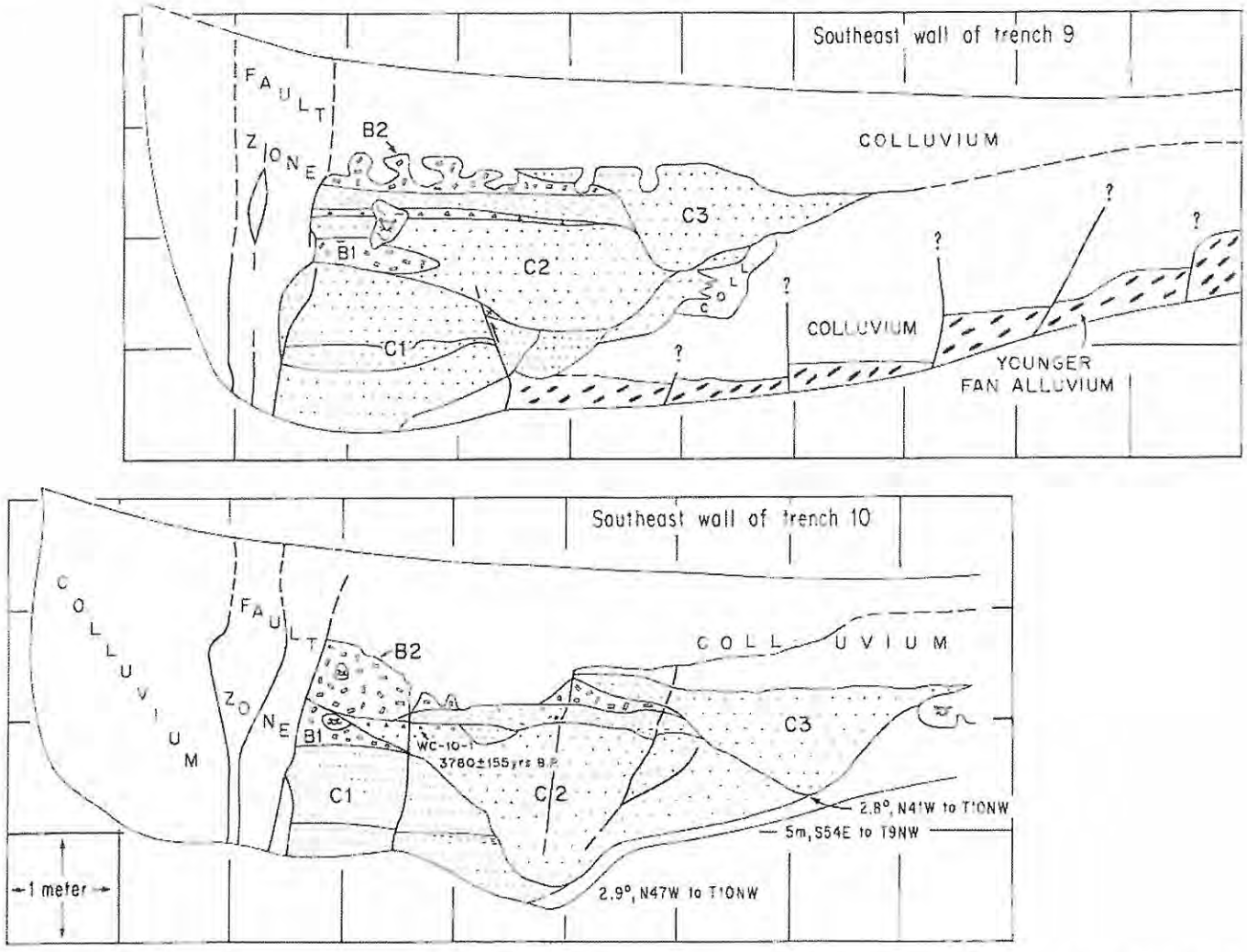

Figure 4. Trenches 9 and 10 reveal the various deposits of the abandoned channel. B_1 and B_2 are scarp-derived breccias. C_1, C_2, and C_3 are fluvial sands and gravels. Solid triangles indicate location of charcoal that yielded date for channel deposits.

Andreas fault early during the Holocene epoch, Wallace Creek developed a bend along the fault that reflected the offset accumulated since entrenchment (Fig. 7d). Water and debris flowing within the channel were diverted to the right at the fault, flowed along the fault for a distance equal to the accumulated offset, and then were diverted left and away from the fault. These two bends in the channel will be referred to hereinafter as the right bend and the left bend.

Trench 5 indicates that by ~6000 yr B.P., 3.0 to 3.3 m of sediment had been deposited within the channel at the right bend. Trench 5 also shows that, locally, at least 1.5 and perhaps 3.3 m of these high-channel deposits subsequently was eroded away. About 3800 yr B.P., after the channel had been offset ~240 m, critical changes began to occur within the channel. For reasons that we do not understand, debris began to accumulate in the channel to greater thicknesses than ever before (Fig. 7e). Trench 5 reveals that at the right bend, the accumulation was at least 5.5 m deep. Trenches 2, 9, and 10 show that this accumulation all but filled the channel at the right bend. This filling set the stage for abandonment of the channel downstream from the right bend and re-entrenchment of Wallace Creek straight across the fault (Fig. 7e). The new channel was cut no more than 8.5 m below the level of the old channel, as the maximum depth of the new channel is only 8.5 m below the top of the high terrace in trench 5.

Offset and Future Re-entrenchment of the New Channel

The new channel has been offset ~130 m subsequent to its creation about 3800 yr B.P. (Fig. 7f). The modern-channel deposits have accumulated in the new channel during this period of time. They are now ~2.5 m thick at the right bend and more than 2.5 m thick at the left bend.

Although the active channel floor is now ~3 m below the crest of the channel bank at the

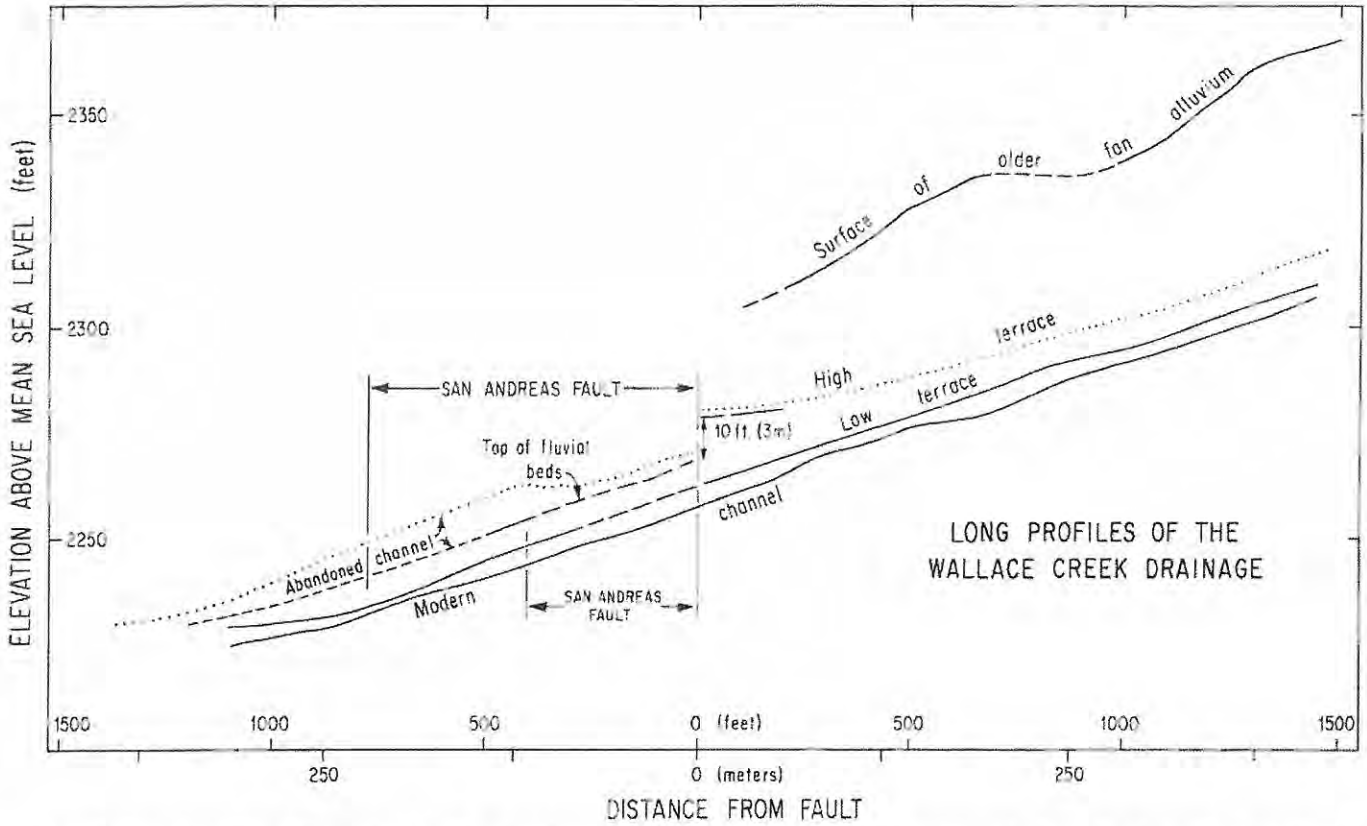

Figure 5. Stream profiles of the modern and the abandoned channels of Wallace Creek. High terrace, indicated by dotted lines, and top of high-channel alluvium, indicated by solid and dashed lines, are offset ~3 m vertically.

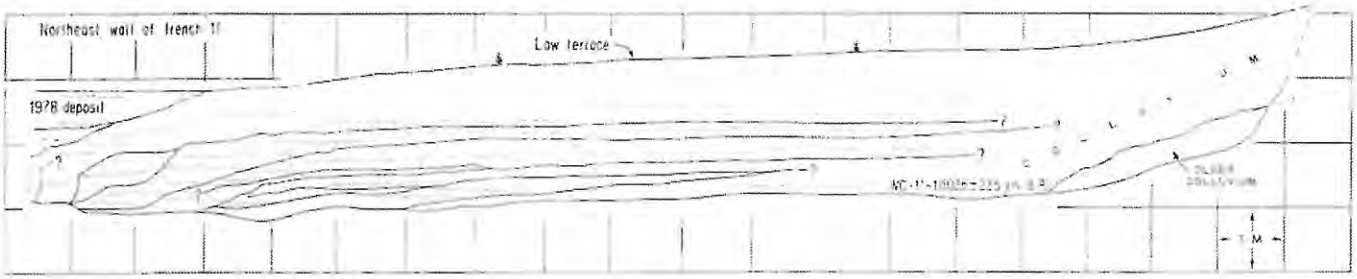

Figure 6. Trench 11 exposes the upper 2.5 m of low-channel deposits in the modern channel. Solid lines are contacts of individual fluvial beds. Dotted lines represent locally visible layering within these beds.

right bend, older modern-channel deposits form a low terrace surface that is only 1 m below the crest of the bank there. Mr. Ray Cavanaugh, who farms at Wallace Creek, reported to us that water actually spilled over the edge at the right bend in the winter of 1971–1972 or 1972–1973. It is not hard to envision a third entrenchment of Wallace Creek (Fig. 7g), given another metre or two of channel filling and a moderately high discharge. Such a re-entrenchment would establish the creek once again straight across the fault.

SLIP RATE OF THE SAN ANDREAS FAULT

Slip Rate during the Late Holocene

Knowing the date of the most recent entrenchment of Wallace Creek and the offset that has accumulated since that entrenchment, one can calculate rather precisely the rate of slip for the San Andreas fault. That rate is 33.9 ± 2.9 mm/yr, and its derivation is explained in detail below.

The offset of the modern channel of Wallace Creek is 128 ± 1 m. This figure is obtained by extrapolating the southwestern edge of the abandoned channel (labeled 1 in Fig. 8) to its

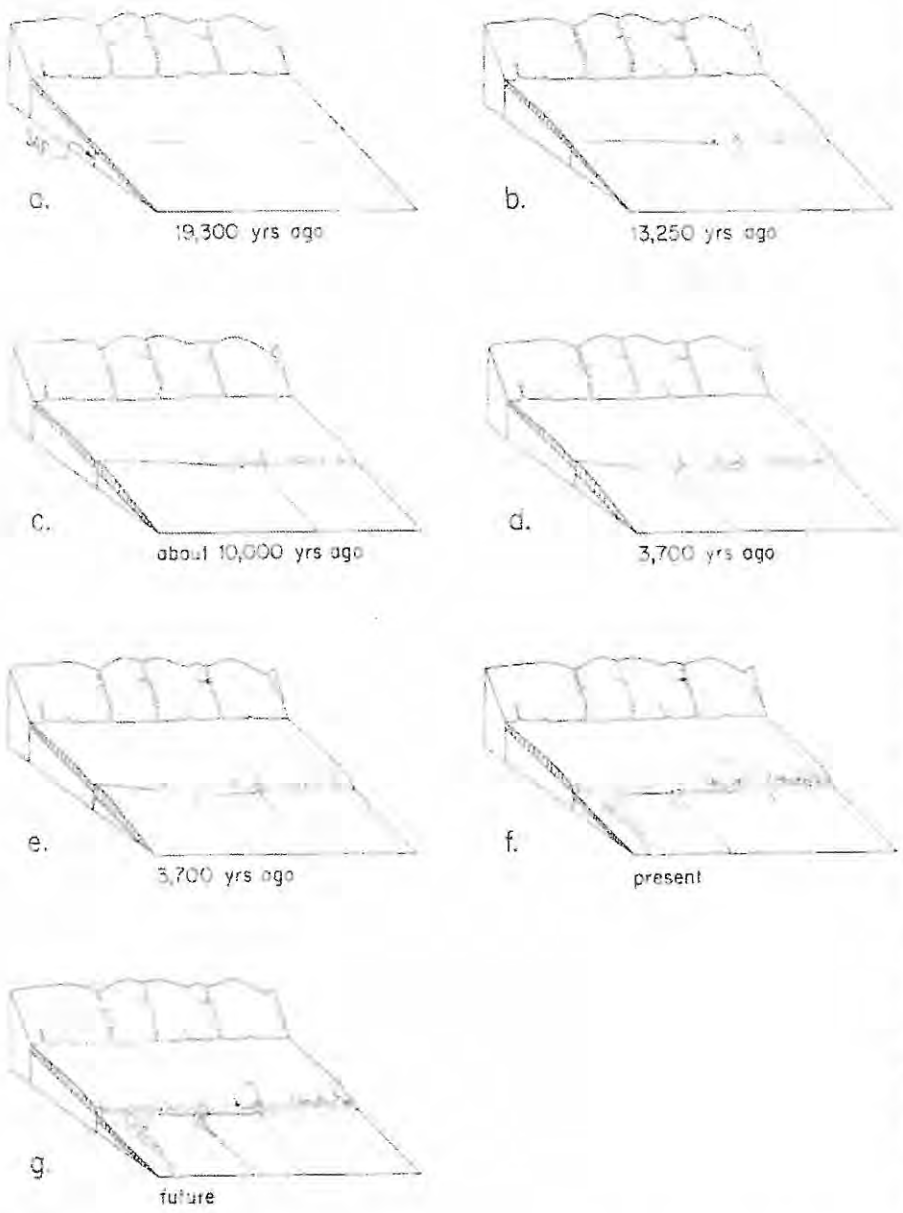

Figure 7. The Holocene–late Pleistocene evolution of Wallace Creek. An aggrading "older alluvial fan" during the period including 19,300 yr ago progressively buried small scarps formed along the San Andreas fault (SAF) during major strike-slip events (a). Right-lateral offsets accumulated during this period, but no geomorphologically recognizable offsets began to form until 13,250 yr ago, when the "older alluvial fan" became inactivated by initial entrenchment of Wallace Creek (b). At this time, erosion of small gullies to the right (southeast) of Wallace Creek also resulted in deposition of the "younger fan alluvium" downstream from the fault. These features then began to record right-lateral offset, and scarps began to grow along the fault. About 10,000 yr ago, a new channel was cut across the fault at Wallace Creek, and the initial channel, downstream from the fault, was abandoned (c). The new channel remained the active channel of Wallace Creek during the early and middle Holocene, during which ~ 250 m of slip accumulated (d). This channel filled with "high-channel alluvium" 3,700 yr ago, and Wallace Creek cut a new channel straight across the fault (e). Between 3,700 yr ago and the present, this youngest channel has registered 128 m of right-lateral offset (f). Aggradation of this channel, accompanied by continued offset, will probably lead to its abandonment and the creation of a new channel, cut straight across the fault (g).

intersection with the fault and then measuring the distance from that intersection to the intersection of the modern channel edge (labeled 2 in Fig. 8) with the fault. The same value is obtained if one measures the distance between the offset segments of the modern channel (labeled 3 and 4 in Fig. 8). In making the latter measurement of offset, it is important to realize that the outside edge of the left bend has been eroded by flood waters that have swept against it as they have passed around the left bend. The right bend has not been eroded in this manner, because it is refreshened each time the fault slips.

The fact that feature 1 and feature 3 (Fig. 8) intersect the fault at almost the same point strongly suggests that the abandonment of the high channel and entrenchment of the modern channel were contemporaneous. This coincidence also indicates that the new channel was cut straight across the fault without any initial nontectonic deflection of the stream along a fault scarp. The absence of any initial, nontectonic deflection is also confirmed by the fact that the modern channel is entrenched through a broad topographic high immediately downstream from the fault (consider contours in Fig. 2). If the channel had been deflected along a fault scarp, one would expect it to have cut through a low point on the downstream side of the fault rather than a high point. The measured separation of 128 m thus is ascribable entirely to tectonic offset.

The youngest date from the deposits of the abandoned high channel (3680 ± 155 yr B.P.) provides a maximum age for the modern channel, because all of the high-channel sediments were deposited before the modern channel was cut. All offset of the modern channel thus occurred between this date and A.D. 1857. The average slip rate, therefore, can be no slower than 35.7 ± 1.9 mm/yr (128 ± 1 m/3,680 − 155 ± 91 yr [the time between A.D. 1950, which has been designated zero B.P., and A.D. 1857.]).

Additional considerations are necessary to provide an upper limit to the slip rate. For this constraint, trenches 9 and 10 (Fig. 4) are useful. The high-channel deposits here consist of three distinct units, labeled C1, C2, and C3, that represent three distinct scourings and fillings. The uppermost sediment of channel C2 in trench 10 contained the radiocarbon sample the age of which is 3780 ± 155 yr B.P. At the time of deposition, C1, C2, and C3 in trenches 9 and 10 must have been at or northwest of the right bend of Wallace Creek. Trench 9 is now 145 m northwest of the right bend, and so no more than 145 m of dextral slip has accumulated since channel C2 was filled 3780 ± 155 yr B.P.

The trend of C2 between trenches 10 and 9 suggests that the edge of C2 actually intersects

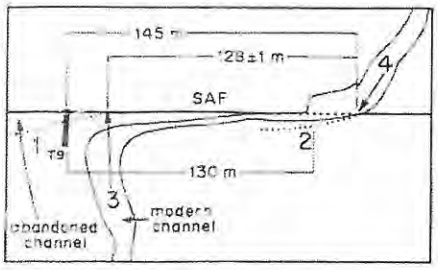

Figure 8. The edge of the abandoned channel (1) intersects the fault 128 ± 1 m northwest of the intersection of the modern channel edge (2) and the fault. The offset of the modern channel (from point 3 to point 4) is also 128 m. These provide the best measure of offset during the past 3,700 yr.

the fault at least 10 m closer to the modern right bend. In support of this, we note that the channel is ~5 m wide and rests entirely southwest of the fault in both trench 9 and trench 10. Sufficient channel width to accommodate a similar deposit southwest of the fault in the modern channel does not exist until at least 15 m downstream from the modern right bend. There, the crest of the channel bank is ~5 m southwest of the fault trace, and, were the channel to fill this year, a 5-m wide deposit analagous to the channel fill in trenches 9 and 10 would be deposited. From trench 9 to this geometrically analagous point in the modern channel (labeled 2 in Fig. 8) is ~130 m. It seems, therefore, that no more than 130 m of dextral slip accumulated between 3780 ± 155 yr B.P. and A.D. 1857. This yields an *upper* limit of 35.3 ± 1.5 mm/yr [130 m/(3,780 ± 155 − 93 yr)] for the slip rate. This maximum limiting rate is indistinguishable from the minimum limiting rate of 35.7 ± 1.9 mm/yr determined previously and independently. The rate must therefore be 35.3 ± 1.5 mm/yr, which includes the highest maximum value (35.3 + 1.5 mm/yr) and the lowest minimum value (35.7 − 1.9 mm/yr).

The calculations thus far have assumed continuous fault displacement between 3680 yr B.P. and A.D. 1857. It is very likely, however, that much, and possibly all, of the slip accumulates sporadically, during large earthquakes, such as that which occurred in 1857. If, as we argue below, this segment of the fault is characterized by coseismic displacements of ~10 m, followed by several centuries of quiet repose, the fault could have been at any point in its earthquake cycle 3680 yr B.P. If, in that year, the region bisected by the fault was in the middle or toward the end of a period of elastic strain accumulation, the rate calculated using this data will be slightly too high, because the 128-m offset accumulated between then and 1857 is in small part due to loading that occurred slightly earlier. Put in a different way, the 3,680-yr date may be any fraction of a recurrence interval younger than the beginning of a strain accumulation cycle. The beginning of the loading cycle corresponding to the earliest increment of the 128-m offset thus may be any time between 3680 yr B.P. and 3680 plus one recurrence interval. As is seen below, the average recurrence interval here is ~310 yr, or 8% of the time between A.D. 1857 and 3680 yr B.P. The actual slip rate thus could be as much as 8% lower than that just calculated, or 32.5 ± 1.5 mm/yr. The late Holocene slip rate thus could be any value between 32.5 ± 1.5 and 35.3 ± 1.5 mm/yr. This range is conveniently expressed as 33.9 ± 2.9 mm/yr.

Slip Rate since 13,250 yr B.P.

An additional determination of slip rate along the San Andreas fault at Wallace Creek comes from the 475-m offset of a 13,250-yr-old alluvial fan from its source gullies. This provides an average slip rate of 35.8 + 5.4/−4.1 mm/yr, which is not appreciably different from the late Holocene rate of 33.9 ± 2.9 mm/yr.

The 13,250-yr-old alluvial fan constitutes the "younger fan alluvium" mapped in Figure 2. The fan radiated from a point that is now located very near the modern left bend of Wallace Creek. Its existence is reflected in the bulging of the 2,240-, 2,250-, and 2,260-ft contours toward the southwest (Fig. 2). Even though it is now buried by 1.5 to 2 m of unmapped slope wash and bioturbated materials, the bulging of the contours and measurements of thickness in trenches 2, 3, 4, and 6 enable construction of the isopach map of the younger fan alluvium shown in Figure 9.

Trench 2 (Fig. 3) exposes the sediments of the fan near its apex. There, the sediments constitute a 1.3-m-thick bed of well-sorted, imbricated sandy gravel. The gravel is composed of tabular pebbles of diatomaceous Tertiary marine mudstone. Imbrication of these tabular pebbles clearly indicates a flow direction toward the southwest. The source of the alluvial fan thus must be on the opposite side of the San Andreas fault. Although the fan is composed of three discrete beds in trench 2 (see detailed log of trenches, available from author), the lack of bioturbation or weathering of the two horizons between these beds suggests that the fan was deposited very rapidly, perhaps in a matter of a few decades or less.

The deposit overlies a massive, poorly sorted sandy loam that represents either a colluvial unit or an alluvial deposit that was extensively bioturbated prior to burial. The unit probably lay at the ground surface for a long time prior to burial by the alluvial fan. The presence of charcoal pebbles and granules in this unit, no more than a centimetre or two beneath the base of the fan, suggests that a range fire occurred just prior to deposition of the fan. The charcoal certainly would have been oxidized if it had not been buried deeply very soon after its formation. Erosion of the fan materials from their source within the burned area may have been a direct result of the fire, which removed protective vegetative cover from the ground surface. The charcoal age of 13,250 ± 1,650 yr B.P. thus represents the age of the basal unit of the overlying alluvial fan.

If the source of the younger fan sediments were Wallace Creek, the fan would be offset a mere 128 m. This would imply that the fault was inactive between about 13,000 yr and about 3700 yr B.P., because we have just shown that 128 m of slip has occurred since about 3700 yr B.P. Such a long period of dormancy along the San Andreas fault seems very unlikely to us, and so we seek a source for the younger fan that is farther to the southeast.

The volume of the fan is ~25,000 m^3. Candidates for the source gully (or gullies) must have total eroded volumes at least as great as this and preferably somewhat larger, because some of the material transported out of the source region must have been carried beyond the alluvial fan as suspended load and bedload.

Given this constraint, only two plausible sources for the fan exist within 1 km of Wallace Creek. The first is a solitary channel ~730 m southeast of the fan apex (E in Fig. 1). This channel originates in the Temblor Range but drains a much smaller area than Wallace Creek. If this is the source, an average slip rate of ~63 mm/yr for the period 13,250 to 3700 yr B.P. is calculated:

$$\frac{(730 - 128)\ \text{m}}{(13{,}250 - 3{,}680)\ \text{yr}} \approx 63\ \text{mm/yr}.$$

This would indicate fluctuations in slip rate of at least several centimetres per year during the past 13,000 yr, because the average rate for the past 3,800 yr has been ~34 mm/yr.

More likely sources for the alluvial fan are four closely spaced gullies several hundred metres southeast of the fan apex (A, B, C, and D in Fig. 1). In Figure 9, these have been restored to their probable location at the time of formation of the fan. None of these four small gullies, which extend only a few hundred metres back from the fault scarp, could have been the sole provider of enough material to construct the entire fan. The volumes of A, B, and C are only ~13,000 m^3 each, and D is much smaller. In any combination, however, they could have delivered enough material.

The proper matching of this multiple source with the younger fan deposit can be determined rather precisely. If the general reconstruction shown in Figure 9 is correct, the southeastern

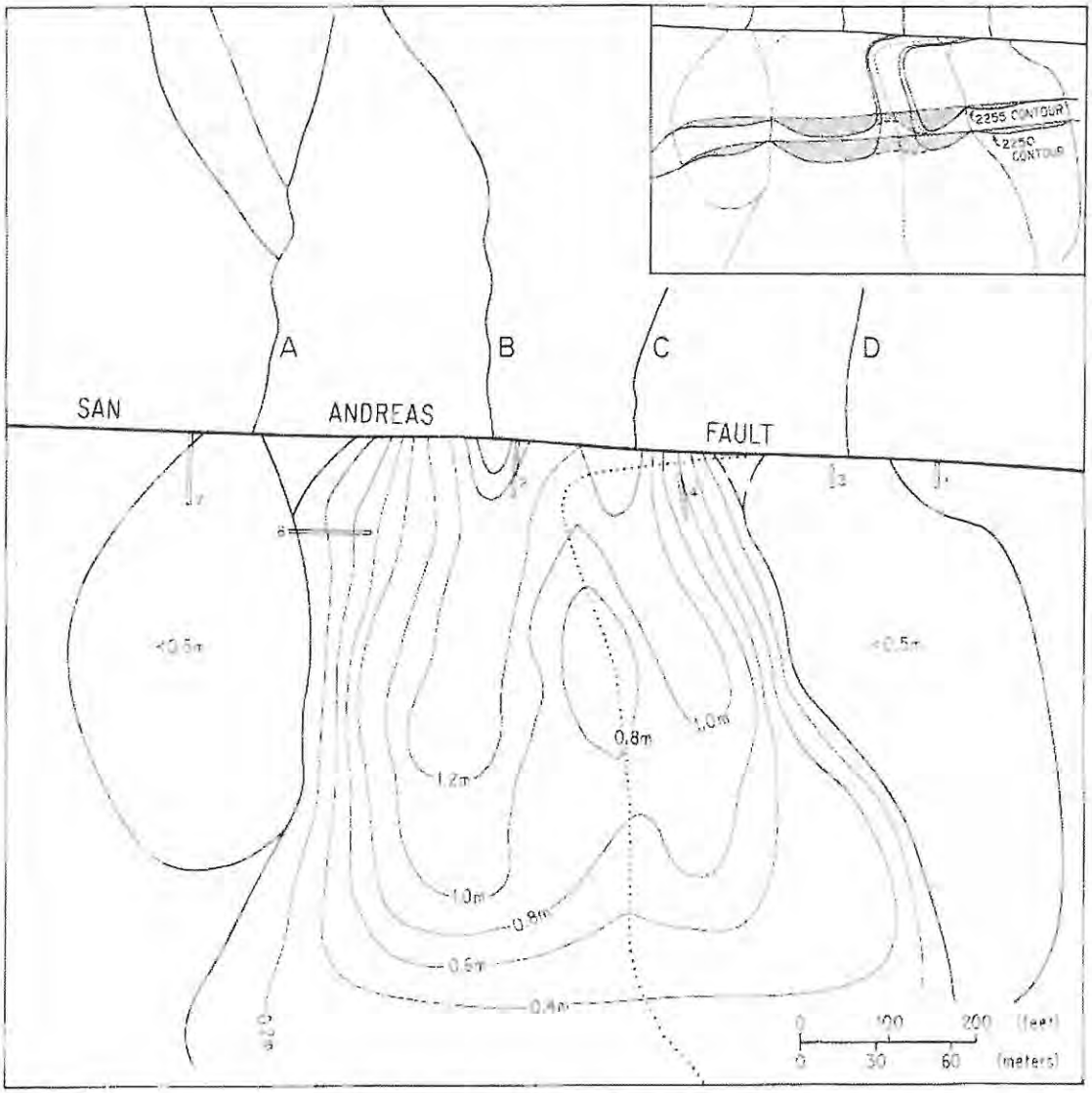

Figure 9. Isopach map of 13,250-yr-old alluvial fan and source gullies B and C. In this figure, the gullies have been restored 475 m to their late Pleistocene position upstream from the fan. The same gullies are indicated by letters B and C in Figure 1b. For reference, dotted line represents location of modern channel of Wallace Creek. Isopach map is based on trench exposures (thick, open bars) and geometry of contours. Insert in upper right illustrates use of topographic contours in constructing isopach map. Lower edge of stippled region is topographic contour. Upper edge is contour prior to deposition of fan. Southwestward bulging of contours indicates presence and thickness of alluvial fan.

flank of the main fan complex had to be southeast of channel C. The offset thus is no less than 472 m. At the same time, the crests of the two distinct lobes of the fan shown in Figure 9 should have had their apexes at the mouths of two of the middle gullies. Only gullies B and C are spaced appropriately to meet this constraint. The mouth of gully B cannot be offset more than 478 m, if B is the source of the northwestern lobe of the fan. It is of interest that the younger fan deposits are offset from gullies A, B, C, and D, only slightly less so than the oldest, beheaded channel of Wallace Creek itself (marked with a white arrow at the left margin of Fig. 1). The creation of gullies A, B, C, and D must, therefore, be nearly contemporaneous with the first entrenchment of Wallace Creek.

These considerations constrain the offset of the younger fan deposits to 475 ± 3 m. In that the younger fan formed 13,250 ± 1650 yr B.P., the average slip rate must be 35.8 + 5.4/ −4.1 mm/yr. Within the level of resolution, this cannot be distinguished from the average late Holocene rate of 33.9 ± 2.9 mm/yr.

RECURRENCE INTERVALS BETWEEN PAST LARGE EARTHQUAKES AT WALLACE CREEK

The average Holocene and late Holocene rates of slip at Wallace Creek are important new measurements of strain across the San Andreas

TABLE 2. SMALLEST STREAM OFFSETS NEAR WALLACE CREEK AND PROPOSED INTERVALS BETWEEN GREAT EARTHQUAKES

(1) Stream offsets (m)	(2) Remarks	(3) Produced by	(4) Slip associated with earthquake (m)	(5) Proposed interval between events (yr)
9.5 ± 0.5 (±1σ)	Average of 5 measurements	1857 event	9.5 ± 0.5(±1σ)	
				240 to 320[a]
21.8 ± 1.1	Average of 4 measurements**	1857 plus one prehistoric event	12.3 ± 1.2*	
				300 to 440[b]
32.8 or 33.5 ± 1.9	Average of 3 measurements**	1857 plus latest 2 prehistoric events	11.0 or 11.7 ± 2.2†	240 to 450[c]

*$21.8 - 9.5 = 12.3$; $\sqrt{1.1^2 + 0.5^2} = 1.2$.
†$32.8 - 21.8 = 11.0$; $\sqrt{1.9^2 + 1.1^2} = 2.2$; $33.5 - 21.8 = 11.7$; $\sqrt{1.9^2 + 1.1^2} = 2.2$.
‡Slip during following earthquake in column 4 divided by average late Holocene slip rate (33.9 ± 2.9 mm/yr).
**Offset gullies are all between Wallace Creek and Gully D in Figure 1.

TABLE 3. SMALLEST STREAM OFFSETS NEAR WALLACE CREEK AND PROPOSED DATES AND CORRELATION OF LATEST FOUR GREAT EARTHQUAKES

(1) Stream offsets (m)	(2) Time required to accumulate offset at elastic strain using average late Holocene slip rate (years)	(3) Proposed dates for latest earthquakes (A.D.)	(4) Possible correlations with events recognized at Pallett Creek	(5) Possible correlations with events recognized at Mill Potrero by Davis (1983)
9.5 ± 0.5 (±1σ)	240 to 320	1857	Z(1857)	Z(1857)
21.8 ± 1.1	560 to 740	1540 to 1630*	V(1550 ± 70)	V(1584 ± 70)
32.8 or 33.5 ± 1.9	840 to 1140	1320 to 1360†	R(1380 ± 65)	
		120 to 1020‡	F(1845 ± 75)	

*1857 - (240 to 320 yr).
†1857 - (560 to 740 yr).
‡1857 - (840 to 1140 yr).

fault in central California, because they are the first to span more than a fraction of a great earthquake cycle of strain accumulation and relief. These millennial averages can be used in conjunction with other data to infer earthquake recurrence intervals.

For example, the length of the cycle of strain accumulation that preceded and led to the great 1857 earthquake can be calculated. In 1857, the San Andreas fault sustained 9.5 m of right-lateral slip at Wallace Creek. This is indicated by five small offset gullies nearby (A, B, C, D, and F in Fig. 1; Table 2), as well as by small offset gullies at distances of as much as several kilometres to the northwest and southeast. These gullies were incised across the fault prior to the 1857 event, but after the previous large event (see Sieh, 1978c, for a more detailed discussion). If one assumes that the 9.5 m of fault slip associated with the 1857 earthquake relieved elastic strains that had accumulated in the adjacent crustal blocks at an average rate of 34 mm/yr, one calculates that the 1857 earthquake was preceded by a 280-yr period of strain accumulation. This calculation does not assume that annual strain accumulation was uniform during the 280-yr period, but only that the *average* annual rate was equal to the millennial average of 34 mm/yr. Periods of faster or slower accumulation thus could be accommodated within the over-all loading cycle. Table 2 (top of col. 5) displays the actual range of values for the period of strain accumulation if the uncertainties in the 1857 offset value and average slip rate are taken into account. In lieu of a direct dating of the large event that preceded the 1857 event at Wallace Creek, this range (240–320 yr) is probably the best estimate that can be made for the recurrence interval between the 1857 earthquake and its predecessor.

Estimates of the duration of two earlier periods of strain accumulation can also be made, using the average late Holocene slip rate and the amount of fault slip associated with each of the last two prehistoric earthquakes. Table 2 lists the data that suggest these 2 events were associated with ~12.3 and 11.5 m of fault slip at Wallace Creek. At 34 mm/yr, these values would have accumulated in 360 and 340 yr, respectively. The actual range in value for both of these recurrence intervals, calculated using the ranges in value for the slip rate and the offsets, is displayed in column 5 of Table 2. From the table, one can see that the latest 3 recurrence intervals are estimated to be within the range of 240 to 450 yr.

Of course, it is possible that the 4,000-yr and 13,000-yr average slip rates do not represent the average rate of strain accumulation during the periods of fault dormancy prior to 1857 and the 2 previous great earthquakes. For example, the rate of accumulation actually could have been much higher during the past millennium and much slower during the previous 4,000-yr interval. If so, the recurrence intervals between the latest few earthquakes would be much shorter than those calculated above. Perhaps a future study of a currently undiscovered 1,000-yr-old feature near Wallace Creek will resolve this issue by providing a 1,000-yr average rate. Alternatively, the past several earthquakes may be dated directly, as has been done at Pallett Creek (Sieh, 1978b, in press). In the meantime, the validity of using the 3,700-yr average slip rate in calculating recurrence intervals of recent and future great earthquakes must be assessed in other ways.

First, the slip rate averaged over the past 3,700 yr (33.9 ± 2.9 mm/yr) does not differ appreciably from the 13,000-yr average (35.8 + 5.4/−4.1 mm/yr), although the 13,000-yr average conceivably could be as much as 10 mm/yr (~30%) faster than the late Holocene average, given the imprecision of the 2 determinations.

Second, geodetic data on modern rates of strain accumulation across the fault are available from the "Carrizo" net, which spans the fault and 80 km of adjacent territory at the latitude of Wallace Creek (Savage, 1983, and 1982, written commun.). These data are available, however, only for the period 1977.6 to 1981.5. The deformation observed during this period averages 0.29 ± 0.06 μstrain/yr (extension) N89°E ± 4°W and −0.09 ± 0.06 μstrain/yr (contraction) north-south. Numerous models of lithospheric deformation can produce this observed surficial deformation. One class of model involves the assumption that the observed deformations are the result of aseismic right-lateral slip on the San Andreas fault beneath its locked, brittle upper 10 or 20 km. In this case, the observed deformations of the Carrizo net are resolved as right-lateral shear strains parallel to the San Andreas fault. The average shear strain over the entire 80-km-wide network is 0.38 ± 0.04 μrad/yr. This translates into a deep slip rate on the fault of 30.4 ± 3.2 mm/yr, if one assumes that the network spans the entire zone of deformation due to slip on the fault. If it does not span the entire zone, the rate of deep slip on the fault must be higher. Like the 13,000-yr average rate, the geodetically determined modern rate does not differ significantly from the 3,700-yr average.

The similarity of the 13,000-yr, 3,700-yr, and 4-yr averages suggests that strain accumulation across the fault may be fairly uniform. Of course, numerous histories could be invented that include these three data points and yet involve large fluctuations in the strain accumulation rate between earthquake cycles or recurrence intervals. To date, however, no known data support large fluctuations. A reasonable assumption, thus, is that the late Holocene average

slip rate represents the average rate of strain accumulation between large earthquakes. The recurrence intervals displayed in Table 2 may, therefore, be realistic estimates of the dormant intervals that preceded the past three great earthquakes.

In the next section, we attempt to assess when the current earthquake cycle will end at Wallace Creek; that is, when the next great earthquake, accompanied by rupture at Wallace Creek, will occur. We also attempt to use the 3,700-yr average slip rate to assess the likelihood of large earthquakes elsewhere along the San Andreas fault.

FORECASTS OF THE BEHAVIOR OF THE SAN ANDREAS FAULT

Along the South-Central (1857) Segment

If the crust adjacent to the San Andreas fault has been accumulating strain at 34 mm/yr since 1857, as much as 4.3 m of potential slip has now been stored and conceivably could be released along all or part of the 1857 rupture. Geomorphologic data, however, suggest that this is likely only along two portions of the 1857 rupture. Wallace Creek is not within either of these portions.

Figure 10 displays offsets measured along the south-central segment of the San Andreas fault. The 1857 segment is divisible into at least three parts, based on slippage during the 1857 earthquake and one to four previous large earthquakes. The southeastern part is ~90 km long and seems to have been characterized by 3- to 4.5-m slip events. The central 160 km, including Wallace Creek, has experienced 7 to 12.3 m of slip during the most recent 3 great earthquakes. The lower values along this central portion occur along the reach between km 90 and km 200, where several other active faults to the north and northeast exist, and so the lower values may reflect distributed deformation, away from the San Andreas fault. A 30-km segment northwest of Wallace Creek experienced 3 to 4 m of slip in 1857 and probably 1 or 2 during previous large earthquakes, as well.

These data suggest that each part of the fault has experienced a characteristic amount of slippage during the past three to four large earthquakes. Although, of course, so few data do not provide a statistically sound basis for predicting all previous and future events, we are confident that this pattern offers some insight into the long-term behavior of the fault.

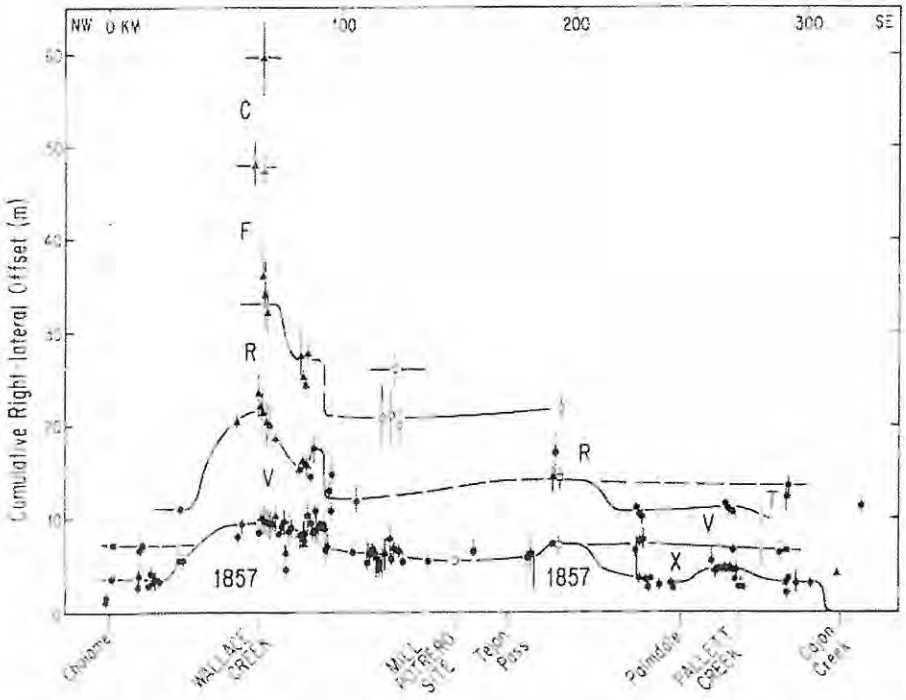

Figure 10. Right-lateral offsets measured along the south-central (1857) segment of the San Andreas fault suggest that slip at each locality is characterized by a particular value. Solid circles are data from Sieh (1978c), with poor-quality data deleted. Open circles are data from Davis (1983). Triangles are new data and remeasurements at sites reported by Sieh (1978c). Open squares are new data. Vertical bars indicate magnitude of imprecision in measurement.

At least two explanations are worth considering. First, we consider the possibility that the northwestern 40 km and southeastern 90 km are loaded more slowly, and, therefore, when the earthquake occurs, they experience lesser amounts of slip than does the central 160-km-long part. This is unlikely, because the average Holocene slip rate along these two parts must be nearly equal to the rate determined at Wallace Creek. Just beyond the south-central segment, at Cajon Creek (Fig. 10), the San Andreas has average Holocene and late Holocene slip rates of 25 ± 3 mm/yr (Weldon and Sieh, 1981). The nearby San Jacinto and related subparallel faults probably carry ~10 mm/yr at this latitude (based on data of Sharp, 1981, and Metzger, 1982). These fault systems end and nearly merge with the San Andreas fault just northwest of Cajon Creek. Farther northwest, the San Andreas fault is the only major active structure, and so northwest of Cajon Creek, it must have a slip rate of ~35 mm/yr. In addition, the average recurrence interval for large earthquakes at Pallett Creek (location in Fig. 10) is in the range of 145 to 200 yr, which is appreciably shorter than the 240- to 450-yr range at Wallace Creek. For this reason, some of the slip events shown in Figure 10 in the Palmdale-Pallett Creek region must have their northwestern rupture tip southeast of Wallace Creek, and 1857-like events cannot be the only type of slip event along this part of the south-central segment.

The northwestern 30 km of the south-central segment (Fig. 10) must also share the long-term average slip rate of Wallace Creek. No diversion of a large fraction of the Wallace Creek rate along other structures is plausible. The only known major active(?) fault nearby is the San Juan Hill fault, which runs 3 to 14 km west of and subparallel to the San Andreas from about Cholame to Wallace Creek (Jennings and others, 1975). Its rate of slip is probably no more than a few millimetres per year.

A second explanation for the different behavior of the three parts of the south-central segment is based on the hypothesis that each part is imbued with a different strength. If, for reasons of geometry or rock properties, the central 160 km of the segment were 2 or 3 times stronger than the 2 other parts, 2 or 3 times as much elastic loading of the adjacent crustal blocks would be necessary before failure occurred.

Each failure thus would result in two to three times as much slippage as on the two adjacent parts. Such an explanation is compatible with our judgments that (1) slip rate does not vary greatly along the south-central segment, and (2) large earthquakes are more frequent at Pallett Creek than at Wallace Creek.

Table 3 lists our best estimates of the dates of large earthquakes at Wallace Creek and proposed correlations with large earthquakes that have been directly dated at Pallett Creek (Sieh, in press) and at Mill Potrero (Davis, 1983). The capital letters in Figure 10 reflect our best judgment regarding correlation of the latest events at Wallace Creek, Pallett Creek, and Mill Potrero. Event X at Pallett Creek (A.D. 1720 ± 50) has no correlative at Wallace Creek, although Davis (1983) discovered evidence for and dated a relatively small slip event at Mill Potrero that may well be event X. Event V at Pallett Creek occurred about A.D. 1550, which is about the time we estimate that the last prehistoric event at Wallace Creek occurred, and also about the time of a large slip event that Davis (1983) discovered at Mill Potrero. Similarly, events R and F at Pallett Creek occurred at about the time we estimate that the third and fourth events occurred at Wallace Creek.

On the basis of the foregoing discussion, we judge that the central 160 km of the south-central segment of the San Andreas fault is unlikely to generate a great earthquake for at least another 100 yr. Recurrence intervals appear to be in the range of 250 to 450 yr, and yet the time elapsed since the great earthquake of 1857 is only 127 yr. Slip during the latest 3 great earthquakes has been 7 to 12.3 m, and yet we suspect that only a little more than 4 m of potential slip has been stored in the past 127 yr.

The southeastern 90 km and the northwestern 30 km of the south-central segment are good candidates for producing a large earthquake within the next several decades. Geomorphologic measurements seem to indicate that 3 to 4.5 m of slip is characteristic during large events, and ~4 m of potential slip may well have been stored in the adjacent crustal blocks since 1857. Based on studies at Pallett Creek, the probability of a great event along the southeastern 90 km of the south-central segment within the next 50 yr is between 26% and 98% (Sieh, in press).

Along the Creeping Segment

The long-term average slip rates determined at Wallace Creek are indistinguishable from the geodetically determined rates of slip at deep levels along the fault from Wallace Creek to Monterey Bay (Savage, 1983; Lisowski and Prescott, 1981). The long-term rates at Wallace Creek are also identical to the historical rate of slip at shallow levels along the central 50 km of the creeping segment (see data compiled by Lisowski and Prescott, 1981, Fig. 6). These similarities could be coincidental, but they suggest that the central 50 km of the creeping segment is creeping annually at its millennial-average rate of slip. If this were true, it would mean that large elastic strains are not accumulating across the central 50 km of the creeping segment, and that this segment will not participate in the generation of the next large earthquakes along the San Andreas fault.

From a geological point of view, it is reasonable to suspect that the long-term slip rate along the San Andreas fault at Wallace Creek should not be different from its long-term rate along the creeping segment, except along its northernmost 50 km, adjacent to which runs the actively creeping Paicines fault (Harsh and Pavoni, 1978). No other large, active structures in the latitudes of the creeping segment can be called upon to absorb a large portion of the slip rate observed farther south at Wallace Creek. Likewise, there are no obvious geological structures near the San Andreas that would lead one to suspect that the long-term slip rate along the creeping segment is appreciably higher than the long-term rate farther south.

Along the 90-km Segment Centered on Cholame

Between the central 50 km of the creeping zone and Wallace Creek, there is a stretch of the San Andreas fault that historically has been a zone of transition between the fully creeping and fully locked portions of the fault. On the basis of available data, this segment is a prime candidate for generating a large earthquake in the near future. In the period of historical record, it has not experienced as much slip as have segments to the northwest or southeast, and it is therefore a "slip gap."

One interpretation of the historical data is illustrated in Figure 11, in which cumulative right-lateral slip for the past two centuries is

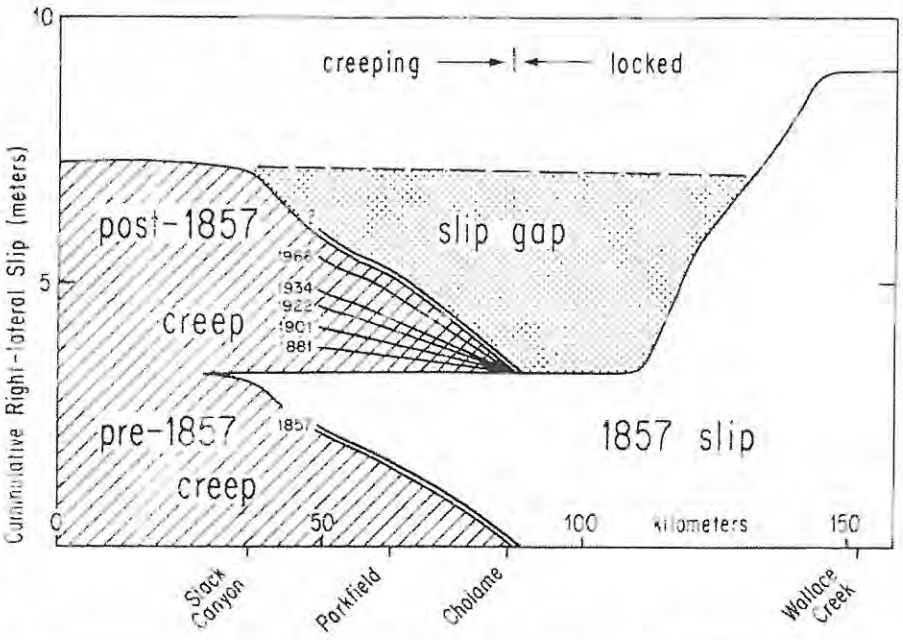

Figure 11. Hypothetical source of future major earthquake along the San Andreas fault includes ~60 km of the currently creeping segment and 30 km of the locked segment. Cumulative right-lateral slip plotted against distance along the fault indicates that this 90-km segment is slip-deficient relative to adjacent stretches of the fault. Slip in 1857 is from Sieh (1978c). Cumulative slip along the creeping segment is extrapolated from alignment array slip rates for period 1968–1979 (Lisowski and Prescott, 1981, Fig. 6). Dates of moderate earthquakes generated by slip along the fault in the Parkfield-Cholame region are shown, because such an event probably triggered the great 1857 rupture and conceivably could trigger the rupture of the slip gap.

plotted as a function of location along the fault. We assume that creep rates northwest of Cholame have been constant for the past few hundred years, so that the alignment array data for the period 1968–1979 are representative of the pre- and post-1857 creep rates. We also assume that Cholame has been the edge of the creep zone throughout this period. In the century preceding 1857, 3 to 3.5 m of slip would have accumulated by creep northwest of Slack Canyon. Less slip would have accumulated by creep, and perhaps during occasional moderate earthquakes, between Slack Canyon and Cholame.

In 1857, ~3.5 m of slip occurred along the 30-km stretch of the fault southeast of Cholame, and 9.5 m of slip occurred in the vicinity of Wallace Creek. The sparse historical accounts are compatible with our inference in Figure 11 that slippage during the earthquake decreased northwestward from Cholame and died out near Slack Canyon (Sieh, 1978c, p. 1423–1424).

Following 1857, creep resumed northwest of Cholame. Northwest of Slack Canyon, ~4.5 m of slip now has accumulated at the full, long-term rate of loading of the fault (that is, 34 mm/yr). The 60-km-long section between Slack Canyon and Cholame, however, has crept at rates that are significantly lower than the loading rate, and strain is being stored in the rocks adjacent to the fault there. Similarly, elastic strains are accumulating in the rocks adjacent to the locked portion of the fault, and the northernmost 30 km of this portion, which seems to fail in 3- to 4-m slip events, may well be loaded nearly to the point of failure.

We suggest that this northernmost part of the locked segment and the southernmost part of the creeping segment might fail in unison and produce a major earthquake. This hypothetical event would be associated with ~90 km of surface rupture and a maximum of ~4.3 m of right-lateral slip.

In discussing this hypothetical event, it is important to note that the great 1857 earthquake seems to have originated in this region. Sieh (1978a) documented that at least 2 moderate foreshocks occurred in this vicinity about 1.5 and 2.5 hr prior to the main shock. Within the past century, 5 moderate (M5.5 to 6) earthquakes have been produced by slippage along the San Andreas fault northwest of Cholame. Sieh (1978a) inferred that the 1857 foreshocks emanated from a source similar to that which produced these historical shocks. If this is true, then the next moderate "Parkfield-Cholame" earthquake might well be a foreshock of the hypothetical major event described above.

ROLE OF THE SAN ANDREAS FAULT IN THE RELATIVE MOTION OF THE NORTH AMERICAN AND PACIFIC PLATES

Minster and Jordan (1978) determined from a circumglobal data set that the relative motion of the Pacific and North American plates has averaged ~56 mm/yr during the past 3 m.y. The geological record at Wallace Creek shows that, at least during the past 13,000 yr, only ~34 mm/yr of this has been accommodated by slip along the San Andreas fault. If one assumes that the 3-m.y. average represents the Holocene average rate across the plate boundary as well, then clearly the San Andreas fault is accommodating only ~60% of the relative plate motion. The remainder of the deformation must be accomplished elsewhere within a broader plate boundary. The San Gregorio–Hosgri fault system, which traverses the coast of central California, may have a late Pleistocene–Holocene slip rate of 6 to 13 mm/yr (Weber and Lajoie, 1977), and the Basin Ranges, to the east of the San Andreas fault, may be opening N35°W on oblique normal faults at a late Pleistocene–Holocene rate of ~7 mm/yr (Thompson and Burke, 1973). Most of the 56 mm/yr plate rate thus may be attributed to the San Andreas, San Gregorio–Hosgri, and Basin Range faults. Long-term slip rates on these three major fault systems are not known precisely enough to preclude or confirm the possibility that the rate of relative plate motion during the Holocene is equal to the 3-m.y. average. No clear basis exists, however, for suggesting that the Holocene rate is less than or more than the longer-term rate.

ACKNOWLEDGMENTS

Wallace Creek is named after Robert Wallace, who elucidated the basic history of the channel more than 15 years ago and provided us with a special topographic base map. N. Timothy Hall drew our attention to the study site. He and Laurie Sieh participated in initial studies. Art Fairfall and John Erickson at the University of Washington provided all of the radiocarbon analyses. Robert Wallace, David Schwartz, David Pollard, Christopher Sanders, and Ray Weldon provided helpful criticisms of earlier manuscripts. This work was supported by the National Earthquake Hazards Reduction Program, U.S. Geological Survey Contract nos. 14-08-0001-15225, 16774, 18385, and 19756.

REFERENCES CITED

Agnew, D., and Sieh, K., 1978, A documentary study of the felt effects of the great California earthquake of 1857: Seismological Society of America Bulletin, v. 68, p. 1717–1729.

Arnold, R., and Johnson, H. R., 1969, The earthquake off Point Sal, Santa Barbara County, California: Science, v. 29, no. 744, p. 558.

Crowell, J., 1962, Displacement along the San Andreas Fault, California: Geological Society of America Special Papers, v. 71, 61 p.

——1981, An outline of the tectonic history of southeastern California, *in* Ernst, W. G., ed., The geotectonic development of California: Englewood Cliffs, New Jersey, Prentice-Hall, p. 583–600.

Dibblee, T., 1968, Late Cenozoic structure and tectonic history of the western "Big Bend" of the San Andreas Fault and adjacent San Emigdio Mountains (Ph.D. dissert.): Santa Barbara, California, University of California, Department of Geological Sciences.

Hurst, P., and Prevott, N., 1978, Slip on the Parkfield fault: Seismological Society of America Bulletin, v. 68, p. 1191–1194.

Hill, M., and Dibblee, T., Jr., 1953, San Andreas, Garlock and Big Pine faults, California—A study of the character, history and tectonic significance of their displacements: Geological Society of America Bulletin, v. 64, p. 443–458.

Jennings, C., and others, 1975, Fault map of California: Division of Mines and Geology California Geological Data Map Series, Map no. 1, scale 1:750,000.

Klein, J., Lerman, J. C., Damon, P. E., and Ralph, E. K., 1982, Calibration of radiocarbon dates: Tables based on the consensus data of the Workshop Calibration of Radiocarbon: Time Scale: Radiocarbon, v. 24, p. 103–150.

Lawson, A., and others, 1908, The California earthquake of April 18, 1906—Report of the State Earthquake Investigation Commission, Washington, D.C., Carnegie Institution of Washington, 2 volumes and atlas, 451 p.

Lisowski, M., and Prescott, W. H., 1981, Short-range distance measurements along the San Andreas fault system in central California: Seismological Society of America Bulletin, v. 71, no. 5, p. 1607–1624.

Metzger, L., 1982, Tectonic implications of the Quaternary history of Lower Lytle Creek, southeastern San Gabriel Mountains (B.S. thesis): Claremont, California, Pomona College.

Minster, J. B., and Jordan, T. H., 1978, Present-day plate motions: Journal of Geophysical Research, v. 83, no. B11, p. 5331–5354.

Nilsen, T., and Link, M. H., 1975, Stratigraphy, sedimentology and offset along the San Andreas fault of Eocene to lower Miocene strata of the western Santa Lucia Range and the San Emigdio Mountains, Coast Ranges, central California, *in* Weaver, D. W., and others, eds., Tectonic framework and volcanic sedimentology: Pacific Section, Society of Economic Paleontologists and Mineralogists Short Course, Annual Meeting, SAPG-SEPM SEG, Long Beach, California, p. 367–400.

Reid, H. F., 1910, Permanent displacements of the ground, *in* The California earthquake of April 18, 1906—Report of the State Earthquake Investigation Commission: Washington, D.C., Carnegie Institution of Washington, v. 2, p. 16–28.

Savage, J. C., 1983, Strain accumulation in western United States: Annual Reviews of Earth and Planetary Science, v. 11, p. 11–43.

Sharp, R. V., 1981, Variable rates of late Quaternary strike slip on the San Jacinto fault zone, southern California: Journal of Geophysical Research, v. 86, p. 1754–1762.

Sieh, K., 1977, Late Holocene displacement history along the south-central reach of the San Andreas Fault (Ph.D. dissert.): Stanford, California, Stanford University, 239 p.

——1978a, Central California foreshocks of the great 1857 earthquake: Seismological Society of America Bulletin, v. 68, p. 1731–1749.

——1978b, Pre-historic large earthquakes produced by slip on the San Andreas fault at Pallett Creek, California: Journal of Geophysical Research, v. 83, p. 3907–3939.

——1978c, Slip along the San Andreas fault associated with the great 1857 earthquake: Seismological Society of America Bulletin, v. 68, p. 1421–1428.

——in press, Lateral offsets and revised dates of large prehistoric earthquakes at Pallett Creek, southern California: Journal of Geophysical Research.

Stuiver, M., 1982, A high-precision calibration of the AD radiocarbon time scale: Radiocarbon, v. 24, no. 1, p. 1–26.

Stuiver, M., and Pollach, H. A., 1977, Discussion: Reporting of ^{14}C data: Radiocarbon, v. 19, no. 3, p. 355–363.

Thatcher, W., 1979, Strain accumulation on the northern San Andreas fault zone since 1906: Journal of Geophysical Research, v. 84, no. B5, p. 2283–2295.

Thompson, G. A., and Burke, D. B., 1973, Rate and direction of spreading in Dixie Valley, Basin and Range province, Nevada: Geological Society of America Bulletin, v. 84, p. 627–632.

Wallace, R. E., 1968, Notes on stream channels offset by the San Andreas fault, southern Coast Ranges, California, *in* Dickinson, W., and Grantz, A., eds., Conference on Geologic Problems of San Andreas Fault System: Proceedings, Stanford University Publications in the Geological Sciences, v. 11, p. 6–21.

Weber, G. E., and Lajoie, K. R., 1977, Late Pleistocene and Holocene tectonics of the San Gregorio fault zone between Moss Beach and Point Ano Nuevo, San Mateo County, California: Geological Society of America Abstracts with Programs, v. 9, no. 4, p. 524.

Weldon, R. J., and Sieh, K. E., 1982, Offset rate and possible timing of recent earthquakes on the San Andreas fault in Cajon Pass, California [abs.]: EOS, American Geophysical Union Transactions, v. 63, no. 45, p. 1068.

Manuscript Received by the Society November 19, 1982
Revised Manuscript Received September 2, 1983
Manuscript Accepted September 22, 1983
Contribution No. 3819, Division of Geological and Planetary Sciences, California Institute of Technology

Printed in U.S.A.

PLAIN HUMOR

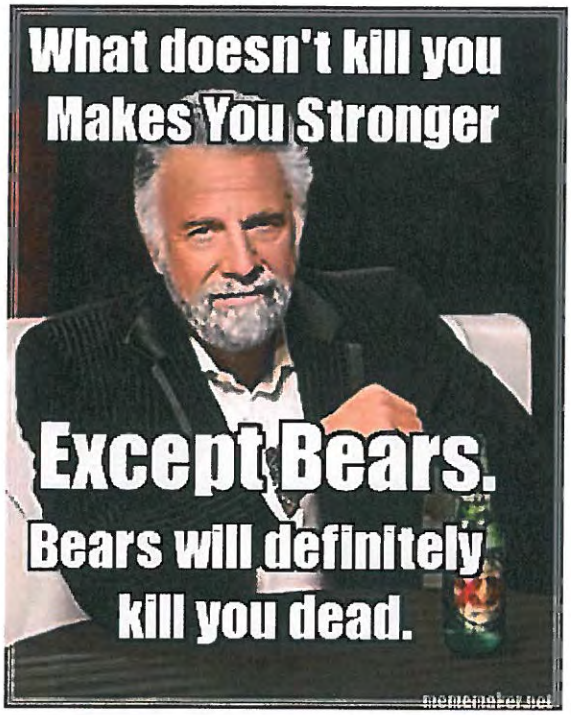
What doesn't kill you
Makes You Stronger
Except Bears.
Bears will definitely
kill you dead.

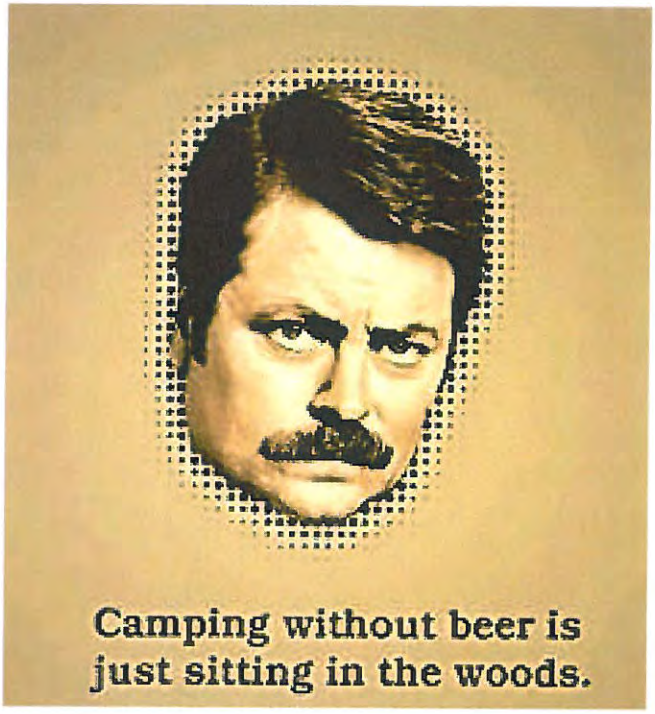
Camping without beer is
just sitting in the woods.


I SEE YOU BROUGHT FOOD WITH YOU
CAMPING
MINE
quickmeme.com

Honestly officer, the salesman said it was overland capable!!

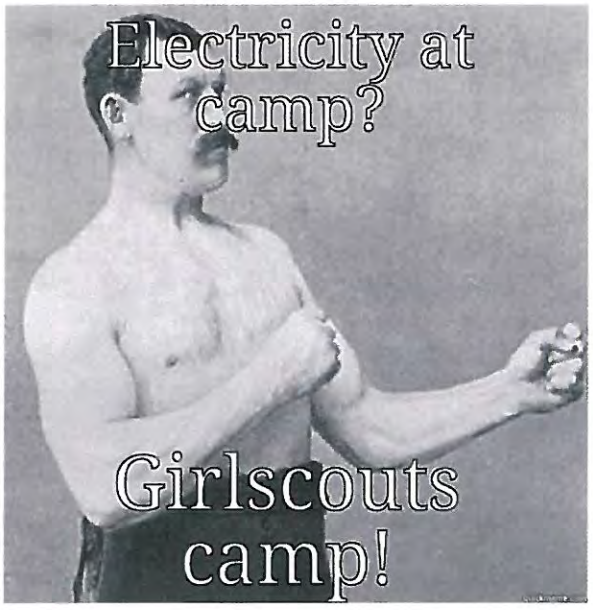

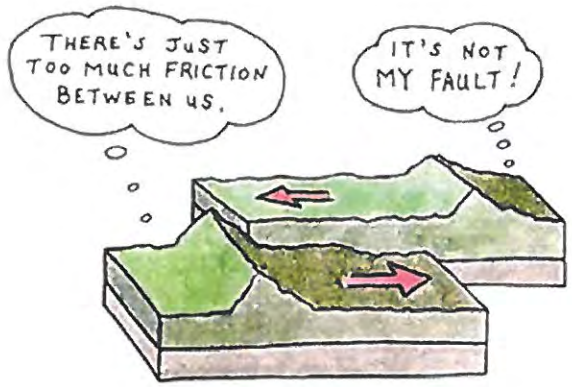

TECTONIC RELATIONSHIPS

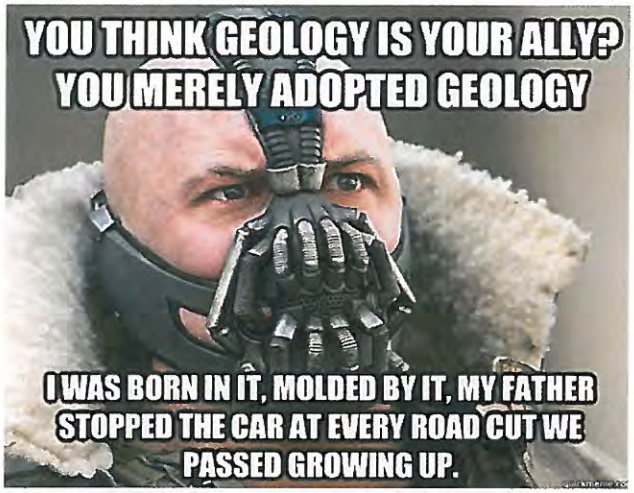

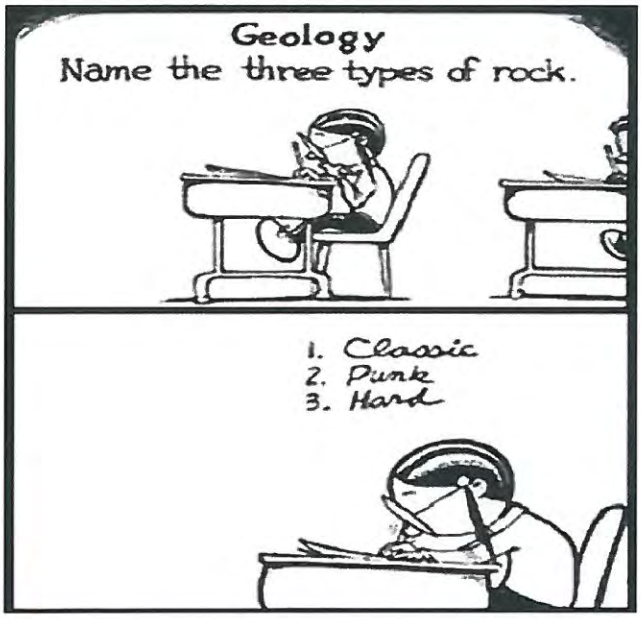

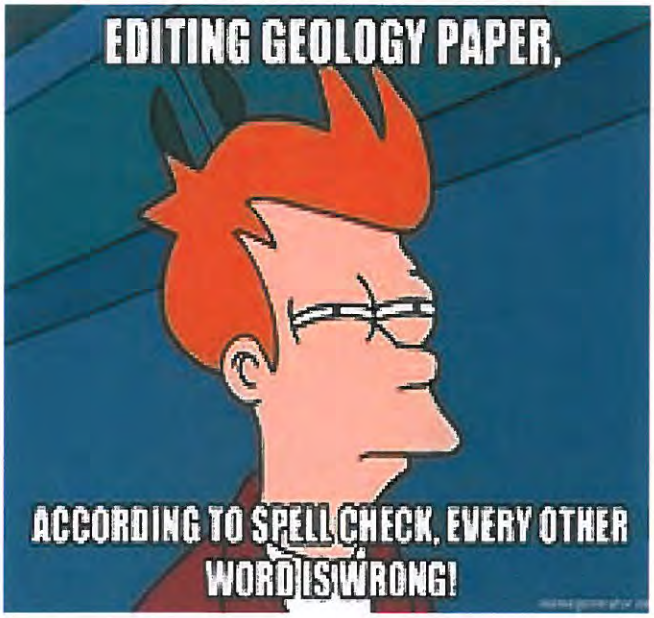

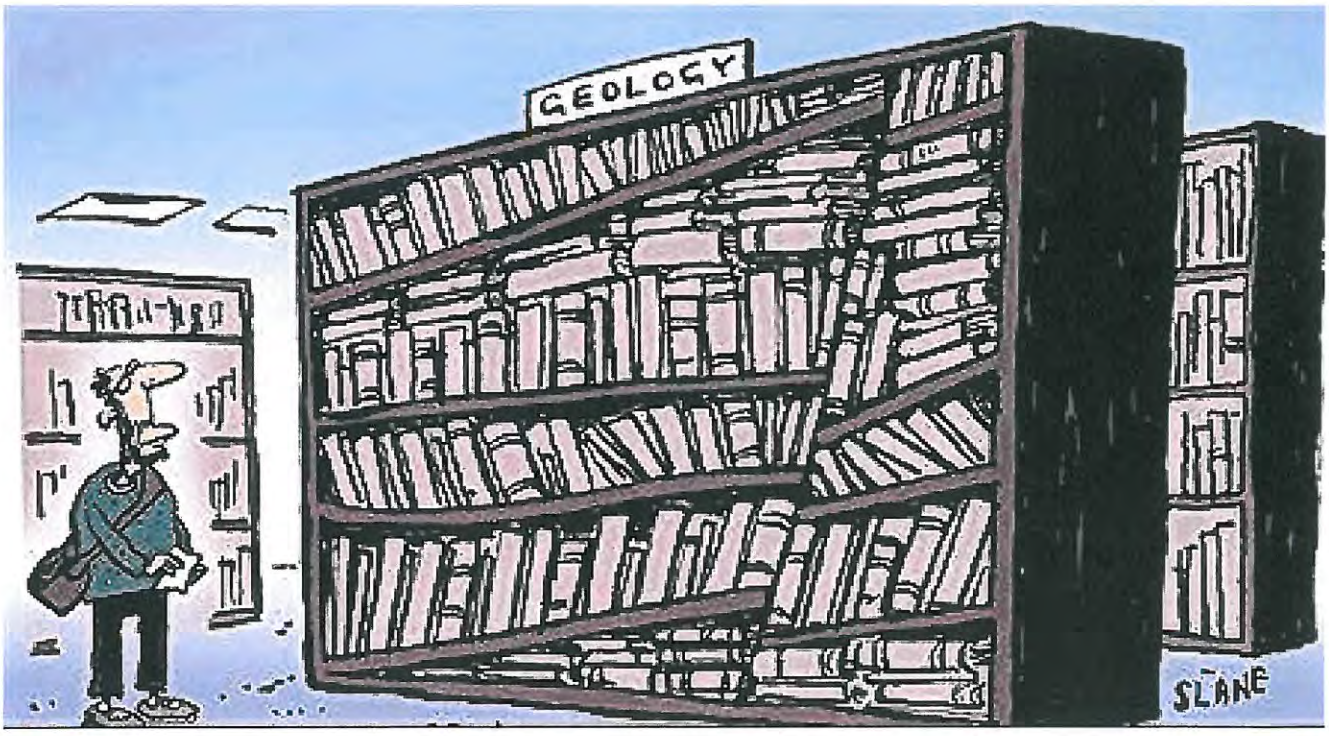

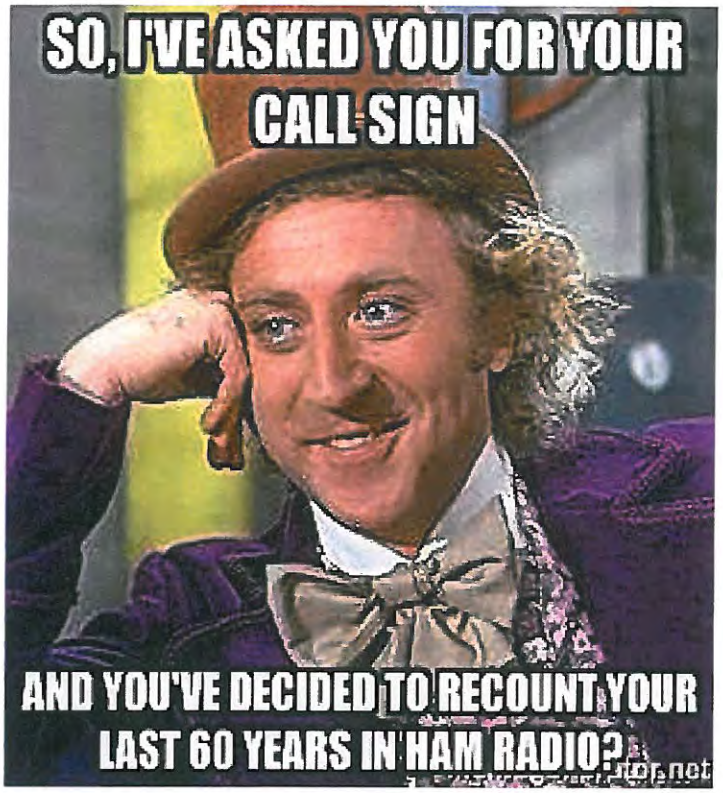

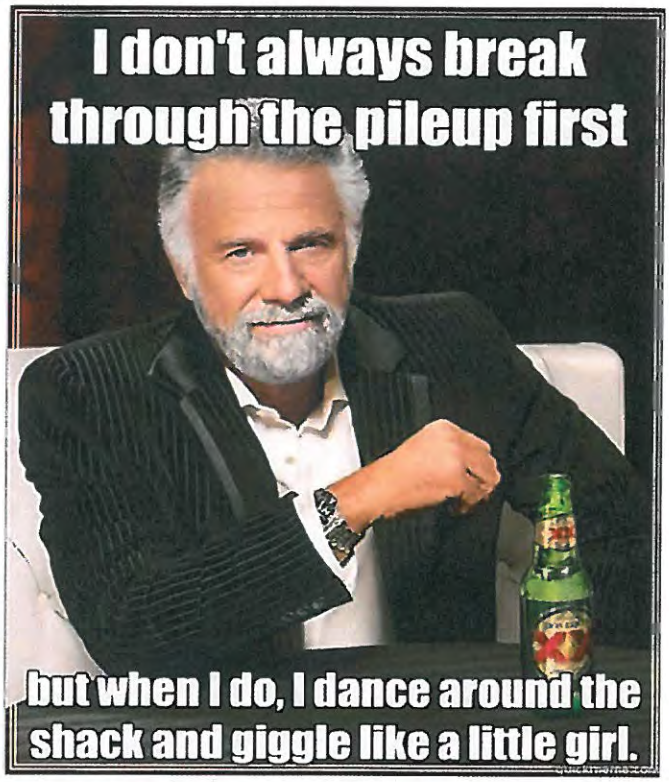

I HATE BEING SEXY BUT I'M A HAM RADIO OPERATOR SO I CAN'T HELP IT

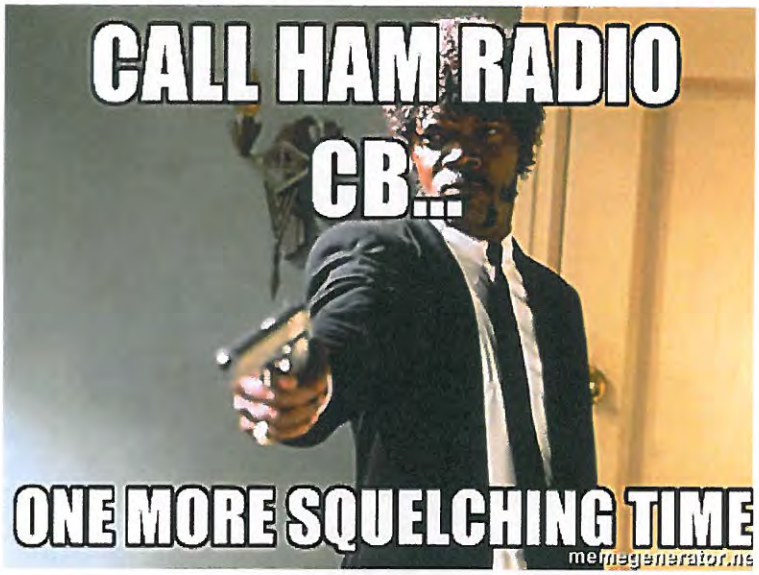

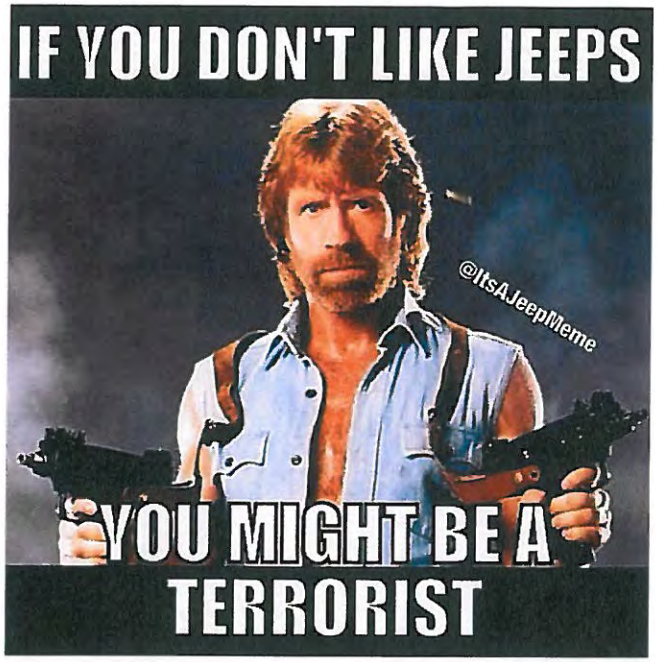
IF YOU DON'T LIKE JEEPS
@ItsAJeepMeme
YOU MIGHT BE A TERRORIST

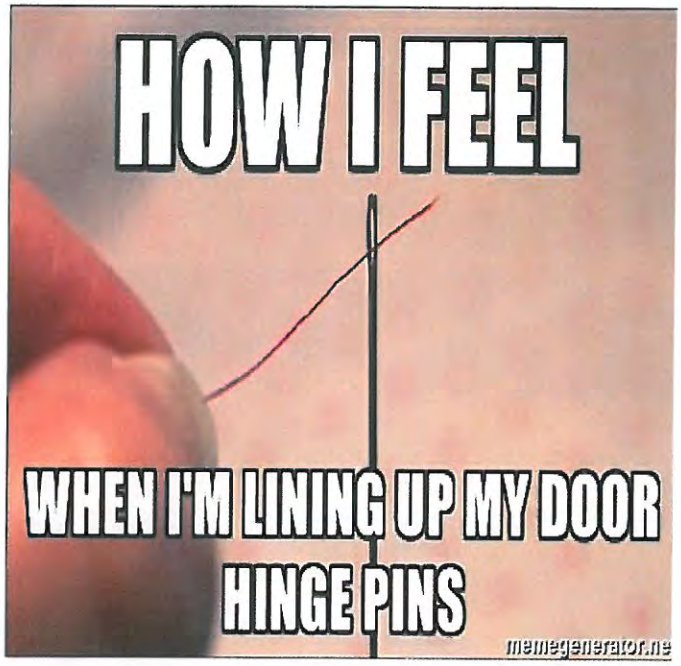
HOW I FEEL
WHEN I'M LINING UP MY DOOR HINGE PINS
memegenerator.net

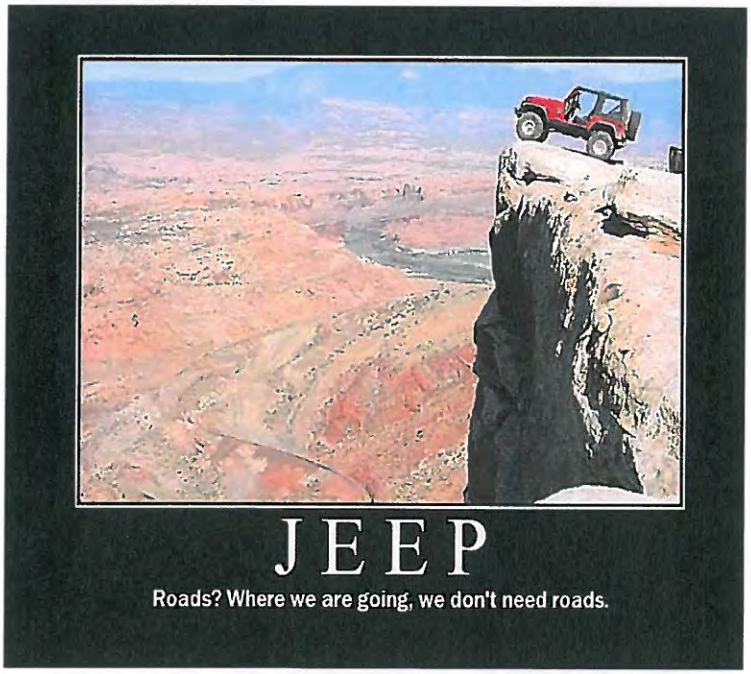
JEEP
Roads? Where we are going, we don't need roads.

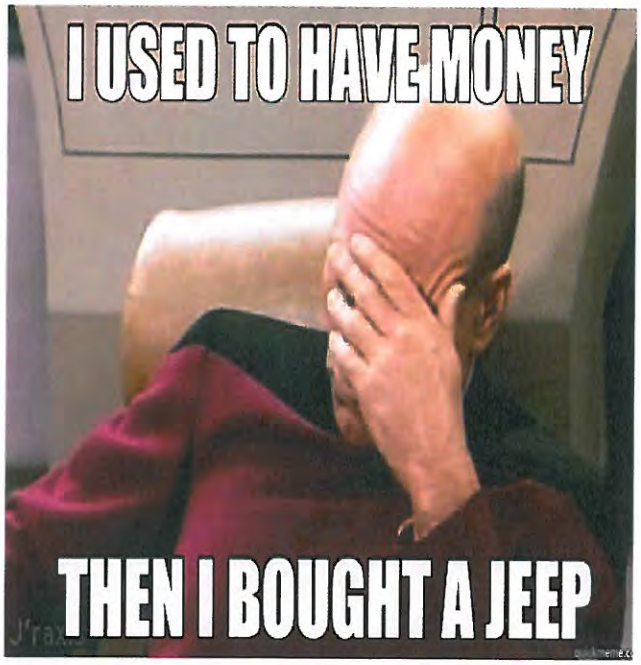
I USED TO HAVE MONEY
THEN I BOUGHT A JEEP

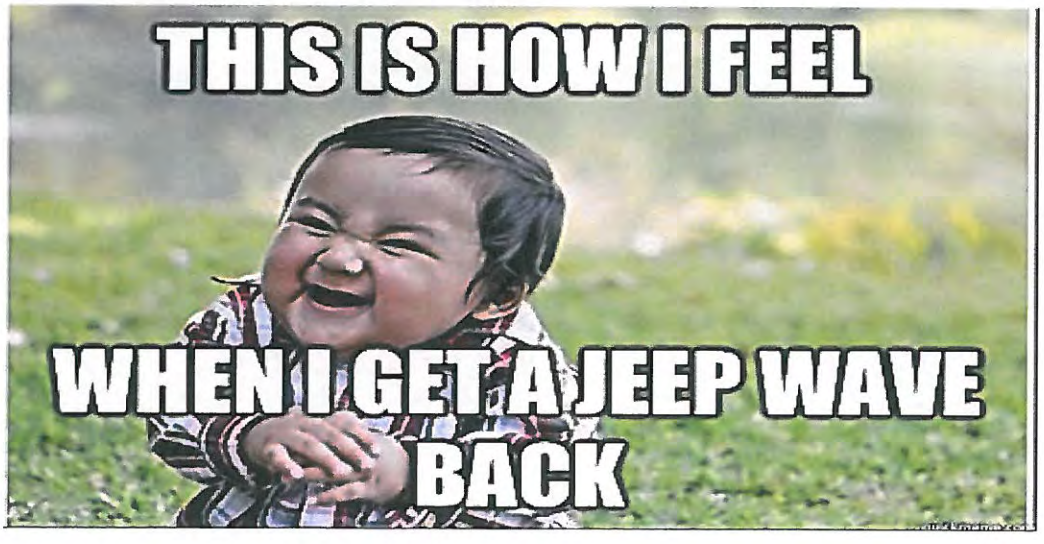
THIS IS HOW I FEEL
WHEN I GET A JEEP WAVE BACK

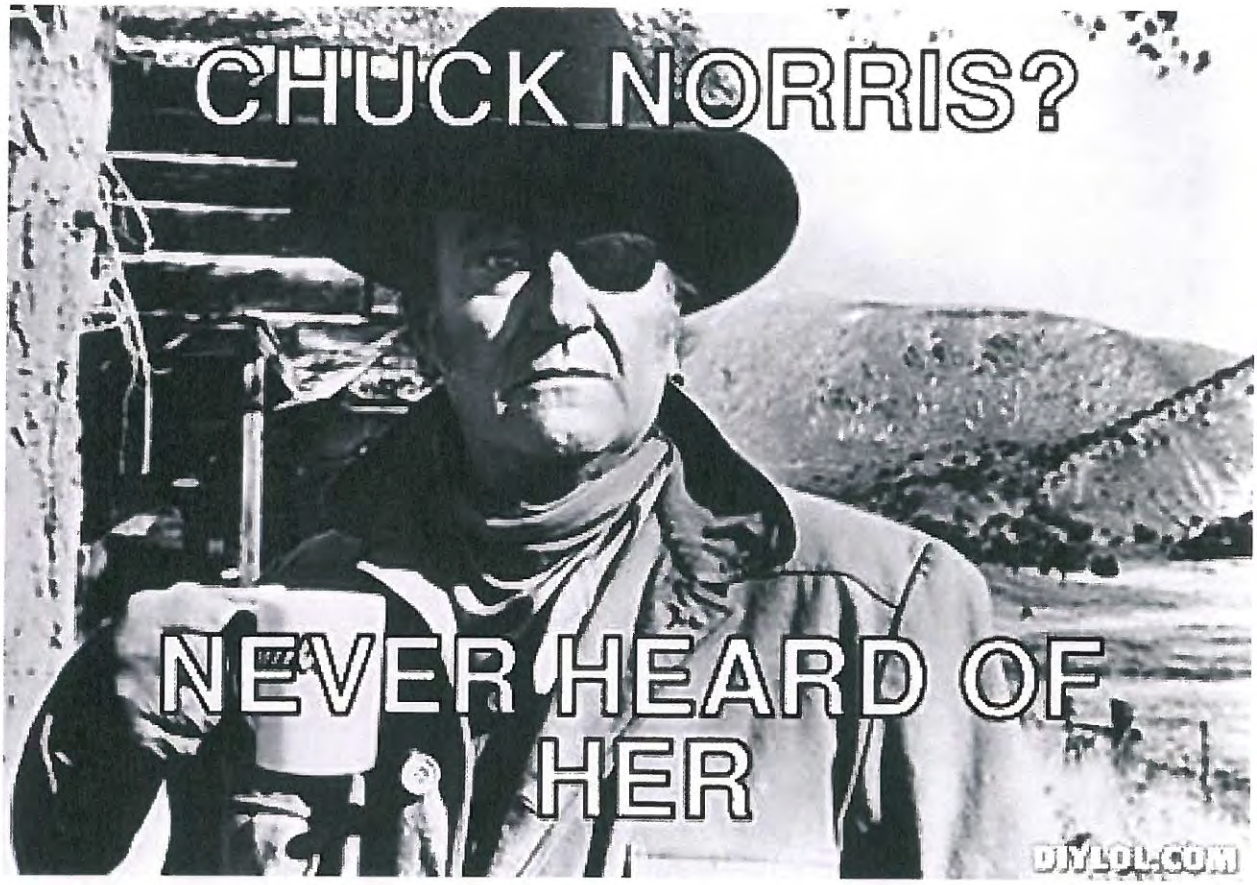
CHUCK NORRIS?
NEVER HEARD OF HER
DIYLOL.COM

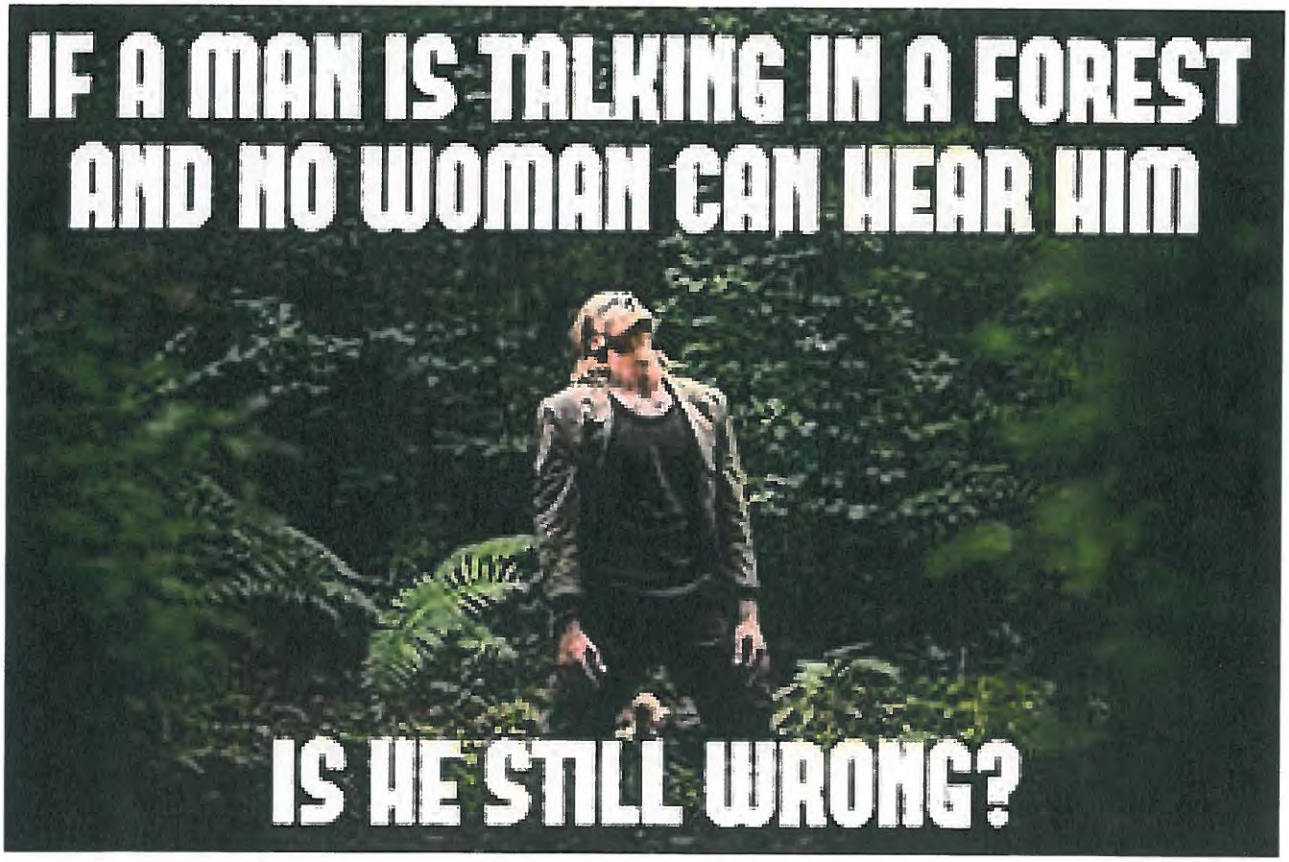
IF A MAN IS TALKING IN A FOREST AND NO WOMAN CAN HEAR HIM
IS HE STILL WRONG?

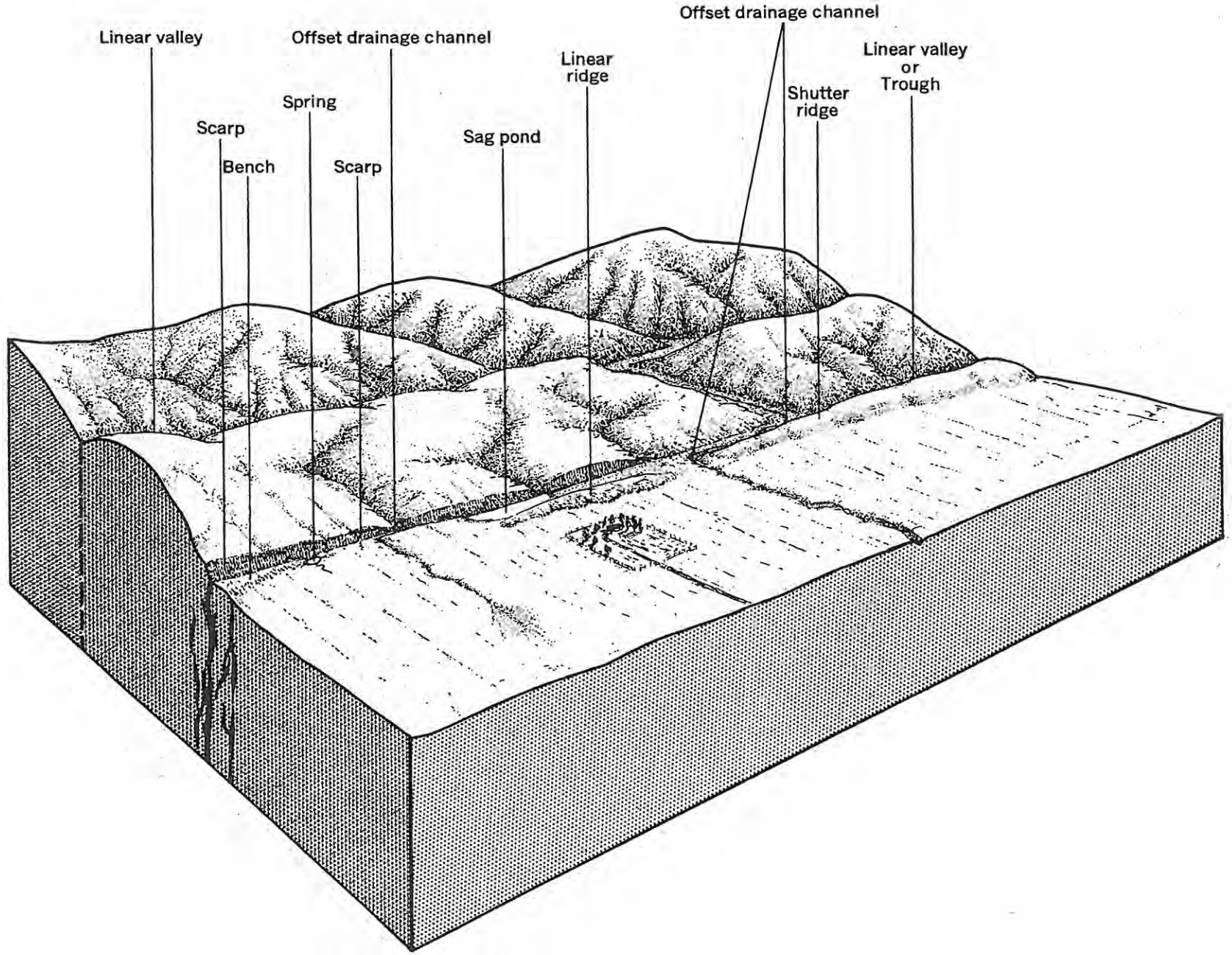

BLOCK DIAGRAM SHOWING LANDFORMS PRODUCED ALONG RECENTLY ACTIVE FAULTS